

00188.26-01f

**En Route Descent Advisor (EDA)  
and  
En Route Data Exchange (EDX)  
ATM Interruption Benefits**

Tara Weidner  
T.Golpar Davidson  
Susan Dorsky



Seagull Technology, Inc.

Prepared for:

National Aeronautics and Space Administration  
Ames Research Center, Moffett Field, CA 94035

Under:

SRC Subcontract No. 99-0249, Task Order No. RTO-26 1266-090  
NASA Prime Contract No. NAS2-98005  
Seagull Project No. C188.26

December 2000

## Acknowledgment

---

*This research was performed by Seagull Technology, Inc., as a subcontract to Systems Resources Corporation, Inc., for the NASA Ames Research Center's Advanced Air Transportation Technologies (AATT) Program. The authors appreciate the discussions and program support of Steve Green and Rich Coppenbarger at NASA Ames, as well as input from NASA researchers Dave McNally, Karl Bilimoria, Russ Paielli, Ralph Bach, and William Chan. The research was performed under the program management of Tara Weidner with software support from Susan Dorsky and Darren Dow, and key technical contributions from Goli Davidson, Lance Birtcil, Tysen Mueller, Jimmy Krozel and Mark Peters, of Seagull Technology. The use of software and algorithms from prior research was greatly appreciated, including conflict detection algorithm developed by Joseph Mitchell and Yi-Jen Chiang at the State University of New York (SUNY) and conflict resolution algorithms developed by Jimmy Krozel and Mark Peters at Seagull Technology. This effort is an extension of previous research [7-8], which focused on the initial development of the ATM Interruptions Model.*

## Table of Contents

---

<b>EXECUTIVE SUMMARY .....</b>	<b>VII</b>
<b>INTRODUCTION.....</b>	<b>1</b>
<b>1. STUDY CASES.....</b>	<b>3</b>
<b>2. ATM INTERRUPTIONS MODEL OVERVIEW .....</b>	<b>7</b>
<b>3. AIRSPACE SIMULATION .....</b>	<b>11</b>
3.1 Airspace.....	11
3.2 Trajectories .....	13
<b>4. METERING CONFORMANCE ATM INTERRUPTIONS.....</b>	<b>21</b>
4.1 Metering Delays.....	21
4.2 Metering Conformance Delay Absorption Strategy.....	23
4.3 Metering Conformance ATM Interruptions Cost Model.....	28
<b>5. SEPARATION ASSURANCE ATM INTERRUPTIONS .....</b>	<b>31</b>
5.1 Incident Database.....	31
5.2 ATM Perception .....	33
5.3 Conflict Resolution and Costs .....	51
<b>6. ATM INTERRUPTIONS BENEFITS .....</b>	<b>56</b>
6.1 Simulated DFW Daily Interruptions .....	56
6.2 ATM Interruptions Costs .....	65
6.3 ATM Interruptions Savings.....	67
<b>7. CONCLUSIONS AND RECOMMENDATIONS.....</b>	<b>76</b>
<b>ACRONYMS .....</b>	<b>82</b>

<b>APPENDIX A MODIFIED ARRIVAL INPUT TRAJECTORIES.....</b>	<b>86</b>
<b>APPENDIX B AIRCRAFT COST RATES AND FUELBURN RATES.....</b>	<b>88</b>
<b>APPENDIX C ATM TRAJECTORY ACCURACY EQUATIONS DERIVATION</b>	<b>94</b>
<b>APPENDIX D ATM TRAJECTORY PREDICTION ACCURACY ERRORS... </b>	<b>100</b>
<b>APPENDIX E 1996 ANNUAL OPERATIONS BY AIRPORT .....</b>	<b>106</b>
<b>REFERENCES.....</b>	<b>108</b>

## List of Figures

---

Figure S.1 ATM Interruptions Model Approach.....	x
Figure S.2 Metering Conformance Delay Absorption.....	x
Figure S.3 Separation Assurance False Alert Probability.....	xii
Figure S.4a EDA Annual Savings by Airport Site.....	xvi
Figure S.4b EDX Annual Savings by Airport Site.....	xvii
Figure 1 ATM Interruptions Model Approach.....	7
Figure 2 Metering Conformance Delay Absorption.....	8
Figure 3 Separation Assurance False Alert Probability.....	10
Figure 4 Location of the Study Airspace Relative to U.S. ARTCC Boundaries.....	11
Figure 5 IFR En Route Chart with DFW Arrival (red) & Departure (blue) Fixes.....	12
Figure 6 Study Day Hourly DFW Arrival and Departure Operations.....	13
Figure 7 Plan View of DFW Study Day STAR (red) and SID (blue) Operations.....	14
Figure 8 Profile View of DFW Study Day Arrival (red), Departure (blue), and Overflight (green) Operations.....	14
Figure 9 COYOTE ONE SID from DFW.....	16
Figure 10 BOWIE ONE STAR from DFW.....	16
Figure 11 Direct Routing Shortens Arrival and Departure Flight Paths.....	17
Figure 12 DFW En Route Trajectories: SID/STAR vs. Direct Routing.....	18
Figure 13 Operations at Top Four DFW Satellite Airports.....	19
Figure 14 Location of Overflight Operations and Top 10 DFW Satellite Airports.....	20
Figure 15 Average Hourly Arrival/Departure Metering Delays.....	22
Figure 16 Average Hourly Arrival/Departure Metering Delays.....	23
Figure 17 Modeled Vectoring Method.....	25
Figure 18 Metering Conformance ATM Interruption.....	26
Figure 19 Histogram of Descent Durations.....	28
Figure 20 Protected Airspace Zone (PAZ) exceeds the FAA Minimum Separation.....	32
Figure 21 Trajectory Prediction Accuracy Initial Position Accuracy & Time Horizon Relationship.....	34
Figure 22 Arrival Conflict Time Horizon.....	41
Figure 23 Acceptable Controller Separation (ACS) Results from Predicted Position Accuracy.....	43
Figure 24 Perceived Miss Distance results from Actual Miss Distance ( $r_f$ ) and Prediction Accuracy.....	46
Figure 25 Comparison of Perceived Miss Distance Curves and Acceptable Controller Spacing (ACS) results in Probability of Conflict and Resolution Costs for Each Type of Incident.....	47
Figure 26 Off-flight Plan Effect on ATM Perception.....	49
Figure 27 Off-Flight-Plan Probability of Conflict Estimation.....	49
Figure 28 Heading (Backside) Resolution Maneuver.....	53
Figure 29 Minimum Cost Resolution between Backside and Frontside Options.....	53
Figure 30 Comparison of Employed Metered Arrival Delay Strategy.....	58
Figure 31 EDA Metering Conformance Savings Per Operation.....	59
Figure 32a EDA Annual Savings by Airport Site.....	73
Figure 32b EDX Annual Savings by Airport Site.....	74
Figure A.1 Original and Modified DFW Arrival Trajectories.....	87
Figure A.2 Original and Modified DFW Arrival Descent Times.....	87

## List of Tables

---

Table S.1 Assumed Metering Conformance Delay Strategy Parameters .....	xi
Table S.2a Assumed ATM Perception Parameters.....	xiii
Table S.3 1996 Operations and Benefits at NAS Deployment Airports.....	xv
Table 1 Characteristics of Top 10 DFW Satellite Airports.....	19
Table 2 DFW Scheduling Criteria.....	22
Table 3 Assumed Metering Conformance Strategy Parameters .....	26
Table 5 Trajectory Prediction Contributing Error values (Jet with FMS).....	37
Table 6 Assumed ATM Trajectory Prediction Accuracy.....	42
Table 7 Acceptable Controller Spacing .....	45
Table 8 Frequency of Off-Flight-Plan Route Intent Error .....	50
Table 9 Resolution Strategies both with and without the CPTP Tool .....	52
Table 10 Metering Conformance Delay Methods .....	57
Table 11 Metered Arrival Delay Comparison.....	58
Table 12 Simulated Metered Arrival Fuelburn Comparison .....	59
Table 13a Number and Category of EDA Separation Assurance ATM Interruptions .....	61
Table 13b DFW EDA Arrival Separation Assurance Conflicts Detail .....	61
Table 13c Number and Category of EDX Separation Assurance ATM Interruptions .....	62
Table 14 Comparison of ATM Interruptions by Operations Type .....	64
Table 15a DFW ATM Interruptions Costs.....	65
Table 15b DFW EDX ATM Interruptions Costs.....	66
Table 16 Average Separation Assurance Resolution Costs by Incident Type.....	66
Table 17a EDA ATM Interruptions Savings, relative to FFP1 Baseline .....	67
Table 17b EDX ATM Interruptions Savings, relative to EDA-Direct Arrivals Baseline.....	67
Table 18 DFW Daily Simulation Interruption Rates and Costs.....	69
Table 19a EDA ATM Interruptions Benefits .....	71
Table 19b EDX ATM Interruptions Benefits.....	72
Table A.1 DFW Radar-based Descent Rates.....	86
Table B.1 Time and Fuelburn Rates by Aircraft Class.....	88
Table B.2 B737 Fuelburn Rates from High-Fidelity Model Simulations.....	89
Table B.3 Climb Fuelburn by Altitude and Aircraft Class [21] .....	90
Table B.4 Cruise Fuelburn by Altitude and Aircraft Class [21] .....	91
Table B.5 Descent Fuelburn by Altitude and Aircraft Class [21] .....	92
Table B.6 BADA “Low” Cruise Speeds by Altitude and Aircraft Class [21].....	93
Table C.1 Dispersion of Trajectory Sensitivities/Partial Derivatives.....	97
Table C.2 TOC Dispersions Due to Jet Aircraft Weight Dispersions3 (%) .....	98
Table C.3. Assumed Trajectory Sensitivities/Partial Derivatives.....	99
Table D.1 Aircraft Takeoff Weight Statistics for American Airlines at DFW5.....	100
Table D.2 Aircraft TOD Weight Statistics for American Airlines at DFW5 .....	101
Table D.3. Thrust and Drag Statistics (%).....	101
Table D.4 Cruise and Descent Speed Adherence Statistics .....	102
Table D.5 Path Distance Error Statistics During Turns (sec).....	102
Table D.6 Rapid Update Cycle 2 (RUC-2) Wind Forecast Accuracy (0000 UTC) .....	103
Table D.7 Rapid Update Cycle 2 (RUC-2) Temperature Forecast Accuracy (0000 UTC) .....	103
Table D.8 ITWS Terminal Wind and RUC Wind Forecast Accuracy11 (kts).....	104
Table D.9 Secondary Surveillance Radar Tracking Accuracy .....	105
Table E.1 Airport Delays and Assumed Interruption Rates.....	106
Table E.2 Rush Arrival Rate Criteria.....	107
Table E.3 CY1996 Domestic ARTCC Operations .....	107

## **En Route Descent Advisor (EDA) and En Route Data Exchange (EDX) ATM Interruption Benefits**

### **Executive Summary**

Air Traffic Controllers must occasionally interrupt flights to avert impending traffic conflicts and to conform to flow-rate restrictions. These interruptions impose deviations from the user's preferred trajectory. The efficiency and effectiveness of such controller-imposed deviations directly affect controller and flight crew workload as well as user costs. The large number of interruptions associated with current air traffic operations have led airspace users to strongly advocate for industry initiatives such as Free Flight. Strong international efforts are underway to develop and deploy new Air Traffic Management (ATM) Decision Support Tools (DSTs) to assist controllers in reducing the frequency and impact of ATM-based flight interruptions. ATM En Route DSTs and their further enhancement with data exchange have the potential to reduce unnecessary deviations and improve the efficiency with which necessary deviations are implemented by more accurately predicting flight trajectories and supporting useful clearance decisions. We refer to these processes that the ATM system uses to interrupt the normal traffic flow in order to mechanize flow-rate conformance and separation assurance conflict resolution as "ATM interruptions," and the DST processes of reducing and imposing more efficient traffic interruptions as "ATM interruption benefits." This study evaluates ATM interruption improvements from advanced DSTs within the Center-TRACON Automation System (CTAS), under development by NASA Ames Research Center.

The CTAS En Route Descent Advisor (EDA) will assist ATM in reducing deviations from the user's preferred trajectory, by generating accurate, fuel-efficient clearance advisories for the merging, sequencing, and separation of high-density traffic as well as provide automation assistance for the prediction and resolution of conflicts between aircraft. EDA integration of metering conformance and conflict probe functions also improves en route operations. Knowledge of metering conformance flight intent enhances trajectory prediction used by the conflict probe. Additionally, the NASA En Route Data Exchange (EDX) program aims to augment the functionality of CTAS through exchange of real-time user flight data, thereby improving CTAS trajectory predictions and allowing CTAS to better accommodate user preferences. CTAS trajectory accuracy will improve with user-CTAS enhanced knowledge of aircraft state and intent, leading to increased controller confidence and reduced unnecessary flight interruptions.

The objective of this effort is to determine the benefits of the EDA and its further enhancement with user-CTAS en route data exchange (EDX), compared to baseline operations. The two types of ATM interruptions under study address functions of arrival metering conformance and conflict probe separation assurance. This effort follows a prior model development effort [7-8], and was performed in conjunction with complementary NASA efforts [1-2].

## Study Cases

In order to determine the effects of EDA and further data exchange enhancements on ATM interruptions, systems with and without these improvements were compared to baseline operations. These cases are discussed below. The EDA system is compared to a baseline FFP1 system, while the EDX cases are compared to a baseline EDA system:

- **Free Flight Phase 1 (FFP1) System** - This system reflects en route operations aided by FAA Free Flight Phase 1 (FFP1) arrival metering and conflict probe tools. This includes the CTAS Traffic Management Advisor (TMA) to schedule and meter arrival flights, as well as a separate User Request Evaluation Tool (URET CCLD) conflict probe and trial-planning tool. TMA sets an arrival aircraft metering fix crossing schedule at the Center/TRACON boundary and displays flight-specific delay advisories to the controller. The controller cognitively creates a strategy to absorb the specified delay to meet the TMA schedule. As each arrival progresses toward the terminal area, and is delayed by the controller, TMA updates the displayed delay estimate to provide feedback to the controller as to the effectiveness of the employed delay strategy. The assumed FFP1 conflict probe independently probes all en route airspace predicted trajectories and alerts controllers of potential separation assurance conflicts, with a trial planner to assist in the development of effective resolution clearances. Because the metering conformance and conflict probe functions are not integrated in FFP1 operations, the conflict probe suffers by being unaware of the controller metering conformance flight changes. Thus, without integration, the aircraft intent does not match conflict probe assumptions, leading the tool to falsely identify some conflicts while missing other real conflicts.
- **CTAS En Route/Descent Advisor (EDA) System** - The CTAS EDA case refers to future en route operations using integrated ATM metering and scheduling capabilities with the En Route/Descent Advisor (EDA) tools. EDA functionality is assumed to include integrated TMA arrival scheduling, EDA-calculated maneuver advisories to meet this schedule, and a conflict probe with both detection and trial planning capabilities. Because the EDA conflict probe is also assumed to enable controllers to clear arrival aircraft to fly direct routes to arrival metering fixes, when operationally feasible, both Standard Terminal Arrival Route (STAR) and Direct Arrival (DIR) cases are analyzed. The EDA maneuver advisories assist controllers in formulating and executing a traffic delay strategy to meet the TMA schedule, allowing the controller to assess quickly and accurately the impact of various delay strategies. The integration of the resulting metering conformance flight changes with the conflict probe tool, reduces false and missed alert rates.

- **En Route Data Exchange (EDX) Systems** - Four en route data exchange (EDX) cases provide CTAS EDA improved perception by supplementing CTAS trajectory prediction capabilities with EDX aircraft-specific flight information. In this study, EDX encompasses four evolutionary cases. The data are assumed to be downlinked from the aircraft in real-time, although significant improvement may also result from sharing airline dispatcher-based estimates. Note that these cases are numbered to match a related study effort:

EDX1 Wx Data Exchange – FMS downlink of airborne wind/temperature measurements. These real-time reports are used to upgrade CTAS weather forecasts, used in CTAS trajectory prediction. Additionally, the improved meteorological forecast is disseminated providing a common weather forecast for ATM, FMS and AOC trajectory modeling.

EDX2 Wx, Aircraft Weight Data Exchange – EDX1 enhanced with user-provided flight-specific aircraft weight estimates as well as aircraft-specific thrust and drag coefficients. Such state and aircraft performance information is critical to modeling ascent/descent flight profiles.

EDX3 Wx, Weight, Speed Intent Data Exchange – EDX2 enhanced with user-provided aircraft-specific speed intent, including the climb/descent intended Mach/CAS speed profile. This is a user preference that ATM will attempt to accommodate.

EDX5 Wx, Weight, Speed Intent, Next Two Waypoints Data Exchange – EDX3 enhanced with downlink of the FMS’s next two waypoints. Waypoint intent (names and/or locations) automatically improves DST trajectory predictions for all DST functions, including conflict probe.

## **Analysis Process and Key Assumptions**

The ATM Interruptions Model, used in this study to analyze ATM improvements to flight interruptions, is summarized in Figure S.1. Initially an airspace model, using user-preferred trajectories for a sample day at a target airport, simulates the target en route ARTCC airspace. The arrival and departure trajectories are then modified to accommodate metering conformance flight changes (i.e., delays) required by airport flow-rate restrictions. Separation Assurance ATM interruptions are then modeled using these metered flights as input. Initially conflicts and near-conflicts detected in the metered traffic scenario are recorded in a conflict-incident database. Based on the characteristics and ATM perception of these incidents, separation assurance resolution strategies and costs are identified. Each metering conformance and separation assurance ATM interruption is recorded, including tabulation of fuel costs and associated technology benefits. A simple method is employed to extrapolate the simulated single-facility daily savings to annual and NAS-wide benefit estimates. This modeling approach facilitates general assessment of various combinations of DST capabilities, supporting technologies (e.g, data exchange, FMS equipage), and controller procedures.

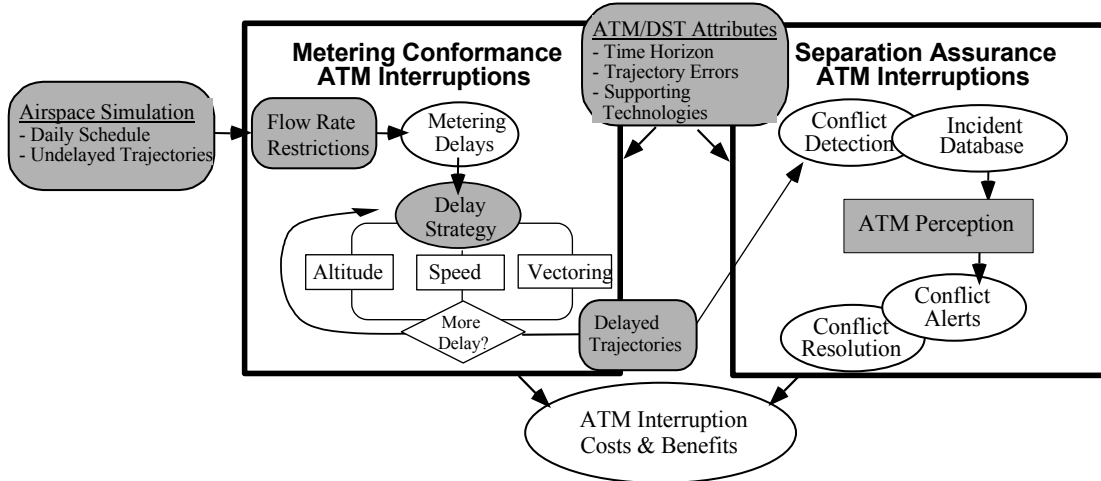


**Figure S.1 ATM Interruptions Model Approach**

Metering Conformance ATM Interruptions

Figure S.2 illustrates the general methodology employed in the model to clear an aircraft to meet a metered (i.e., delayed) arrival fix crossing time. Combinations of speed, altitude, and vectoring maneuvers are considered, where the maximum amount of delay is absorbed by each method before moving onto the next method. The affect of time horizon where the maneuver is initiated is also illustrated. Note that at larger time horizons (right figure), speed and altitude changes can absorb more delay. As the effective time horizon decreases (left figure), the need for more expensive vectors (path stretching) increases since the speed and altitude changes cannot absorb as much delay.

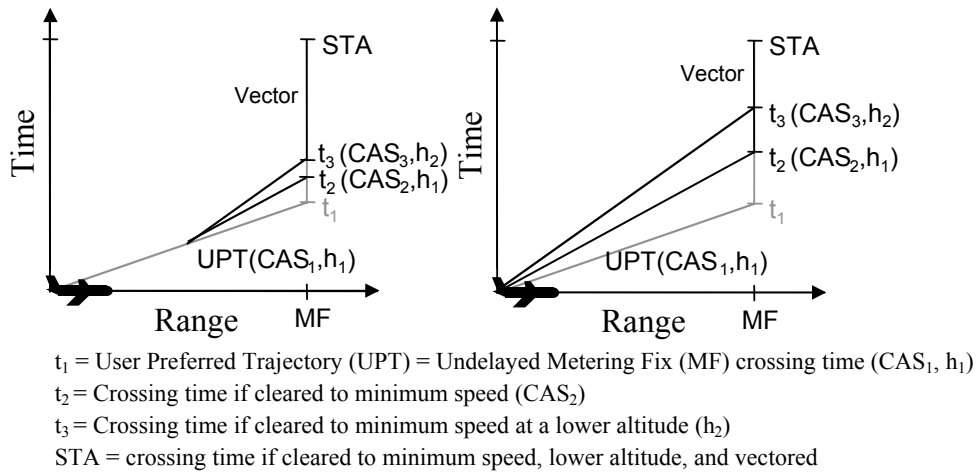


**Figure S.2 Metering Conformance Delay Absorption**

The effectiveness of the delay absorption clearance depends on the amount of delay to be absorbed by any one flight, the time available to absorb the delay (i.e., effective time horizon), and the delay absorption strategy. Differences in delay-absorption performance are modeled through differences in the technology-specific time horizon and delay strategy.

In all cases, departure metering delays are absorbed by holding the aircraft on the ground, effectively shifting the takeoff time but not altering its three-dimensional trajectory. Arrival metering delays employed a mix of airborne delay absorption methods including changes in speed, cruise altitude, and routing. Although the same approach was used for all cases, key differences include the ordering of the various delay absorption methods, the assumed time horizon, and baseline altitude and minimum speed limitations, as shown in Table S.1. Note that for simplicity, EDX was assumed to apply the same assumptions as EDA, with no resulting incremental benefits.

**Table S.1 Assumed Metering Conformance Delay Strategy Parameters**

	FFP1	CTAS EDA
<b>General</b>		
Strategy Order	Altitude Speed Vectoring Time Shift	Speed Altitude/Speed Vectoring Time Shift
Time Horizon	16 min	18 min
<b>Speed</b>		
Speed Increments	10 kt	5 kt
Speed Error	+ 10 kt	None
Min Cruise Speed	BADA(1)	BADA(1) – 10 kts
Min Descent Speed	BADA (1)	BADA(1) – 20 kts
<b>Altitude (Jets only)</b>		
Permitted Altitudes	Min Altitude	FAR Altitudes
Min Altitude	FL230/FL240	FL230/FL240
<b>Vectoring</b>		
Heading Increment	1°	1°
Max Vector Angle	60°	60°
Turn back Error	± 60 seconds	± 30 seconds

(1) Reflecting a lack of automation to help controllers identify efficient speeds, the minimum cruise/descent speeds for FFP1 used Eurocontrol BADA model [37] “low” cruise speeds included in Appendix B (e.g. 250 kts for jets). EDA minimum speeds were modeled as 10 kts (20 kts in descent) lower than BADA, a conservative estimate closer to best endurance speed.

Separation Assurance ATM Interruptions

The approach used to evaluate Separation Assurance ATM interruptions involves detection and resolution of ATM perceived conflicts. Potential incidents are filtered through an ATM perception model to identify whether ATM would perceive the incident as a conflict requiring interruption. This perception model reflects the level of conflict probe technology in terms of trajectory prediction accuracy, time horizon, and separation criteria. ATM is assumed to intervene and interrupt trajectories that fall below an acceptable controller spacing, as perceived by a conflict probe tool. Because of uncertainty and lack of integration with other DST functions, intervention may result in correct or false alerts, and no-intervention may lead to a missed alert, that will need to be resolved tactically. ATM perceived probability of conflict, based on trajectory prediction accuracy is used to weight the overall interruption cost of each incident. Consider the incident described in Figure S.3, assuming a minimum separation of 5.0 nm (±M), an Acceptable Controller Spacing of 6 nm (±ACS), and a simulated point of closest approach (PCA) of 7 nm. With perfect ATM perception, the separation minimum and

PCA would be compared, no conflict would be identified, and ATM would not interrupt the aircraft. However, when adjusted for imperfect ATM perception and acceptable controller spacing buffers, a certain portion of the time (as shown by the shaded region) a conflict would be perceived by ATM requiring intervention. The assumed ATM interruption for this false alert would accrue a fuel cost penalty. Alternatively, a probability (unshaded region) exists that ATM would perceive no conflict and correctly avert a false interruption (at no cost or controller workload). An overall weighted cost of the incident would be calculated from the Probability of Conflict and the resolution costs of the alternate resolution actions (e.g. false/no alert). Under improved ATM perception, the Figure S.3 curve would tighten around the correct PCA. As a result, ATM would perceive the aircraft to be in conflict less frequently limiting ATM intervention and its associated fuel penalties.

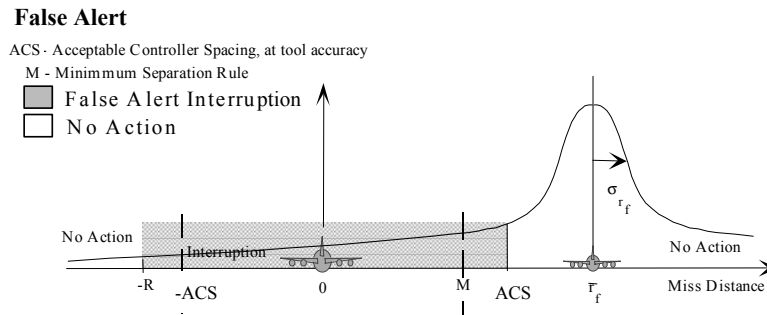


**Figure S.3 Separation Assurance False Alert Probability**

Table S.2 summarizes the attributes of ATM Perception used to identify whether ATM would perceive each incident as a conflict, requiring intervention to ensure separation. These attributes include the conflict probe time horizon, and predicted trajectory prediction accuracy of climb (CL), cruise (CR), and descent (D) flight segments. This prediction accuracy is used to identify the vertical and horizontal acceptable controller spacing (ACS) or protected airspace zone (PAZ) dimensions. To account for prediction uncertainties, controllers are assumed to apply a safety buffer to FAA minimum spacing requirements, as shown in Table S.2. A final assumption was the extent of unrecorded off-flight plan clearances. Such changes in flight intent not documented as a flight plan amendment, go undetected by the conflict probe and result in increased false and missed alerts. For this analysis, no additional conflict (missed alerts) was assumed to result from the off-flight plan route, and the recording of such routings were assumed to improve for metered arrivals under EDA and for all flights under EDX5.

**Table S.2a Assumed ATM Perception Parameters**

		FFP1 Baseline					EDA				
		DEP		OVR	ARR		DEP		OVR	ARR*	
		CL	CR	CR	CR	D	CL	CR	CR	CR	D
<b>12-minute Trajectory Prediction Error</b>											
Predicted Position Error	nm	13.8	4.7	4.7	4.7	4.5	13.8	4.7	4.7	3.7	1.6
<b>Horizontal ACS</b>											
En Route	nm	8.00	8.00	8.00	8.00	8.00	8.00	8.00	8.00	7.37	6.07
<b>Vertical ACS</b>											
>FL290	Ft	3000	2000	2000	2000	3000	3000	2000	2000	2000	2357
<=FL290	Ft	2000	1000	1000	1000	2000	2000	1000	1000	1000	1357
<b>Off-Flight Plan Frequency</b>											
Off-FP	%	15%	15%	15%	15%	15%	15%	15%	15%	0%	0%
		EDX1 (Weather)					EDX2 (Aircraft Weight)				
		DEP		OVR	ARR*		DEP		OVR	ARR*	
		CL	CR	CR	CR	D	CL	CR	CR	CR	D
<b>12-minute Trajectory Prediction Error</b>											
Predicted Position Error	nm	13.7	4.7	4.6	3.6	1.37	12.2	4.7	4.6	3.6	1.44
<b>Horizontal ACS</b>											
En Route	nm	7.98	7.91	7.91	7.26	5.95	7.66	7.91	7.91	7.26	5.91
<b>Vertical ACS</b>											
>FL290	Ft	2994	2000	2000	2000	2318	2886	2000	2000	2000	2303
<=FL290	Ft	1994	1000	1000	1000	1318	1886	1000	1000	1000	1303
<b>Off-Flight Plan Frequency</b>											
Off-FP	%	15%	15%	15%	0%	0%	15%	15%	15%	0%	0%
		EDX3 (Speed Intent)					EDX5 (Next 2 Waypoints)				
		DEP		OVR	ARR*		DEP		OVR	ARR	
		CL	CR	CR	CR	D	CL	CR	CR	CR	D
<b>12-minute Trajectory Prediction Error</b>											
Predicted Position Error	nm	9.4	3.6	3.6	3.6	1.4	9.4	3.6	3.6	3.6	1.4
<b>Horizontal ACS</b>											
En Route	nm	7.04	7.26	7.26	7.26	5.91	7.04	7.26	7.26	7.26	5.91
<b>Vertical ACS</b>											
>FL290	Ft	2680	2000	2000	2000	2303	2680	2000	2000	2000	2303
<=FL290	Ft	1680	1000	1000	1000	1303	1680	1000	1000	1000	1303
<b>Off-Flight Plan Frequency</b>											
Off-FP	%	15%	15%	15%	0%	0%	0%	0%	0%	0%	0%

\* Applies to metered arrivals only.

## Findings

The ATM Interruptions Model is used to evaluate key EDA and EDX benefits. Table S.3 presents the annual cost savings estimated for each mechanism at each study site. The savings are plotted graphically by airport in Figures S.4a and S.4b for EDA relative to the FFP1 Baseline, and EDX relative to an EDA-Direct Arrivals Baseline, respectively. In addition to the ATM interruptions flight efficiency and workload benefits quantified here, other EDA and EDX benefit mechanisms are discussed in references [1] and [2], respectively.

This effort quantified EDA metering conformance and EDA/EDX separation assurance ATM interruption savings. Metering conformance interruptions delay arrival aircraft to meet airport capacity constraints. EDA maneuver advisories assist controllers in formulating and executing a traffic delay strategy to meet arrival metering fix crossing schedule. EDA allows controllers to quickly and accurately assess the impact of various delay strategies, and more effectively use fuel-efficient strategies, such as speed control, resulting in lower cost metering conformance interruptions. It was found that EDA saved an average of 59 lbs and 2.6 seconds or \$6.80 per arrival metering conformance interruption, for a total savings of \$25.09M annually assuming NAS-wide deployment at 37-airports. In addition, the EDA metering conformance procedures are more strategic and require less overall workload than those currently used by the FFP1 Baseline. Metering conformance improvements represent 90 percent of the estimated EDA interruptions benefits.

For separation assurance interruptions, ATM relies on accurate predictions of flight trajectories within its conflict probe tool to accurately identify the location and nature of pending separation violations. With more accurate EDA arrival trajectory predictions (EDA advisories and EDA/EDX updated state/intent) ATM would less frequently perceive aircraft to be incorrectly or out of conflict (missed and false alerts), resulting in fewer ATM flight interventions and associated resolution fuel penalties. Additionally, improved traffic conflict prediction will include more accurate estimation of conflict geometry and speeds, leading to more efficient resolution maneuvers. It was found that EDA reduced separation assurance interruptions by 7.7 percent with each interruption saving an average of 0.8 lbs or \$0.08 per interruption, for a total savings of \$2.80M annually NAS-wide. More significantly, the EDA separation assurance conflicts required less overall workload primarily because of the integration with metering conformance flight intent, reducing missed and false alert rates by 50 and 40 percent, respectively. Relative to the EDA-Direct arrival Baseline, it was found that EDX reduced separation assurance interruptions by 10 percent with each interruption savings an average of 2 lbs or \$0.21 per interruption, for a total savings of \$3.6M annually assuming NAS-wide deployment at 37-airports. More significantly, the EDX separation assurance conflicts required less overall workload primarily because of the integration with metering conformance flight intent, reducing the number of missed and false alerts by 25 and 7 percent, respectively. Additionally other interruption benefits are noted but not quantified, including EDA and EDX enhancement to overall safety, strategic controller planning across multiple sectors, and reduced nuisance conflict alerts.

**Table S.3 1996 Operations and Benefits at NAS Deployment Airports**

<u>Airport</u>	<u>Apt/ARTCC</u>		Annual Savings (\$000s)**					
	<u>EDX1</u>	<u>EDX2</u>	<u>EDX3</u>	<u>EDX5</u>	<u>EDX1</u>	<u>EDX2</u>	<u>EDX3</u>	<u>EDX5</u>
Atlanta	ATL	ZTL	1,549.6	1,666.7	22.0	59.8	205.5	224.1
Nashville	BNA	ZME	276.0	309.6	15.5	42.1	144.7	157.8
Boston	BOS	ZBW	362.3	403.5	17.7	48.2	165.7	180.7
Bradley	BDL	ZBW	1,069.0	1,150.2	15.5	42.1	144.7	157.8
Baltimore	BWI	ZDC	430.7	479.5	20.9	56.8	195.3	213.0
Cleveland	CLE	ZOB	484.9	542.2	25.7	70.0	240.5	262.2
Charlotte	CLT	ZTL	808.5	881.1	22.0	59.8	205.5	224.1
Cincinnati	CVG	ZID	702.5	766.5	19.9	54.2	186.1	203.0
Washington National	DCA	ZDC	586.8	645.0	20.9	56.8	195.3	213.0
Denver	DEN	ZDV	585.1	635.3	13.7	37.2	128.0	139.5
Dallas – Ft. Worth	DFW	ZFW	1,707.2	1,830.5	19.0	51.6	177.4	193.5
Detroit	DTW	ZOB	940.6	1,025.3	25.7	70.0	240.5	262.2
Newark	EWR	ZNY	1,168.4	1,258.6	18.3	49.7	170.9	186.4
Ft. Lauderdale	FLL	ZMA	347.9	383.9	13.8	37.6	129.2	140.9
Houston Hobby	HOU	ZHU	383.4	424.6	16.6	45.2	155.2	169.3
Washington Dulles	IAD	ZDC	617.0	676.9	20.9	56.8	195.3	213.0
Houston – Intercontinental	IAH	ZHU	678.8	737.7	16.6	45.2	155.2	169.3
N.Y. Kennedy	JFK	ZNY	873.6	946.1	18.3	49.7	170.9	186.4
Las Vegas	LAS	ZLA	639.2	697.1	17.7	48.3	165.9	181.0
Los Angeles	LAX	ZLA	1,506.5	1,616.4	17.7	48.3	165.9	181.0
N.Y. LaGuardia	LGA	ZNY	929.7	1,005.6	18.3	49.7	170.9	186.4
Orlando	MCO	ZJX	482.8	530.3	16.8	45.8	157.4	171.6
Chicago Midway	MDW	ZAU	538.8	599.7	25.9	70.6	242.5	264.4
Memphis	MEM	ZME	512.7	562.9	17.7	48.2	165.7	180.7
Miami	MIA	ZMA	885.8	954.2	13.8	37.6	129.2	140.9
Minneapolis	MSP	ZMP	822.4	891.7	18.1	49.4	169.9	185.2
Oakland	OAK	ZOA	643.9	696.0	12.2	33.4	114.6	125.0
Chicago O'Hare	ORD	ZAU	2,072.4	2,225.3	25.9	70.6	242.5	264.4
Portland	PDX	ZSE	415.3	453.9	12.5	34.0	116.7	127.2
Philadelphia	PHL	ZNY	858.2	929.8	18.3	49.7	170.9	186.4
Phoenix	PHX	ZAB	880.6	948.3	13.5	36.7	126.1	137.5
Pittsburgh	PIT	ZOB	818.8	896.1	25.7	70.0	240.5	262.2
San Diego	SAN	ZLA	381.3	423.7	17.7	48.3	165.9	181.0
Seattle	SEA	ZSE	660.2	713.5	12.5	34.0	116.7	127.2
San Francisco	SFO	ZOA	1,126.6	1,207.7	12.2	33.4	114.6	125.0
Salt Lake City	SLC	ZLC	496.2	540.8	13.5	36.8	126.4	137.9
St. Louis	STL	ZKC	1,199.0	1,290.5	17.8	48.4	166.4	181.5
Total All Airports *	NA	NA	19,189	20,726	351	956	3,284	3,582

\* Totals include only one instance of each ARTCC, excluding the shaded ARTCC operations separation assurance operations.

\*\* EDA Savings are relative to FFP1 Baseline and EDX Savings are relative to EDA-DIR Baseline.

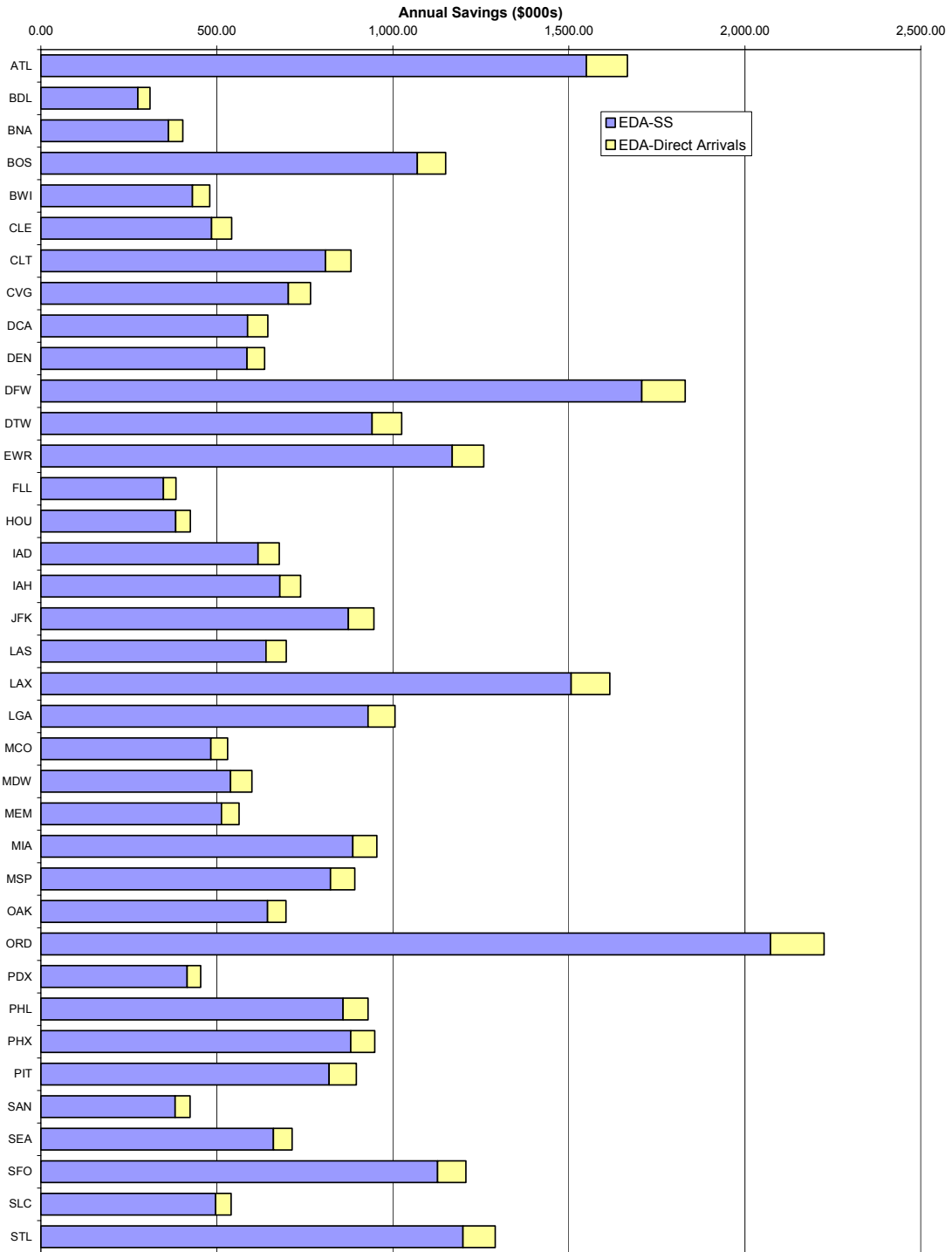


**Figure S.4a EDA Annual Savings by Airport Site**

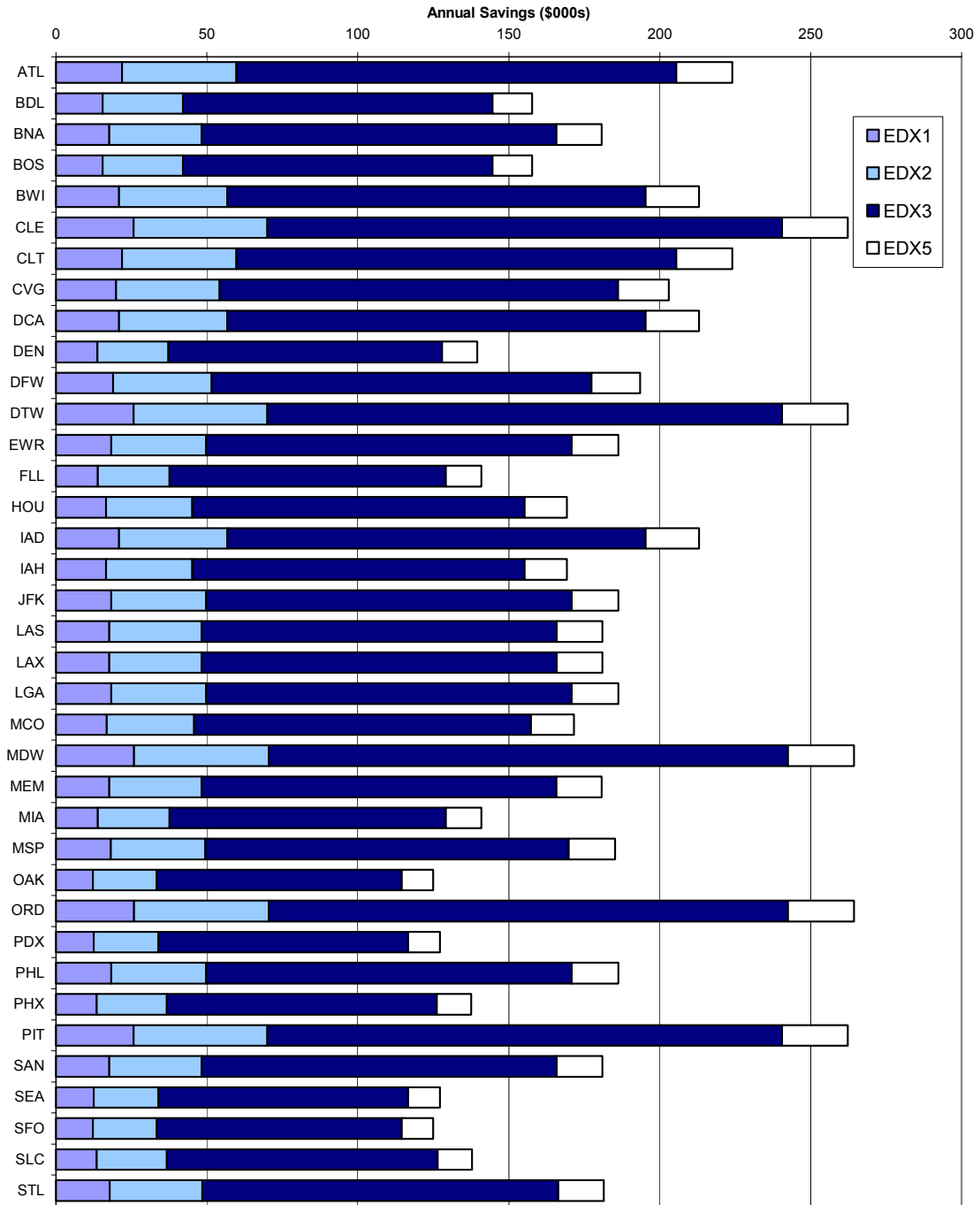


**Figure S.4b EDX Annual Savings by Airport Site**

It should be noted that the direct operating cost estimates do not directly account for the significant controller workload. In all cases, safety improves with enhanced surveillance under EDA and EDX metered arrival trajectory prediction. Under EDA, controller workload is enhanced by EDA assistance in strategic planning to meet the dual objectives of separation assurance and compliance with flow-rate restrictions. The improved metered arrival prediction and integration of flow-rate conformance flight changes with

conflict probe functions, greatly reduces the probability of missed or nuisance (false) conflict alerts. Indeed, the analysis identified a reduction in the number of missed and false alerts by 30 and 21 percent, respectively, in addition to the EDA reduction in overall detected conflicts. Under EDX, controller workload is enhanced by EDX improved conflict probe trajectory prediction accuracy, through incorporation of user-supplied aircraft conditions, weather forecasts, and intent. The improved trajectory prediction, especially the EDX5 downlink of next two waypoint intent, greatly reduces the probability of missed or nuisance (false) conflict alerts. Indeed, the analysis identified a 25 percent reduction in the number of missed and 7 percent reduction in false alerts under EDX, supporting a 10 percent reduction in overall detected conflicts.

Controller workload is also enhanced with EDA metering conformance operations. The EDA-generated maneuver advisories embody an efficient inter-sector approach to metering restrictions, easing controller strategy and clearance development. By identifying an appropriate strategy as well as magnitude, EDA reduces controller workload. Indeed, in early EDA testing, over two-thirds of the EDA clearances provided to controllers required no modification, being acceptable in both method (speed, heading, altitude) and magnitude. Additionally, the use of a high-fidelity model to develop the EDA maneuver advisories improves their accuracy over cognitively-developed interruptions, reducing the need for additional corrective interruptions closer to the restriction, and limiting the use of vectoring which requires two clearances (i.e., turnout and turn back).

## **Recommendations**

This report has assessed the performance of en route ATM DST technologies for reducing the frequency and impact of ATM-based deviations to the user's preferred trajectories. Cases studied include the CTAS En Route Descent Advisor (EDA) and EDA enhanced with user-CTAS data exchange (EDX). This work, summarized in related NASA AATT efforts for EDA and EDX, estimated both metering conformance and separation assurance ATM interruptions benefits. The ATM Interruptions Model used in this effort provided an approach to evaluating the trajectory costs of en route ATM interruptions by modeling specific controller metering and conflict resolution actions, aided by automated DST technology. Specific recommendations to enhance the analysis can be found in Chapter 6. They include the update of model parameters and assumptions, model enhancement to improve the approach to specific topics as well as the capture new related benefit mechanisms, and sensitivity analyses. Implementation of these recommendations would reinforce the ATM Interruptions modeling approach as a powerful and efficient mechanism for evaluating a variety of en route operational impacts at the air traffic controller clearance level.

## **Introduction**

---

Air Traffic Controllers must occasionally interrupt flights to avert impending traffic conflicts and to conform to flow-rate restrictions. These interruptions impose deviations from the user's preferred trajectory. The efficiency and effectiveness of such controller-imposed deviations directly affect controller and flight crew workload as well as user costs. The large number of interruptions associated with current air traffic operations have led airspace users to strongly advocate for industry initiatives such as Free Flight. Strong international efforts are underway to develop and deploy new Air Traffic Management (ATM) Decision Support Tools (DSTs) to assist controllers in reducing the frequency and impact of ATM-based flight interruptions. ATM En Route DSTs and their further enhancement with data exchange have the potential to reduce unnecessary deviations and improve the efficiency with which necessary deviations are implemented by more accurately predicting flight trajectories and supporting useful clearance decisions. We refer to these processes that the ATM system uses to interrupt the normal traffic flow in order to mechanize flow-rate conformance and separation assurance conflict resolution as "ATM interruptions," and the DST processes of reducing and imposing more efficient traffic interruptions as "ATM interruption benefits." This study evaluates ATM interruption improvements from advanced DSTs within the Center TRACON Automation System (CTAS), under development by NASA Ames Research Center.

The En Route Descent Advisor (EDA)[3], is a set of ATM automation DSTs within CTAS. EDA is designed to manage traffic within and between Air Route Traffic Control Centers (Centers) and facilitate Free Flight. EDA will service all phases of en-route flight, including climb, cruise, and descent with the goal of reducing deviations from the user's preferred trajectory. The various EDA tools will generate accurate, fuel-efficient clearance advisories for the merging, sequencing, and separation of high-density traffic. EDA will also provide automation assistance for the prediction and resolution of conflicts between aircraft [4]. These features give en route controllers the flexibility and confidence to manage aircraft more efficiently while meeting Air Traffic Control (ATC) constraints where, currently, conservative advisories may result in less efficient trajectories.

NASA Ames researchers are also proposing an extension of the CTAS EDA tool to include user-CTAS data exchange [5]. This concept, known as the En Route Data Exchange (EDX) program, is intended to augment the functionality of CTAS through receipt of real-time user flight data to improve CTAS trajectory predictions as well as to allow CTAS to better accommodate user preferences. A field evaluation of an initial user-CTAS data exchange is being pursued jointly between the NASA EDX program and the FAA's FMS-ATM Next Generation (FANG) program for Fall 2000 [6].

With improved descent trajectory prediction provided by EDA and data exchange, controllers will have better knowledge of aircraft state and intent. This improvement to CTAS trajectory accuracy will improve DST performance leading to controller confidence and reduce flight interruptions due to misidentified potential conflicts.

Airport flow-rate or metering restrictions also need to be considered in addition to conflicts in aircraft separation minima. The benefits associated with a focus on separation alone are unrealistic in that many ATM interruptions are due to dynamic capacity overloads that result in flight delays independent of conflict occurrences. The benefit of reductions in conflict deviations and route restrictions for any one flight will be negated if downstream congestion forces the flight to be delayed anyway. A hybrid approach is needed to model the impact of, and interactions between, ATM interruptions for conflicts and flow-rate restrictions due to congestion.

Integrated DST functions entail important coupling interactions, which also need to be captured. One coupling involves the inefficiency of solutions that do not consider the entire problem domain. For example, accommodating a faster direct route/UPT just to reach a metering situation does not necessarily improve fuel efficiency. Second, not knowing the outcome of one DST function may limit the effectiveness of other functions. For example, lack of aircraft intent without knowledge of metering conformance changes degrades trajectory prediction used by the conflict probe.

The objective of this effort is to determine the benefits of the EDA and its further enhancement with user-CTAS en route data exchange (EDX), compared to baseline operations. The study investigates the benefits of more fuel-efficient as well as reduced Air Traffic Management (ATM) interruptions. The two types of ATM interruptions under study address functions of arrival metering conformance and conflict probe separation assurance. This effort follows a prior model development effort [7-8], and was performed in conjunction with complementary NASA efforts, which summarize EDA [1] and EDX [2] benefits. These related studies address many other benefit mechanisms of EDA and EDX.

This research effort improves upon the basic modeling methodology developed in previous work [7-8]. Improvements include modifications to the underlying model logic with significant emphasis on improving model inputs and parameter assumptions in order to better represent the technology cases under study. The input parameters were obtained from recent conversations and documentation provided by NASA researchers. However, due to ongoing research in this area, model parameters should be updated with new field tests and supporting research findings to continually improve the ATM interruptions benefit estimates.

This report is organized as follows. After defining the study cases and overviewing the ATM interruptions model methodology in Chapters 1 and 2, the remaining chapters detail the individual model components and parameter assumptions. Chapter 3 reviews the underlying airspace trajectory simulation of the Fort Worth Air Route Traffic Control Center (ZFW) en route airspace. Chapters 4 and 5 discuss the investigation of the two ATM interruptions under study: Metering Conformance and Separation Assurance. This includes the identification of the number and type of interruptions, assumed interruption strategies and the estimated interruption costs. Chapter 6 summarizes the number and cost of ATM interruptions by case and the associated daily benefits as well as extrapolating the daily ZFW savings to annual levels at 37 airports, representing NAS-wide deployment. Conclusions and recommendations are discussed in Chapter 7.

## 1. Study Cases

---

In order to determine the effects of the EDA tool and EDX enhancements on ATM interruptions, systems with and without these improvements were compared to baseline systems. EDA was evaluated relative to a baseline system, which loosely represents the arrival metering and conflict probe capabilities of the Free Flight Phase 1 (FFP1) program. The EDA enhancement case represents a future system with CTAS EDA capabilities including EDA-metering conformance maneuver advisories integrated with conflict probe functionality. This EDA case was used as the baseline for evaluating EDX benefits, including four evolutionary EDX cases, which improve EDA functions through user-CTAS data exchange of aircraft state, intent, and preference data. These cases are discussed further in the following paragraphs. Note that the assumed DSTs merely provide information to an air traffic controller who retains full authority and responsibility for safe separation of air traffic. Additionally, aircraft in all cases are assumed to operate with highly accurate FMS flight control throughout their en route flight.

### **Free Flight Phase 1 (FFP1) System**

The modeled baseline reflects en route operations aided by FAA Free Flight Phase 1 (FFP1) arrival metering and conflict probe tools. This includes the CTAS Traffic Management Advisor (TMA) to schedule and meter arrival flights [9], as well as a separate URET CCLD conflict probe and trial-planning tool [10]. TMA creates an optimal time-based arrival schedule for an airport and establishes scheduled times of arrival (STAs) at TRACON-boundary meter fixes to control the flow into the TRACON airspace. TMA scheduling is based on predicted arrival trajectories using high-fidelity aircraft performance models, meteorological forecasts, and aircraft flight plans [5]. The TMA schedule is continually updated from radar returns flight data from the ARTCC Host computer system in response to changing events, until an aircraft's metering-fix Estimated Time of Arrival (ETA) is within 19 minutes (the “freeze horizon”), at which point the aircraft's Scheduled Time of Arrival (STA) is frozen. TMA STAs are distributed to each en route sector managing arrival traffic. The STAs and TMA estimates of delay to be absorbed are displayed directly on the controller's Display System Replacement (DSR) in an alphanumeric meter list. In the FFP1 baseline, the controller cognitively creates a strategy to absorb the specified delay to meet the TMA schedule. As each arrival progresses toward the terminal area, and is delayed by the controller, TMA updates the displayed delay estimate to provide feedback to the controller as to the effectiveness of the employed delay strategy.

The initial conflict probe assumed in the FFP1 system independently probes all en route airspace predicted trajectories and alerts controllers of potential separation assurance conflicts, with a trial planner to assist in the development of effective resolution clearances. Because the controller metering conformance flight changes and conflict probe functions are not integrated in FFP1 operations, the conflict probe suffers by being unaware of the controller metering conformance flight changes. Thus, without

integration, the aircraft intent does not match conflict probe assumptions, leading the tool to falsely identify some conflicts while missing other real conflicts.

### **CTAS En Route/Descent Advisor (EDA) System**

The CTAS EDA case refers to future en route operations with integrated ATM metering and scheduling capabilities with the En Route/Descent Advisor (EDA) tools [3]. EDA functionality is assumed to include integrated TMA arrival scheduling (as in the FFP1 case), EDA-calculated maneuver advisories to meet this schedule, and a conflict probe with both detection and trial planning capabilities. With integration, all these functions rely on CTAS high-fidelity trajectory modeling to predict future aircraft positions. EDA employs a Required Time of Arrival (RTA)-capable trajectory modeling with horizontal and vertical trajectory-optimization tools to develop maneuver advisories to meet the TMA scheduled arrival fix crossing times and/or resolve en route airspace traffic conflicts. The EDA maneuver advisories assist controllers in formulating and executing a traffic delay strategy to meet the TMA schedule, allowing the controller to assess quickly and accurately the impact of various delay strategies. The integration of the resulting metering conformance flight changes with the conflict probe tool, through EDA assistance in documentation of flight changes, reduces false and missed alerts.

The EDA conflict detection and resolution capability is also assumed to enable controllers to clear arrival aircraft to fly direct routes to arrival metering fixes, when operationally feasible. Additional arrival trajectory optimization benefit mechanisms, which further improve flight efficiency have also been investigated in other efforts [1,11].

### **En Route Data Exchange (EDX) Systems**

Four en route data exchange (EDX) cases provide the CTAS EDA with improved perception over the current system through enhanced CTAS trajectory prediction capabilities, supplemented with EDX aircraft-specific flight information [12]. As a result, EDX enhanced CTAS tools can more accurately predict aircraft position, leading to more accurate conflict detection and generation of more efficient conflict resolutions relative to the EDA case. More accurate position information results in fewer false and missed alerts, and reducing unnecessary or excessive resolution maneuvers. Although, no improvement is assumed in metering conformance, in reality, some savings may result due to more accurate EDA-generated maneuver advisories as CTAS trajectory prediction accuracy is improved through user-CTAS data exchange.

EDX encompasses four evolutionary cases. Initial fielding of these cases is underway through a joint NASA/FAA EDX Phase 2 field evaluation [6]. The data is assumed to be downlinked from the aircraft in real-time, although significant improvement may also result from sharing airline dispatcher-based estimates. Note that these cases are numbered to match a related study effort:

**EDX1 Wx Data Exchange** – FMS downlink of airborne wind/temperature measurements. These real-time reports are used to upgrade CTAS weather forecasts, used in CTAS trajectory prediction [13]. Additionally, the improved meteorological forecast is disseminated providing a common weather forecast for ATM, FMS and AOC trajectory modeling.

**EDX2 Wx, Weight Data Exchange** – EDX1 enhanced with user-provided flight-specific aircraft weight estimates as well as aircraft-specific thrust and drag coefficients. Such state and aircraft performance information is critical to modeling ascent/descent flight profiles.

**EDX3 Wx, Weight, Speed Intent Data Exchange** – EDX2 enhanced with user-provided aircraft-specific speed intent, including the climb/descent intended Mach/CAS speed profile. This is a user preference that ATM will attempt to accommodate.

**EDX5 Wx, Weight, Speed Intent, Next Two Waypoints Data Exchange** – EDX3 enhanced with FMS downlink of its next two waypoints. Waypoint intent (names and/or locations) automatically improves CTAS trajectory predictions for all DST functions, including conflict probe.



## 2. ATM Interruptions Model Overview

The overall ATM Interruptions Model benefits methodology used in this study to analyze the improvements to ATM interruptions based on the study cases of Chapter 1, is summarized in Figure 1. An airspace model, using user-preferred trajectories for a sample day at a target airport, simulates the target en route airspace. The arrival and departure trajectories are then modified to accommodate metering conformance flight changes (i.e., delays) required by airport flow-rate restrictions. Separation Assurance ATM interruptions are then modeled using these metered flights as input. Initially conflicts and near-conflicts detected in the metered traffic scenario are recorded in a conflict-incident database. Based on the characteristics and ATM perception of these incidents, separation assurance resolution strategies and costs are identified. Each metering conformance and separation assurance ATM interruption is recorded, including tabulation of fuel costs and associated technology benefits. This modeling approach facilitates general assessment of various combinations of DST capabilities, supporting technologies (e.g, data exchange, FMS equipage), and controller procedures. The function of each model component is discussed briefly below.

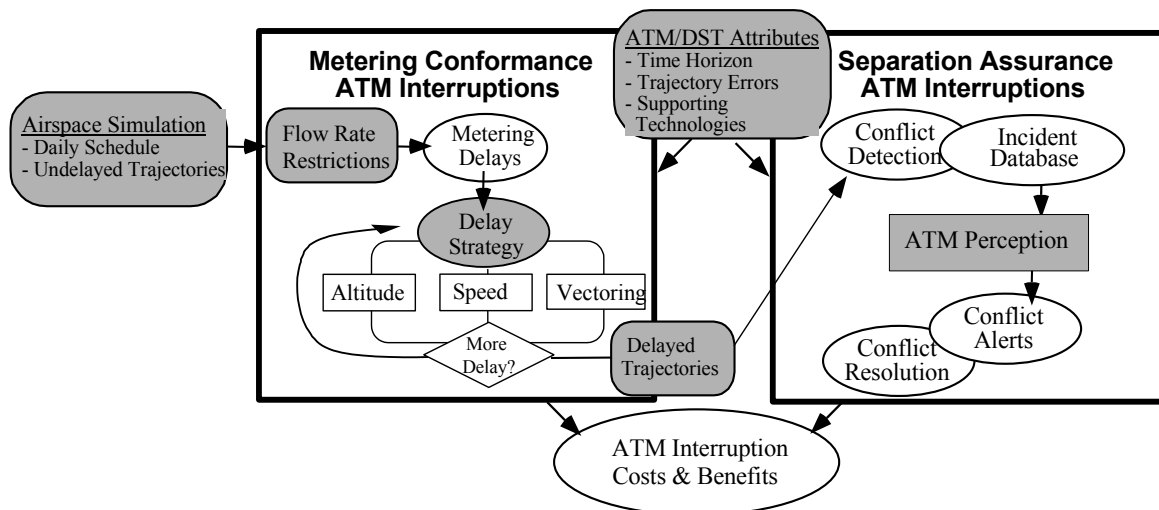


**Figure 1 ATM Interruptions Model Approach**

**Airspace Simulation** – An airspace simulation simultaneously tracks multiple trajectories in a block of en route airspace. These trajectories represent the geometry and timing of scheduled arrival,<sup>1</sup> departure, overflight and satellite airport operations over a 24-hour period, given initial user preferred flight plans (filed route and preferred vertical profile). Standard Instrument Departure (SID) and Standard Arrival Route (STAR) filed routes may be modified to allow arrival direct routing. This simulation generates a set of 4-dimensional “undelayed” trajectories, representing what each flight would do if left alone to fly a user preferred trajectory. These trajectories define a common traffic scenario for ATM interruptions evaluation under the various study cases.

<sup>1</sup> Descents have been updated since the previous studies [7-8], as discussed in Appendix A.

**Metering Conformance ATM Interruptions** – Metering Conformance ATM interruptions reflect flight modifications to realistically absorb the delay necessary to meet airport/airspace capacity restrictions. Initially the undelayed flights are analyzed to determine the level of congestion and determine aircraft-specific arrival/departure metering delays. Although departure delays are absorbed as ground holds in all cases, the particular arrival delay strategy, a mix of changes to the speed profile, cruise altitude, and routing, depends on the assumed DST case. The resulting aircraft-specific delay maneuvers employed and their costs are tabulated, and a second set of arrival/departure flight trajectories are generated which reflect these delay maneuvers.

Figure 2 illustrates the general methodology employed to clear an aircraft to meet an (delayed) arrival fix STA. Multiple possible orderings of speed, altitude, and vectoring maneuvers are considered, where the maximum amount of delay is absorbed by each method before moving onto the next method.

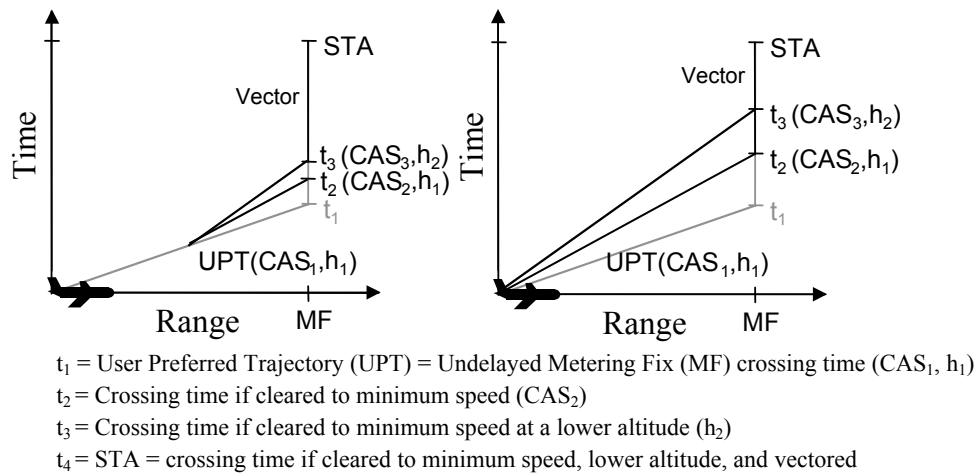


**Figure 2 Metering Conformance Delay Absorption**

The effectiveness of the delay absorption model depends on the amount of delay to be absorbed by any one flight, the time available to absorb the delay (i.e., effective time horizon), and the delay absorption strategy. The affect of time horizon is illustrated in Figure 2. Note that at larger time horizons (right figure), speed and altitude changes can absorb more delay. As the effective time horizon decreases (left figure), the need for more expensive vectors (path stretching) increases since the speed and altitude changes cannot absorb as much delay. Differences in delay-absorption performance are modeled through differences in the technology-specific time horizon and delay strategy.

**Separation Assurance ATM Interruptions** - The assessment of Separation Assurance ATM interruptions requires detection, and resolution of ATM perceived conflicts. The Airspace and Metering Conformance trajectory simulation reflects en route activity where no attempt was made to resolve traffic conflicts other than arrival and departure metering requirements. These data allow for the identification of actual and potential conflicts that would occur without ATM separation assurance intervention, as embedded in actual radar track data. Initially, a method is employed to step through the simulated

trajectories and detect all actual and possible traffic conflicts. The resulting Incident Database identifies all aircraft pairs perceived by ATM as requiring intervention. The database also identifies attributes of the aircraft pair's point of closest approach (PCA). These incidents may or may not be perceived as conflicts by ATM. ATM is assumed to intervene and interrupt trajectories that fall below an acceptable controller spacing, as perceived by a conflict probe tool. One component of perception is the accuracy of the expected PCA attributes reported by the conflict probe at the tool's assumed time horizon, given technology-specific trajectory errors. A second component of perception is identification of Acceptable Controller Spacing, a function of both the required FAA minimum separation and an intentional buffer, used to limit separation violations. When the Acceptable Controller Spacing is compared with the conflict probe reported PCA attributes of each event in the Incident Database, a Probability of Conflict is calculated which identifies the likelihood that a controller would perceive the incident as a conflict requiring intervention. Because of uncertainty and lack of integration with other DST functions, intervention may result in correct or false alerts, and no-intervention may lead to a missed alert, that will need to be resolved tactically. For each perceived conflict of the Incident Database, a resolution cost is defined. This fuel cost penalty represents the cost to just avert a conflict when initiated at the given time horizon. The particular aircraft geometry and severity of the incident are taken into account when resolving conflicts. Missed alerts are resolved in a tactical manner by assuming a more expensive shorter time horizon.

ATM perceived probability of conflict value, based on case perception, is used to weight the overall interruption cost of each incident. Consider the incident described in Figure 3, assuming a minimum separation of 5.0 nm ( $\pm M$ ), an Acceptable Controller Spacing of 6 nm ( $\pm ACS$ ), and a simulated PCA of 7 nm. Using a perfect ATM Perception model, the separation minimum and PCA would be compared, no conflict would be identified, and ATM would not interrupt the aircraft. However, when adjusted for imperfect ATM Perception and Acceptable Controller Spacing buffers, a certain portion of the time (as shown by the shaded region) a conflict would be perceived by ATM requiring intervention. The assumed ATM interruption for this false alert would accrue a fuel cost penalty. Alternatively, a probability (unshaded region) exists that ATM would perceive no conflict and correctly avert a false interruption (at no cost or controller workload). An overall weighted cost of the incident would be calculated from the Probability of Conflict and the resolution costs of the alternate resolution actions (e.g. false/no alert). Under improved ATM perception, the Figure 3 curve would tighten around the correct PCA. As a result, ATM would perceive the aircraft to be in conflict less frequently limiting ATM intervention and its associated fuel penalties.

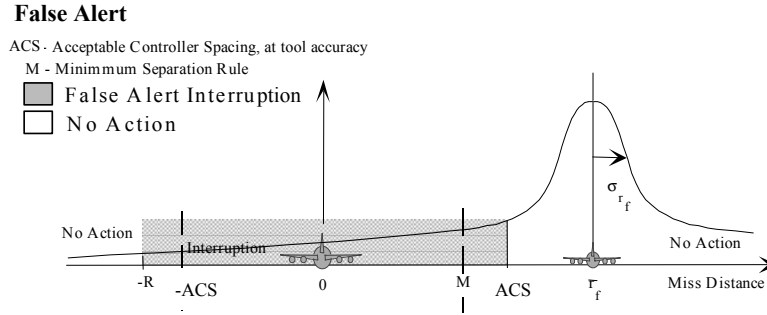


**Figure 3 Separation Assurance False Alert Probability**

**ATM Interruptions Costs & Benefits** – The number and cost of ATM Metering Conformance and Separation Assurance interruptions is tallied. This includes the delay maneuvers employed for metering conformance and additional clearances for separation assurance, as perceived by ATM. Fuel and time costs of resolving all ATM perceived conflicts from the 24-hour incident database are tabulated. By comparing the costs of ATM interruptions of two systems, expected daily fuel cost savings are identified. These daily benefits are annualized and extrapolated to the NAS by applying simulated interruption rates to the annual operations at likely deployment sites.

### 3. Airspace Simulation

---

The airspace simulation model component defines a set of scheduled en route arrival, departure and overflight trajectories for a typical day in the target en route airspace. These trajectories define the traffic scenario used to evaluate both metering conformance and separation assurance ATM interruptions.

#### 3.1 Airspace

The airspace simulated in this investigation consists of the en route ARTCC airspace near the Dallas-Fort Worth International Airport (DFW). Flight trajectories were analyzed between an outer perimeter, 250 nm from DFW, to arrival/departure metering fixes at the Center/TRACON boundary, estimated at 40 nm from DFW. This sample airspace is represented relative to the US ARTCC boundaries in Figure 4.

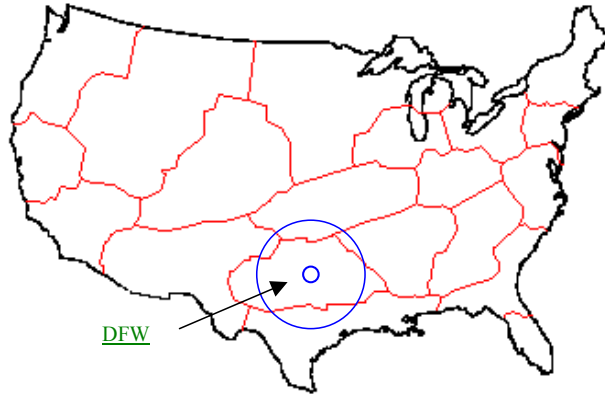


**Figure 4 Location of the Study Airspace Relative to U.S. ARTCC Boundaries**

The study en route airspace consisted of altitudes at or above 10,000 ft, the nominal metering fix altitude. Both DFW arrival and departure operations, as well as overflight operations within the DFW en route airspace were analyzed. Overflights contain both high-altitude through flights as well as arrival and departures to and from numerous DFW satellite airports within the studied airspace. Figure 5 illustrates this sample airspace [14].

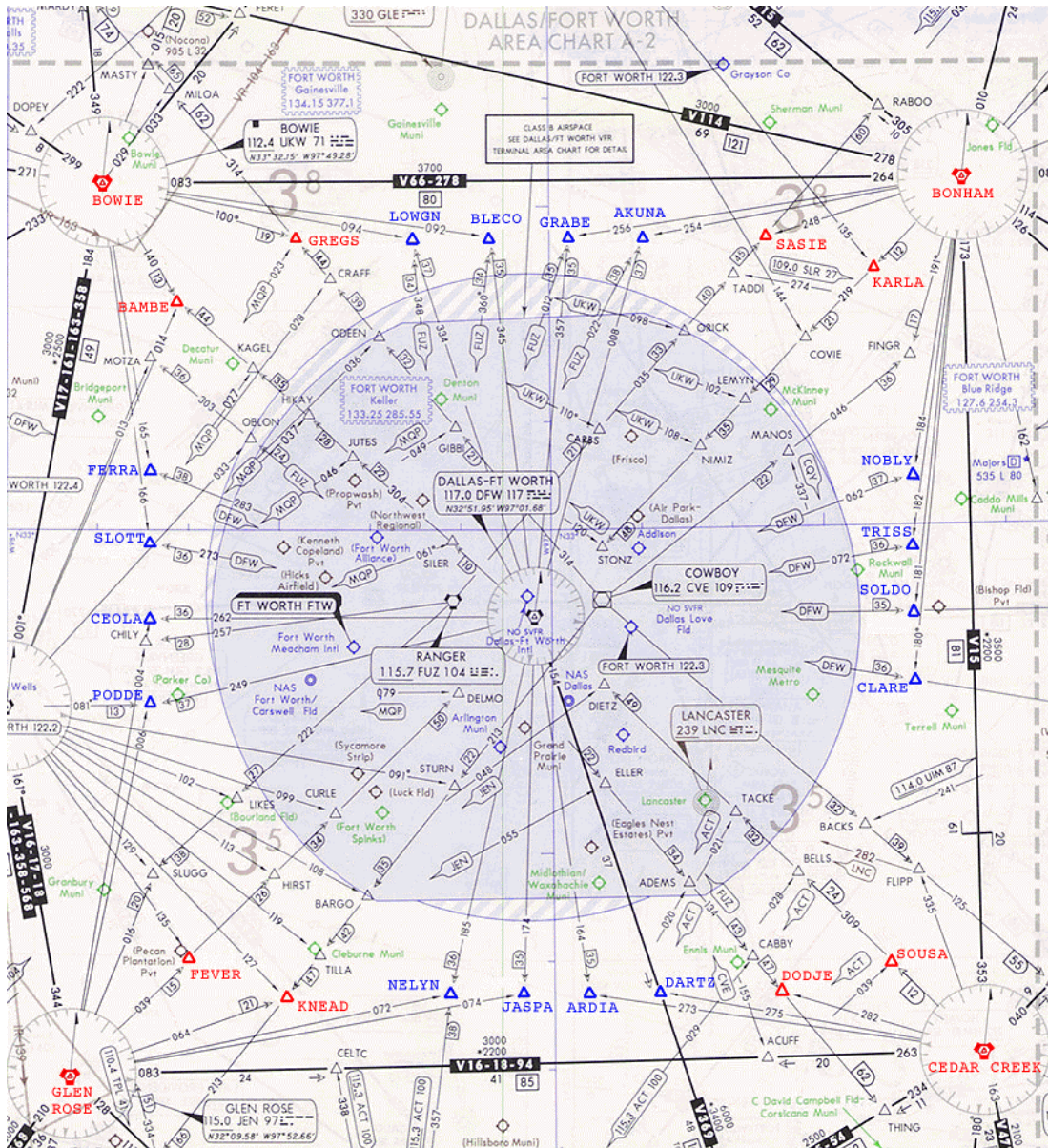


**Figure 5 IFR En Route Chart with DFW Arrival (red) & Departure (blue) Fixes**

Letters of agreement between Center and TRACON facilities often mandate that aircraft enter or exit a TRACON through predetermined gates, or arrival/departure fixes. Such agreements are made in order to better control and separate traffic entering the TRACON. Depending on the volume of traffic entering the TRACON, these fix restrictions may be in effect all or part of the day. Figure 5 illustrates arrival and departure fixes at the DFW TRACON boundary. Flight publications and charts identify the standard instrument departures (SID) and standard terminal arrival (STAR) routes.

### 3.2 Trajectories

Traffic demand data describing four-dimensional (4D) flight trajectories for a selected clear-weather day in 1996 were provided by NASA [16]. The daily traffic sample was derived from Enhanced Traffic Management System (ETMS) flight plan data and FAA radar track data for active flights in the entire domestic US airspace. The traffic sample for Friday, June 14, 1996, a relatively busy clear-weather day, was selected for use in this study. These data were adjusted to construct trajectories that represent user-preferred (filed route and preferred vertical profile) DFW en route flights over a typical day. The sample includes commercial, general aviation, and military flights, and accounts for both domestic and international flights with origins or destinations in the US. The traffic data for each flight defines a 4D trajectory. The data specifies:

- Unique flight identification,
- Aircraft equipment type,
- Origin and destination airports,
- Route of flight (waypoints),
- Waypoint altitude profile, and
- Waypoint crossing times.

Figure 6 describes the hourly operations at DFW for the study day. Sample arrival and departure operations are illustrated in plan view in Figure 7. A profile view of all operations is provided in Figure 8. Note that only flights above 10,000 ft are part of the study despite their presence, for reference, in Figure 8.

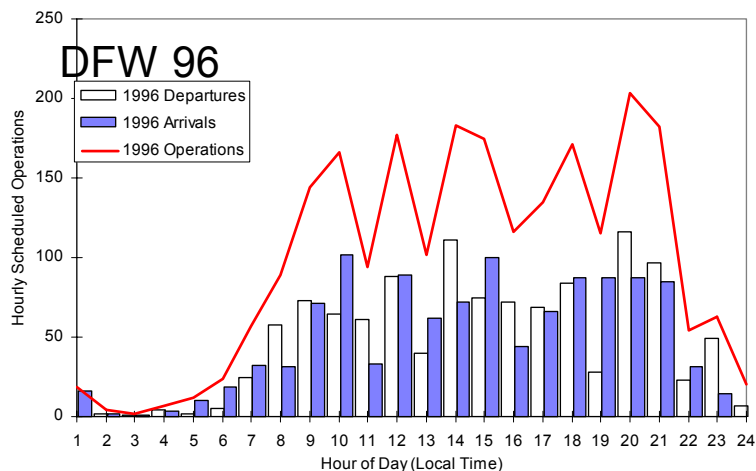


**Figure 6 Study Day Hourly DFW Arrival and Departure Operations**

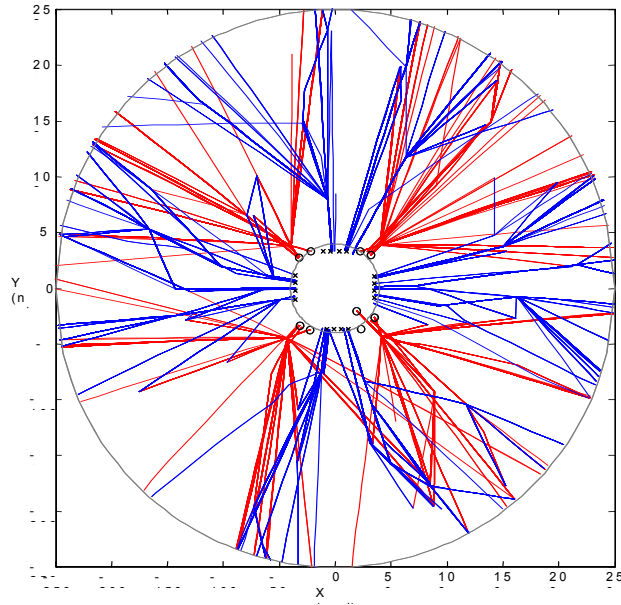


**Figure 7 Plan View of DFW Study Day STAR (red) and SID (blue) Operations**

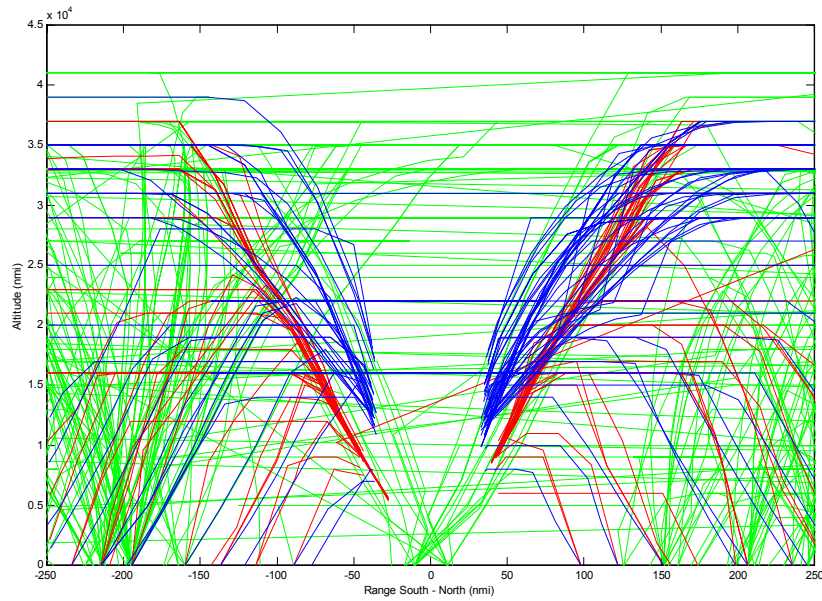


**Figure 8 Profile View of DFW Study Day Arrival (red), Departure (blue), and Overflight (green) Operations**

### **3.2.1 Arrival and Departure Operations**

All of the arrival profiles simulated in this investigation were assumed to follow a typical descent from cruise to metering fix altitude, based on their aircraft class. DFW arrival aircraft typically cross metering fixes at an altitude of 10,000 ft and airspeed of 250 kt. In order to meet these metering fix restrictions, aircraft must begin their descent early enough to reach the prescribed bottom-of-descent altitude before crossing the metering fix. Similarly, the departure profiles simulated in this investigation were assumed to follow a nominal aircraft departure trajectory representative of a typical climb from departure metering fix to cruise altitude at DFW. Baseline FFP1 operations assumed adherence to current published SID/STAR routings. EDA was assumed to enable arrival direct routes. In order to isolate EDA benefits from routing benefits, an EDA SID/STAR case was also modeled. Details of the SID/STAR and arrival direct routing are discussed below.

#### **SID/STAR Routing**

Letters of agreement between Center and TRACON facilities often mandate that aircraft enter or exit a TRACON through predetermined gates, or arrival/departure metering fixes. Such agreements are made in order to better control and separate traffic entering the TRACON. Depending on the volume of traffic, these fix restrictions may be in effect all or part of the day.

Standard departure and arrival routes, commonly known as Standard Instrument Departure (SID) routes and Standard Terminal Arrival Routes (STAR), are published procedures to aid in the coordination and routing of air traffic between Center and TRACON airspace. SIDs and STARS are characterized by information including specific waypoints, headings, runways, speeds, and other parameters. These procedures simplify clearance delivery procedures, separate arrival and departure corridors, and avoid areas of high-density traffic. SID/STAR charts also allow ATM to manage a greater number of aircraft without repeating the same procedure to every pilot. The use of SID/STAR procedures requires that the pilot have the approved textual description or its graphic format (SID/STAR charts) for that particular airport, to use SID/STAR routings as directed by ATM. Each SID and STAR is uniquely defined. Figures 9 and 10 show sample DFW SID and STAR charts, respectively [17]. The nominal trajectory data set was modified to impose DFW SID and STAR routing.

Previous work [7-8] indicated that the original arrival descent trajectories were much shallower than observed at DFW. As such, the original arrival trajectories were modified in this study to reflect the observed DFW rates of descent. The details of this update are included in Appendix A.

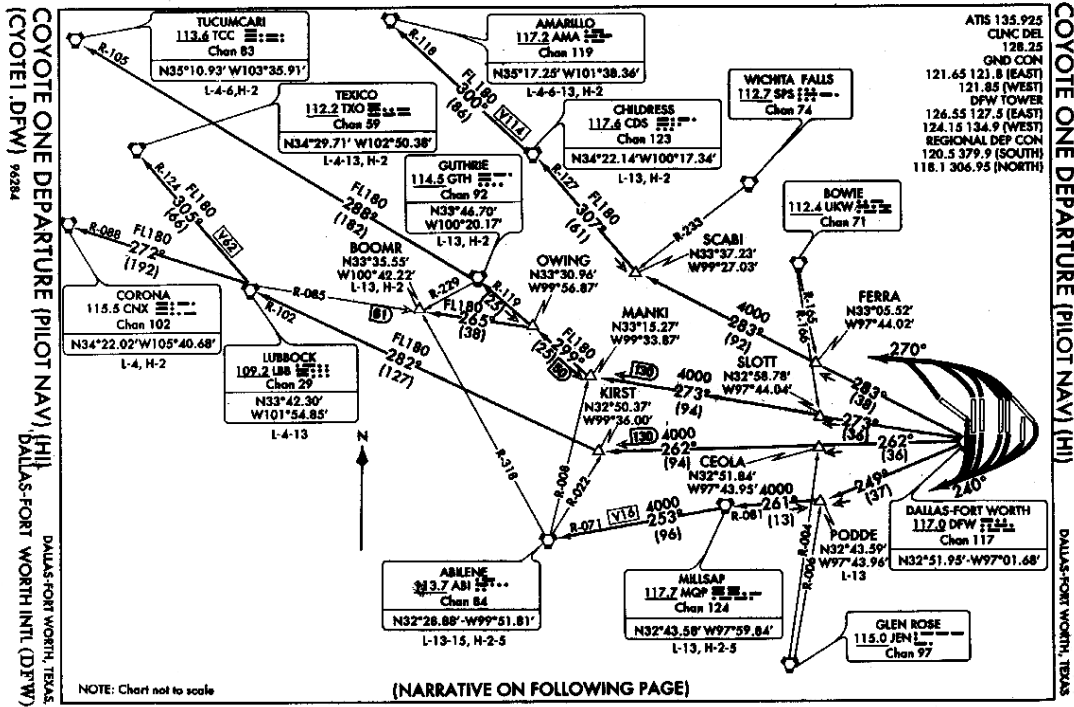


Figure 9 COYOTE ONE SID from DFW.

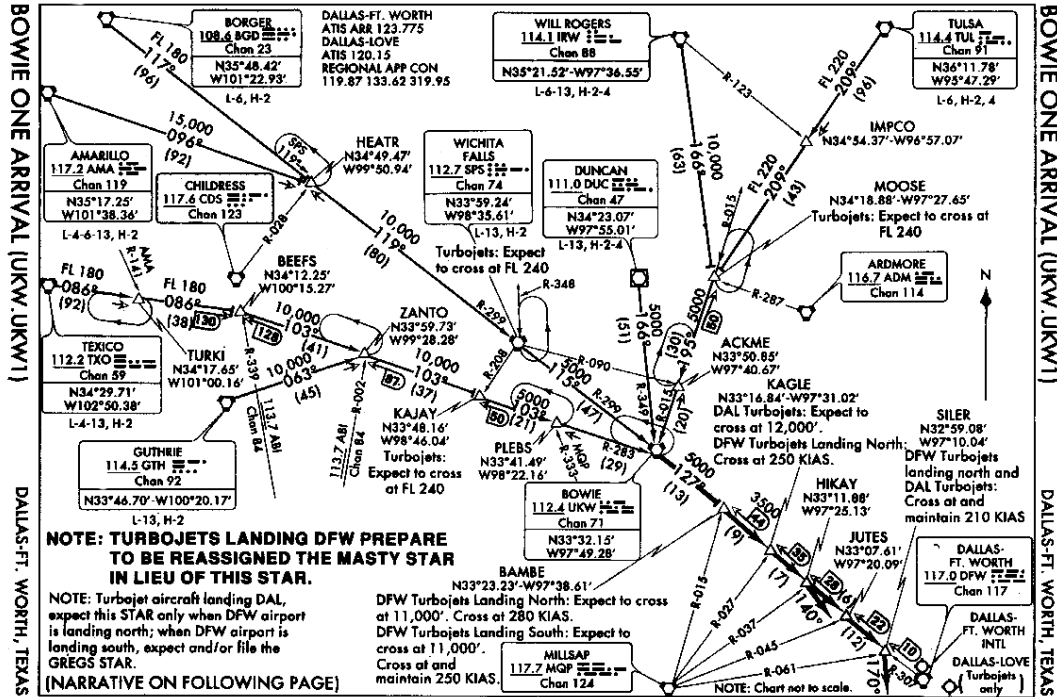
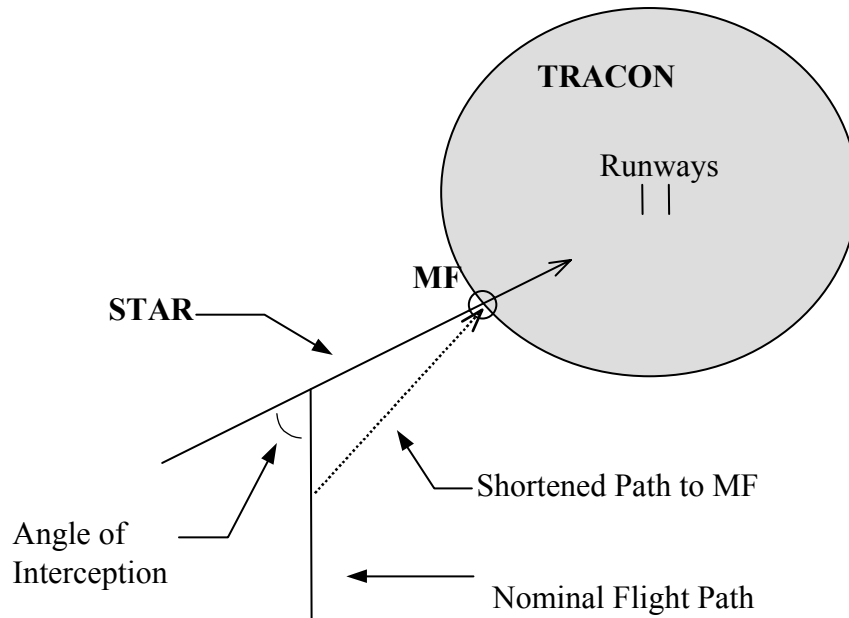


Figure 10 BOWIE ONE STAR from DFW.

### EDA Direct Routing

Arrival direct routing was assumed to be enabled by EDA. As such, arrival trajectories not already on direct routes into the TRACON were re-routed to fly a direct route to the arrival-metering fix. Direct routing allows an aircraft to improve flight efficiency by altering the horizontal-path of the aircraft trajectory. Currently, a typical terminal-area arrival path into a TRACON includes interception of a STAR route, which the aircraft follows to the metering fix. Direct routing shortens the actual path length flown. “Cutting the corner” and flying directly to the metering fix, as shown in Figure 11, can reduce the length of the path to the metering fix. In converting the STAR routes to direct routes, the arrival metering fix crossing times were held constant.



**Figure 11 Direct Routing Shortens Arrival and Departure Flight Paths**

A separate estimate of the potential benefits of arrival direct routing are documented in References [1,11] and vary with the number of segments, or “dog legs,” in the nominal STAR flight path. Figure 12 illustrates the horizontal-path differences between trajectories flying SID/STAR with those flying direct routes.

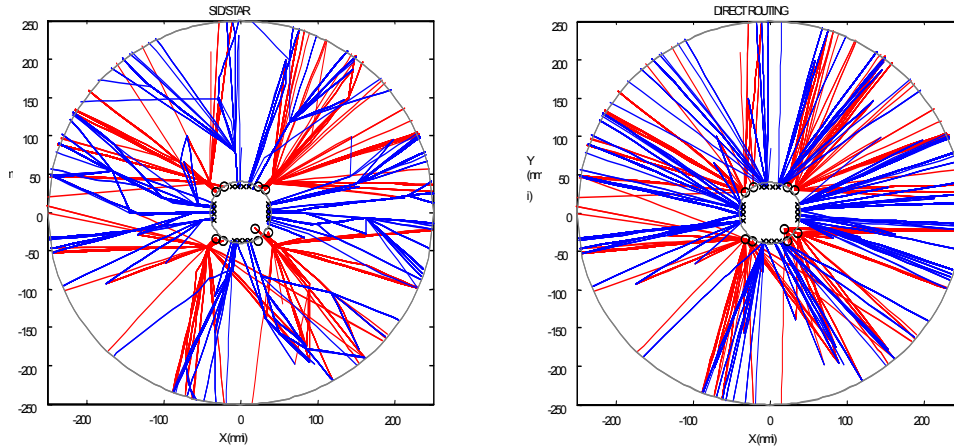


**Figure 12 DFW En Route Trajectories: SID/STAR vs. Direct Routing**

### 3.2.2 Overflight and Satellite Airport Operations

Beyond DFW arrivals and departures, 4,527 flights were identified as penetrating the en route DFW airspace on the study day. These tracks consist primarily of flights to or from DFW satellite airports (4,005 flights) and true high-altitude overflight operations (522 flights). Satellite airports were considered to be all airports within 250 nm of DFW. 199 DFW satellite airports were identified. Most of the satellite operations have little connection to DFW, other than sharing common en route airspace, although several flights do travel between DFW and the satellite airports. These overflight and satellite operations remain unchanged in all cases under study.

The top 10 DFW satellite airports are listed in Table 1 with their daily operations and location relative to DFW. The remaining 189 satellite airports each operate less than 100 operations per day, for an additional 2,048 daily operations in the DFW en route airspace. The study day operations at the top four DFW satellite airports are shown in Figure 13. All overflight/satellite airport operations and the top 10 satellite airport locations are shown, relative to DFW, in Figure 14. In both the table and figure, only operations within the defined DFW en route airspace are reflected.

**Table 1 Characteristics of Top 10 DFW Satellite Airports**

		Airport Characteristics				
<u>DFW Satellite Airport</u>		<u>Latitude (minutes)</u>	<u>Longitude (minutes)</u>	<u>Distance to DFW</u>	<u>Azimuth to DFW</u>	<u>Daily</u>
IAH	Houston Intercontinental	29.980	-95.340	196	153	1,043
HOU	William Hobby Apt	29.645	-95.279	215	155	497
DAL	Dallas Love Field Apt	32.847	-96.852	10	107	468
SAT	San Antonio Intl Apt	29.534	-98.470	215	200	432
AUS	Robert Mueller Muni Apt	30.299	-97.702	160	192	377
OKC	Will Rogers World Apt	35.393	-97.601	153	350	276
TUL	Tulsa Intl Apt	36.198	-95.888	206	16	261
SPS	Wichita Falls Muni Apt	33.985	-98.492	98	312	156
SHV	Shreveport Regional Apt	32.447	-93.826	165	99	136
LBB	Lubbock Intl Apt	33.664	-101.823	245	282	128
Top 10 DFW Satellite		NA	NA	NA	NA	3 774 (83%)
All DFW Satellite Airports		NA	NA	NA	NA	4,005

(1) Reflects only daily operations that pass through the DFW en route airspace. Touch-and-Go's treated as 2 operations.

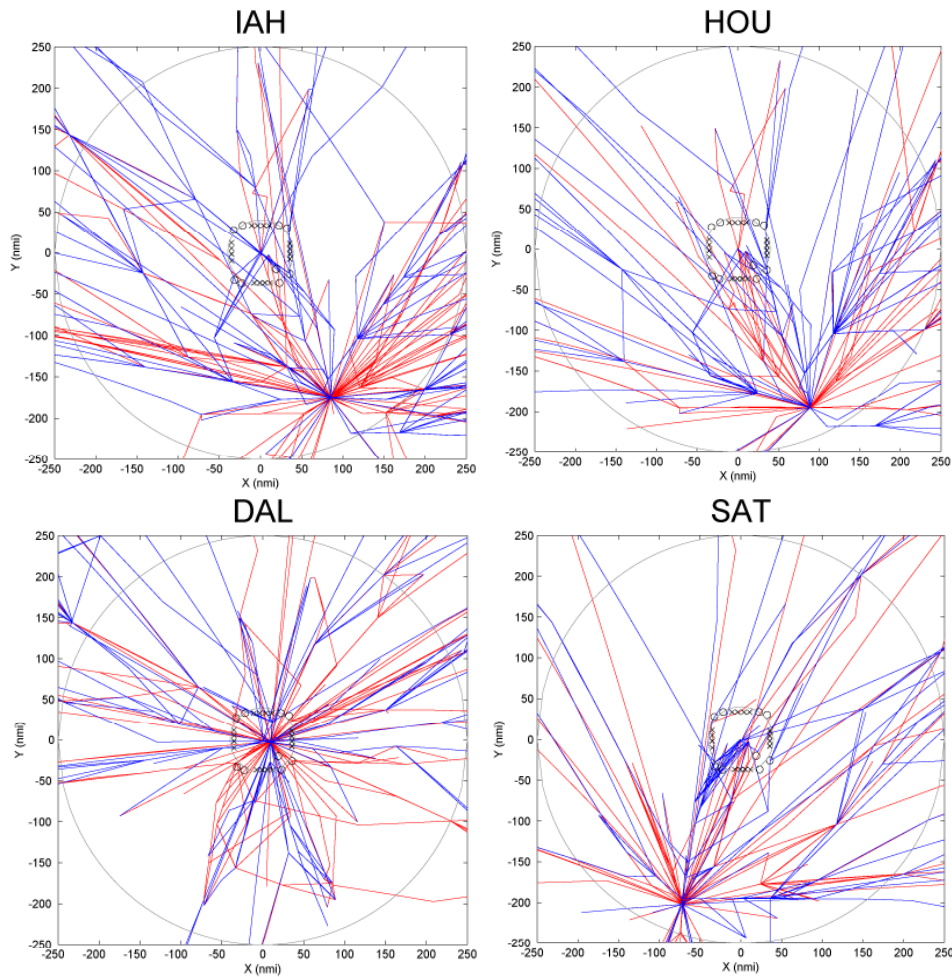


**Figure 13 Operations at Top Four DFW Satellite Airports**

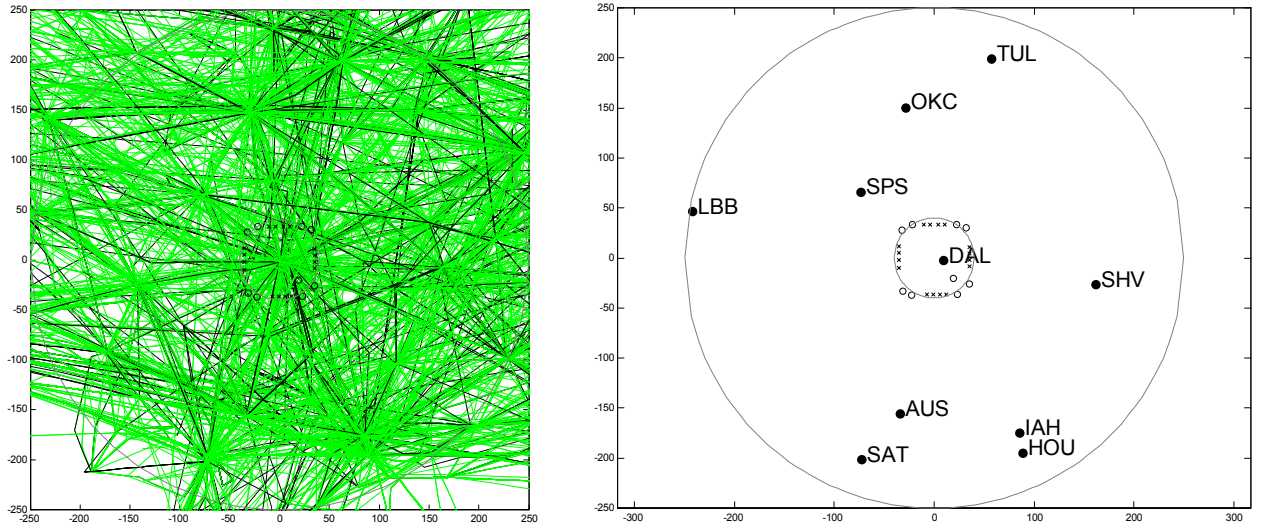


**Figure 14 Location of Overflight Operations and Top 10 DFW Satellite Airports**

## 4. Metering Conformance ATM Interruptions

---

During peak periods more arrival and departure traffic is scheduled at high-density airports than can be accommodated. As a result of airport capacity flow-rate restrictions, both arrival and departure trajectories must be metered by ATM. To reflect realistic flight trajectories for conflict DST evaluation, the simulated trajectories were modified to absorb the delays necessary to meet airport capacity constraints. The absorption of arrival and departure metering delay is essentially the resolution of intra-stream or meet-time conflicts produced by traffic intending to converge/diverge at common arrival or departure fixes. Air traffic controllers must interrupt the metered arrival and departure flights to impose delays, referred to here as metering conformance ATM interruptions. Under EDA, arrival metering conformance methods are enhanced resulting in more fuel efficient interruptions for a given metering delay. EDA has no impact on departure metering conformance.

For arrival aircraft, all cases are assumed to employ the CTAS Traffic Management Advisor (TMA) to identify the delays necessary to meet the TMA time-based metering fix crossing schedule. Departure delays are identified without DST assistance. Departure metering delays are assumed to be absorbed as ground holds, prior to take-off and the departure metering conformance delay strategy does not improved under EDA. Conversely, strategies to absorb arrival metering delays vary, each employing a combination of changes to the speed profile, cruise altitude, and routing. The specific arrival delay strategy depend on the amount of delay (constant for all cases), the time available to absorb the delay, and the case-specific ordering and attributes of the delay absorption strategy. Under TMA, controllers cognitively develop arrival delay strategies. Under EDA, EDA-generated aircraft maneuver advisories are provided to the controller that will sufficiently delay each arrival aircraft to meet the TMA schedule. No further improvement is modeled with EDX, although future analysis and model development could capture the benefits of more accurate EDA metering advisories as CTAS trajectory prediction accuracy is improved through user-CTAS data exchange.

The remainder of this chapter discusses the calculation of aircraft-specific arrival and departure metering delays; the ATM metering conformance delay strategies, which identify case-specific maneuvers to absorb this delay; the effective time horizon of these maneuvers; and the calculation of associated Metering Conformance ATM Interruptions costs.

### 4.1 Metering Delays

CTAS TMA creates an optimum time-based schedule for arrival aircraft crossing each arrival metering fix, the boundary between Center and TRACON airspace. TMA establishes aircraft-specific metering-fix STAs to control flow into the TRACON airspace. TMA STAs are distributed to each en route sector managing arrival traffic. The STAs and TMA estimates of delay to be absorbed are displayed directly on the controller's Display System Replacement (DSR) in an alphanumeric meter list. The TMA schedule is continually updated from radar returns and flight data from the ARTCC

Host computer system in response to changing events and controller inputs. Once an aircraft's metering-fix Estimated Time of Arrival (ETA) is within 19 minutes (the “freeze horizon”) the aircraft's STA is frozen. Departure delays are assumed to be identified without DST assistance.

A simplified model of TMA scheduling was developed to estimate both arrival and departure metering delays by aircraft. Arrival and departure fix STAs at the TRACON boundary and associated metering delays were determined by assuming the maximum TRACON entry and exit rates and minimum in-trail arrival/departure fix separations of Table 2.

**Table 2 DFW Scheduling Criteria**

<u>Scheduling Criteria</u>	<u>Parameter Value</u>
Arr/Dep Fix Separations	5.50 nm
TRACON Rates	
Arrival (4 arr rwys)	150 ac/hr
Departure (3 dep rwys)	115 ac/hr

The arrival/departure schedule and associated metering delays were held constant for all cases. Figure 15 shows the resulting average hourly arrival and departure delays necessary to meet the constraints of Table 2 over the course of the study day. For reference, Figure 15 also shows overall DFW (arrival and departure) throughput. Figure 16 shows the distribution of the individual arrival and departure aircraft delays required to meet the assumed DFW airport flow-rate constraints.

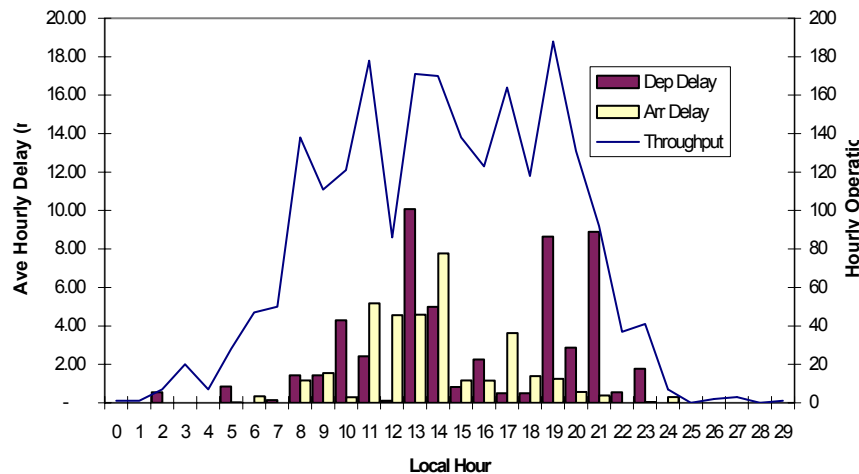


**Figure 15 Average Hourly Arrival/Departure Metering Delays**

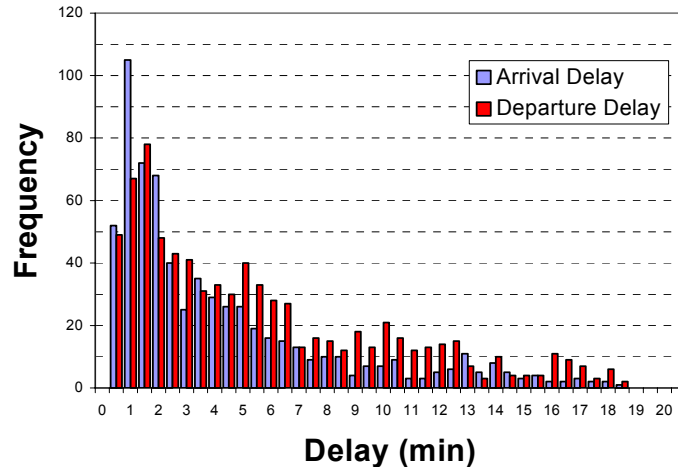


**Figure 16 Average Hourly Arrival/Departure Metering Delays**

## 4.2 Metering Conformance Delay Absorption Strategy

As aircraft are metered the incurred delay must be absorbed prior to reaching the constrained arrival and departure fixes. Under all cases, it was assumed that departure metering delays are absorbed by holding the aircraft on the ground. This effectively shifts the takeoff time of the flight but does not alter its three-dimensional trajectory.

A more complex metering conformance delay-absorption algorithm was developed to alter arrival trajectories to absorb TMA-calculated delays prior to the arrival metering fix under baseline and EDA cases. Arrival aircraft metering delays were absorbed en route, using a mix of airborne delay absorption methods including changes in speed, cruise altitude, and routing. Although the same approach was used for all cases, the cases differ in both their ordering of the various delay absorption methods as well as the assumed time horizon.

### 4.2.1 Overview of Modeled Delay Methods

The delay absorption strategies employed in the metering conformance ATM interruptions analysis are discussed individually below. While arrivals employ a combination of these methods which varies by case, departures were assumed to only employ the timeshift method, essentially a pre-departure ground-hold at DFW. These delay methods are an extreme simplification of the complexity of actual operations, which are restricted, especially in the baseline case, by such issues as sector airspace boundaries, rush/non-rush conditions, in-trail separation constraints, and controller workload.

- Speed Control** - Aircraft are delayed by reducing their cruise and descent CAS along the initial routing and altitude profile. Chosen speeds are limited by aircraft performance-based minimum speeds and subject to ATM controller rounding/increment limitations. For this study, the descent speed is set to essentially “balance” cruise and descent CAS speeds, keeping sequential aircraft at similar speeds. The higher of cruise/descent CAS is initially decremented until both speeds are equal.

Then each speed is alternately decremented until sufficient delay is absorbed or the aircraft hits its minimum speed. This represents the CTAS C=D strategy employed in previous research [18-20]. Although actual controller techniques may not be so precise, this approach conservatively represents controller actions. Reduction in speed profile results in an earlier TOD location. EDA minimum speeds are assumed to approach best endurance speeds with FFP1 Baseline operations at 10 kts above EDA speeds, reflecting their lack of automation to assist in identifying appropriate speeds. EDA minimum speeds were modeled with as 10 kts (20 kts in descent) lower than aircraft-class specific Eurocontrol Base of Aircraft Data (BADA) “low” cruise speed data (see Appendix B) [21].<sup>2</sup>

- **Altitude Change** - Aircraft are directed to descend and maintain a new cruise altitude (until final top of descent) down to the floor of the high-altitude sector airspace (flight level (FL) 230/240). Ground speed is reduced by descending in altitude while holding constant CAS. Prior to EDA, cognitive processes are assumed to limit the controller’s ability to assess the impact of intermediate altitudes.<sup>3</sup> Thus only a drop to the minimum altitude is allowed in the FFP1 Baseline. EDA, with its trajectory prediction capabilities, was assumed to allow intermediate altitudes. Beginning with the initial cruise altitude, available Federal Aviation Regulation (FAR) altitudes were tried, until all delay was absorbed or the minimum altitude (bottom of the sector) was reached. EDA allowed FAR altitudes, based on FAA separation requirements and hemispherical rule guidelines [22], are shown below by Flight Level (FL):<sup>4</sup>

Eastbound: FL230, FL250, FL270, FL290, FL330, FL370, FL410, and FL450

Westbound: FL240, FL260, FL280, FL310, FL350, FL390, and FL430

Additionally, with future EDA technology, speed is also allowed to change at the new altitude, providing an optimal combined speed/altitude approach, difficult to assess without high-fidelity aircraft-specific DST modeling capabilities.

- **Vectoring** - Simple, symmetric out-and-back vectors were performed at constant speed and altitude to increase path length at cruise altitude and speed, up to a maximum heading change. The vectoring angle was chosen to absorb the required delay starting at the DST time horizon and concluding with a symmetric heading change to meet the TOD. An error is imposed on the timing of the final return vector to reflect ATM clearance limitations that may lead to arrival fix STA deviations, as shown in Figure 17. A turn back error is modeled as a random sample from a

---

<sup>2</sup> For example a typical B-737 aircraft at nominal weight has a best endurance cruise speed of approximately 210-220 kts CAS. The BADA B-737 “low” cruise speed value is 250 kts. Thus TMA B-737 minimum speeds were assumed to be 250/250 kts CAS in cruise/descent, with EDA at 240/230 kts.

<sup>3</sup> This is a simplification of actual DFW TMA-based metering conformance operations [55], where the bottom of En Route Sector floor is FL240 for all arrival aircraft, regardless of heading, and aircraft are primarily dropped to either FL290 or FL240, based on the magnitude of delay.

<sup>4</sup> Actual controller altitude procedures are more complex. ZFW controllers using TMA indicate primarily dropping aircraft to two altitudes regardless of direction, FL290 or FL240 (bottom of the sector), based on level of delay. Additionally controllers use more elaborate step-downs schemes to assist when merging streams are vectoring toward each other [55].

distribution, with bounds reflecting ATM/DST accuracy. Although actual controller vectoring may be far more elaborate (e.g. s-turns), this approach captures the first order vectoring impact.

- **Time Shift** – Any remaining delay that could not be sufficiently absorbed using the above methods was adjusted using the time shift method. This method was employed for all departure delays, essentially giving them a pre-departure ground hold. For arrivals, this was assumed to represent additional vectoring at cruise altitude/speed, essentially shifting ARTCC entry times to absorb any remaining delay. Controllers typically employ holding patterns for vectoring delays in excess of 8 minutes [23]. Although not modeled geometrically, the time-shift method adequately models the economic affects of such vectoring.

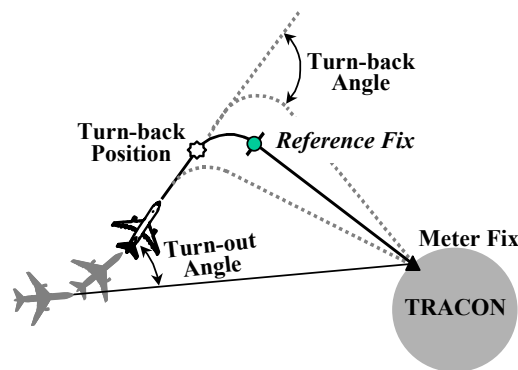


**Figure 17 Modeled Vectoring Method**

#### 4.2.2 Arrival Metering Conformance Strategies

As discussed in the previous section, arrival metering conformance was modeled as a combination of four possible methods that altered the trajectory of each arrival flight such that the proper amount of metering delay was absorbed. The four delay methods are graphically illustrated in Figure 18. In the figure, the arrival begins its metering conformance maneuver at the starting point (SP), a technology-specific duration before the metering fix crossing time. The metering conformance maneuver can include (i) a change in cruise altitude ( $H_0$  to  $H_1$ ) with a corresponding change in True Airspeed, (ii) an addition adjustment in cruise speed ( $V_{C0}$  to  $V_{C1}$ ), and/or (iii) vectoring on the cruise segment prior to TOD. The timeshift method was approximated as additional vectoring at final cruise altitude for cost purposes, but shifted the flight entry time (R250). Note that changes in speed and altitude alter the TOD location. TOD shifts due to speed changes were accounted for in the cost model, but not incorporated into the delayed 4D arrival trajectories. Likewise the cost of errors in implementing the vectoring method were addressed in the cost model, but not in the updated trajectories. These limitations result in simplistic vectoring and altitude profiles in the 4D trajectories.

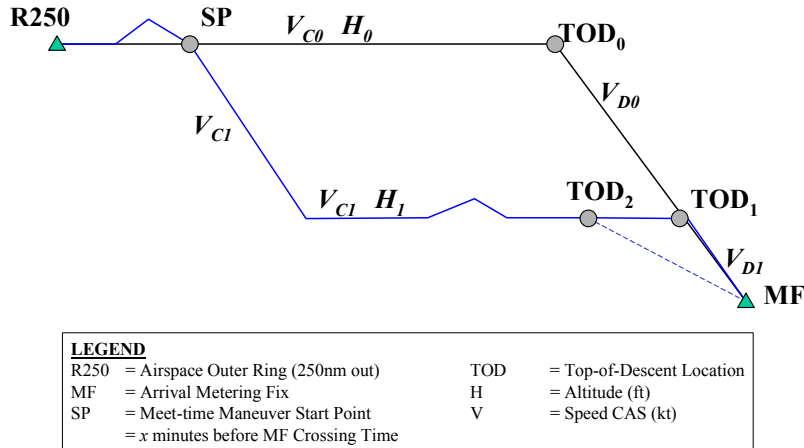


**Figure 18 Metering Conformance ATM Interruption**

The different Metering Conformance strategies and parameters assumed for FFP1 Baseline and EDA cases, are shown in Table 3. As modeled, each case assumes a strategy ordering where the maximum amount of delay is absorbed by each method before moving onto the following method within the strategy.

**Table 3 Assumed Metering Conformance Strategy Parameters**

	FFP1	CTAS EDA
General		
Strategy Order	Altitude Speed Vectoring Time Shift	Speed Altitude/Speed Vectoring Time Shift
Time Horizon	16 min	18 min
Speed		
Speed Increments	10 kt	5 kt
Speed Error	+ 10 kt	None
Min Cruise Speed	BADA(1)	BADA(1) – 10 kts
Min Descent Speed	BADA (1)	BADA(1) – 20 kts
Altitude (Jets only)		
Permitted Altitudes	Min Altitude	FAR Altitudes
Min Altitude	FL230/FL240	FL230/FL240
Vectoring		
Heading Increment	1°	1°
Max Vector Angle	60°	60°
Turn back Error	± 60 seconds	± 30 seconds

(2) Reflecting a lack of automation to help controllers identify efficient speeds, the minimum cruise/descent speeds for FFP1 used Eurocontrol BADA model [37] “low” cruise speeds included in Appendix B (e.g. 250 kts for jets). EDA minimum speeds were modeled as 10 kts (20 kts in descent) lower than BADA, a conservative estimate closer to best endurance speed.

### FFP1 Baseline

The FFP1 Baseline delay strategy reflects current ZFW Center metering conformance methods, based on discussions with NASA ATM experts familiar with ZFW en route airspace [23]. In this cognitively developed strategy, controllers are assumed to first employ altitude control by descending aircraft to the floor of the high-altitude sector airspace. Additional delay is absorbed using speed reductions, based on controller experience, down to a minimum speed applicable to most aircraft types. Without additional information/automation, controllers are unable to routinely identify acceptable lower speeds for clearance. A speed error is added to the optimal case to represent cognitive limitations in developing the metering conformance clearance without automation assistance. Finally, vectoring is implemented to absorb any residual delay. The magnitude of the vectoring turn back error [24] reflects controller cognitive limitations in identifying the optimal vector turn back location/time.

### CTAS EDA

EDA delay strategies [3], employ high-fidelity trajectory modeling to predict future aircraft positions and generate metering conformance maneuver advisories. The maneuver advisories assist controllers in quickly formulating and executing a traffic delay strategy. With a longer time horizon, speed control can be implemented more effectively, and because of its fuel efficiency, is attempted first. EDA automation provides controllers with more efficient speeds that are closer to the aircraft's best endurance speed than manually possible. If speed control alone is not sufficient, a combination of altitude/speed adjustments are used instead. Here, EDA advises an optimal speed/altitude combination, difficult to calculate without EDA data and computational assistance. Vectoring, the least precise and least efficient strategy is reserved for large delays. EDA vectoring advisories are designed to bring the flight within speed-control range using precise "turn-back" advisories to reduce uncertainty [24].

#### **4.2.3 Arrival Time Horizon**

The effectiveness of the various delay strategies is dependant upon the time available for their application. This time begins when the metering conformance clearance is executed by the pilot, calculated as the TMA freeze horizon, less any lag time in acting upon the displayed TMA delay advisory. Although the TMA freeze horizon of 19 minutes (undelayed time to metering fix crossing) is the same for all cases, the controller/pilot response time to develop and begin execution of the advisory is expected to improve with the automated EDA advisories.

In the FFP1 Baseline system, the aircraft metering conformance clearance is cognitively developed by the controller. Thus, a time horizon of 16 minutes is assumed, allowing a 3-minute lag after the TMA delay advisory is displayed to the controller.

The EDA maneuver advisories assist controllers in formulating and executing a traffic delay strategy to meet the TMA schedule, allowing the controller to more quickly identify a metering conformance strategy. As such, a longer 18-minute time horizon is assumed, a one-minute lag from when the TMA delay advisories are displayed.

In addition to variable initiation times, most strategies are modeled to be completed before the top of descent (TOD). As a result, the portion of time spent in descent (post-TOD) is an important indicator of the potential effectiveness of the various delay absorption strategies. A histogram of descent times (TOD to MF crossing) is shown in Figure 19.<sup>5</sup> Note that the greatest frequency of descent times occurs at approximately 10 minutes, leaving almost half of the total 16-18 minute time horizon for pre-TOD delay absorption maneuvers.

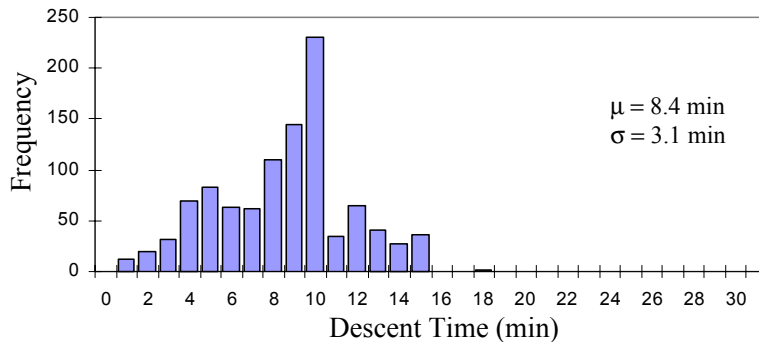


**Figure 19 Histogram of Descent Durations**

### 4.3 Metering Conformance ATM Interruptions Cost Model

Metering conformance ATM interruptions, which delay metering fix arrivals to meet airport capacity constraints, result in both time and fuel penalties. Time costs were calculated directly from the arrival metering delay combined with FAA-based airborne cost rates included in Appendix B. Time costs include both crew and maintenance components and vary by aircraft class.

Departure fuel costs were calculated by applying ground hold fuelburn rates to the metering delay time. Appendix B lists the ground hold fuelburn rates (lbs/min) by aircraft class. A conservative fuel cost of \$0.10 per pound was assumed.

Arrival fuel costs were primarily calculated using Equation (1). Additional cost components were added to account for changing TOD location and turn back error corrections, not implemented geometrically in the delayed trajectories.

$$Arrival\ FuelCost = Fuelburn\ Rate \times Distance_{Cruise} / Speed_{Cruise} \tag{1}$$

Equation (1) essentially applies a fuelburn rate to the cruise flight time. This flight time is calculated as the distance flown during the case-specific time horizon. Arrival fuel rates were calculated based on cruise speed and altitude assuming an average aircraft weight per type. Time shift delays were evaluated as additional vectoring time at the vectoring cruise altitude and speed. Arrival fuelburn rates used in the cost model are included in

---

<sup>5</sup> Descents have been updated since the previous studies [7-8] to reflect steeper profiles observed at DFW, as discussed in Appendix A.

Appendix B. The fuelburn rates were based on high-fidelity simulations [25] of a B737 aircraft under various conditions normalized to determine the fuelburn rates (lbs/min) at each altitude and airspeed. Thus delay strategies causing reductions in speed or altitude employed different fuelburn rates. Vectoring or time shift methods increased fuel costs by increasing the time or distance spent at constant speed/altitude with its associated fuelburn rate. The B737 simulation results were extrapolated to all aircraft classes by applying a scale factor, derived from FAA-based airborne fuel cost rate data found in Appendix A [27-28]. As with departures, a conservative fuel cost of \$0.10 per pound was assumed. This approach assumes no fuel impact with speed changes on the descent segment, a simplification of the assumed idle descent conditions.

Additionally, the fuel impact of the vectoring turn back error was also added to the delayed arrival trajectory fuel cost. Vectoring turn back error impacted fuel costs as increased vectoring distance pre-TOD (late turn), or post-TOD on descent (early turn). Additional vectoring on descent was assumed at the descent speed and MF altitude using the B737-based fuelburn rates just discussed. A fuel and time penalty was imposed when vectoring turn back error caused the flight to arrive late to the metering fix. The impact of such arrival fix delivery error on inefficient metering fix throughput was not addressed.

Finally, the above speed change fuelburn estimate (jets only) was adjusted to account for the fuel impact of a modified TOD location under the new descent speed. The fuel impact of the new TOD location leads to additional or reduction of fuel consumption depending upon the extended (faster) or shortened (slower) cruise segment. The TOD location, relative to nominal, was calculated using Equation (2) for both the original (undelayed) and metered flight, with the difference representing the shift in TOD location due to metering conformance speed changes.

$$TOD\ Shift = 0.00001 \times (Altitude_{Cruise} - Altitude_{MF}) \times (Speed_{Descent} - 280) \quad (2)$$

where:  $Altitude_i$  = Arrival cruise and metering fix (MF) altitudes (ft)  
 $Speed_{Descent}$  = Descent speed (kt)

Equation (2) assumes a typical jet descent rate of 3 nm per 1000 vertical ft, at a nominal 280 kts CAS descent speed. The descent rate was assumed to shift by 0.1 nm per 1000 ft, for every 10 kt deviation from the nominal descent speed. The fuelburn impact of this TOD location was calculated by applying the B737-based cruise fuelburn rates, to the cruise distance shift in TOD location. The speed fuelburn estimates were adjusted accordingly.

This cost method was used to calculate the total fuel expended for each simulated metered arrival and departure trajectory under the FFP1 Baseline and EDA strategies. Metering Conformance ATM Interruption benefits (arrivals only) were calculated as the difference between the total metering conformance maneuver costs (time and fuel) under the two cases under study. This reflected the Metering Conformance ATM Interruption benefits in the study airspace over a single day.



## 5. Separation Assurance ATM Interruptions

---

In addition to metering conformance ATM interruptions discussed above, separation assurance interruptions are the second type of ATM flight interruptions under study. These interruptions are made by controllers to avoid crossing traffic and ensure minimum aircraft separation.

The modeling of Separation Assurance ATM interruptions benefits, begins with the detection of potential conflicts from the simulated airspace trajectories, collected in a conflict-incident database. These incidents reflect actual or near-conflicts based on the metered trajectories, as defined by the FFP1 and EDA metering conformance strategies discussed in the previous section. The incident database reflects the true attributes of the conflict, without intervention. This information is then filtered through technology-specific ATM perception to identify whether ATM would perceive the incident as a conflict requiring interruption. This perception model reflects the level of conflict probe technology in terms of trajectory prediction accuracy, separation criteria, and time horizon. A conflict resolution algorithm is used to identify representative ATM interruption heading maneuvers to avoid the perceived ATM conflicts and provide estimates of the associated resolution fuel costs. These model components are discussed in the remainder of this chapter.

### 5.1 Incident Database

After defining metered trajectories (arrival, departure and overflights) within the ZFW target ARTCC airspace for each case, an incident database was developed that identified all conflicts/near-conflicts that occurred in each set of trajectories. This is the “truth” set, identifying the true attributes of the potential conflict incident that are later filtered through ATM perception. To locate these incidents a conflict detection algorithm developed in previous research [29], was employed which used inputs of trajectory data and Protected Airspace Zone (PAZ) bounds. In creating the incident database, a PAZ larger than the minimum FAA separation requirement was assumed to allow a margin of safety imposed by controllers as well as to facilitate analysis of false alerts. In addition to locating potential incidents, the incident database identified incident attributes, most important of these being the minimum horizontal distance, or miss distance between the conflicting aircraft pair. These incidents are later combined with perception, which indicate whether the potential incident is perceived as a conflict requiring ATM intervention. With improved perception, fewer incidents from the incident database will be perceived as requiring intervention.

#### Identifying Conflict Pairs

The primary function in developing the Incident Database is to locate all unique two-aircraft conflicts/potential conflicts from the trajectory databases. This was accomplished using a conflict detection stepping algorithm developed by the State University of New York (SUNY) in previous research [29]. This code uses inputs of trajectory data (piecewise-linear trajectories with 3D waypoints and time) and minimum

vertical and horizontal bounds, defining a Protected Airspace Zone (PAZ). As shown in Figure 20, the PAZ is assumed to be larger than the minimum separation requirement, to allow a margin of safety. A “conflict” is identified if an aircraft enters the PAZ of another aircraft. This is done in a geometric hashing approach which discretizes (tiles) the airspace into boxes equal in size to the chosen PAZ dimensions. Additionally, time is partitioned into discrete time steps. The conflict thus steps through the grid checking for aircraft in conflict within the same or adjacent boxes, in each time step. The code returns all aircraft pairs that violate the PAZ criteria.

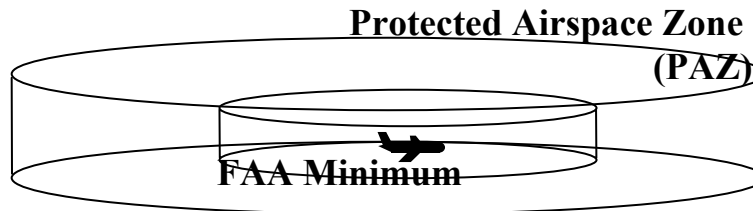


**Figure 20 Protected Airspace Zone (PAZ) exceeds the FAA Minimum Separation**

The outer PAZ limits used in the conflict detection code are:

- 12 nm horizontally, and
- up to 3,000/2,000 ft vertically, depending on the aircraft flight mode (climb, cruise, descent) and whether the aircraft are  $>FL290/\leq FL290$ .

These values were chosen to be larger than the FAA required separation minima [22] to allow for excess spacing buffers imposed by controllers for safety as well as the potential for false alerts.

#### **Incident Database Attributes**

Once conflicts/near-conflicts have been identified from each trajectory set, additional information about the conflict or the involved aircraft is identified and stored with each incident. This information includes attributes of the specific conflicting flights as well as the time, location, and attributes of the point of closest approach (PCA). The attributes stored in the Incident Database are listed below:

- Aircraft ID – for both aircraft
- Operations Type – DFW arrival, DFW departure, or overflight for both aircraft
- Flight Mode – climb, cruise, descent for both aircraft
- Arr/Dep Fix – name of arrival/departure fix if DFW arrival/departure for both aircraft
- Metered Flight Flag– flag indicating whether each flight was subject to metering conformance interruptions
- Time of PCA – Time of the conflict’s PCA
- Location of PCA– (x,y,z) location of the conflict’s PCA
- PCA Miss Distance – Horizontal separation at the conflict’s PCA
- PCA Miss Altitude –Altitude separation at the conflict’s PCA

The PCA is defined as the closest horizontal distance between the aircraft that violates the minimum PAZ altitude. A PCA was calculated in each timestep of the stepping

algorithm that the PAZ was violated. The smallest horizontal miss distance that violated the vertical PAZ bounds was chosen as the PCA. The flight mode and operations type is used to categorize the conflict. The arrival/departure fix information is used to identify if the aircraft pair is heading toward the same fix, while the metering flag is used to indicate metered arrival flights, for which trajectory prediction accuracy improves under EDA operations.

## 5.2 ATM Perception

ATM is assumed to intervene and alter conflicting trajectories that are perceived by the operating conflict probe tool to violate Acceptable Controller Spacing (or the controller's PAZ). With improved perception, fewer incidents will be perceived as requiring intervention. ATM perception is characterized by four metrics:

- Trajectory Prediction Accuracy
- Acceptable Controller Spacing (ACS)
- Perceived Miss Distance
- Probability of Perceived Conflict

These perception parameters vary both by technology case and phase of flight. Initially, ATM conflict probe trajectory prediction accuracy is calculated, based on current system position and velocity errors and uncertainties that occur in trajectory prediction and grow over the conflict prediction time horizon. These values are then used to derive the remaining perception parameters. Acceptable Controller Spacing (ACS) represents the vertical and horizontal limits at which a controller will typically intervene to resolve a conflict. Perceived Miss Distance is the level of accuracy with which the conflict probe can accurately predict the severity of the potential incident, i.e., how close two aircraft will get. Finally, the Probability of Perceived Conflict combines the Acceptable Controller Spacing with the Perceived Miss Distance in a stochastic manner to determine the likelihood that the controller would perceive the incident as a conflict, requiring intervention. The determination of these perception parameters for each case is discussed in the remainder of this section and Appendices C and D. When perception parameters vary between aircraft in the conflicting aircraft pair, the more limiting value is chosen for both.

### 5.2.1 Trajectory Prediction Accuracy

Good conflict prediction requires accurate trajectory prediction. Some inaccuracy is inherent in ATM automation trajectory predictions as a result of errors in the automation's aircraft dynamic models, aero-propulsive and weight models, navigation and radar surveillance data, flight intent data, and weather models. The proposed cases will serve to reduce these errors. For example, when FFP1 is updated with EDA [7] [30] or when EDA is enhanced through user-CTAS data exchange (EDX), ATM trajectory prediction models or model inputs improve, which leads to improved ATM conflict probe performance.

Trajectory prediction accuracy is defined as a position accuracy at a specific time horizon. As the prediction time horizon is reduced, errors in the projected trajectory position become smaller because less time is available for speed, weather, and actuation

errors to propagate. This relationship is shown conceptually in Figure 21, as curves of constant technology are shown to have increased trajectory prediction error with time horizon. With improvements in technology, overall prediction accuracy may improve, resulting in a new curve, better at all time horizons than the original curve. The points identified on the curves of Figure 21 represent a chosen time horizon/predicted position error combination for each technology. Assuming the black dot on the FFP1 Baseline technology represents current conflict probe operations, improved EDA technology accuracies would suggest use of a time horizon somewhere between the white dots on the EDA curve. The white dots assume adherence to either the FFP1 position accuracy or FFP1 time horizon. A similar situation occurs with each new technology curve.

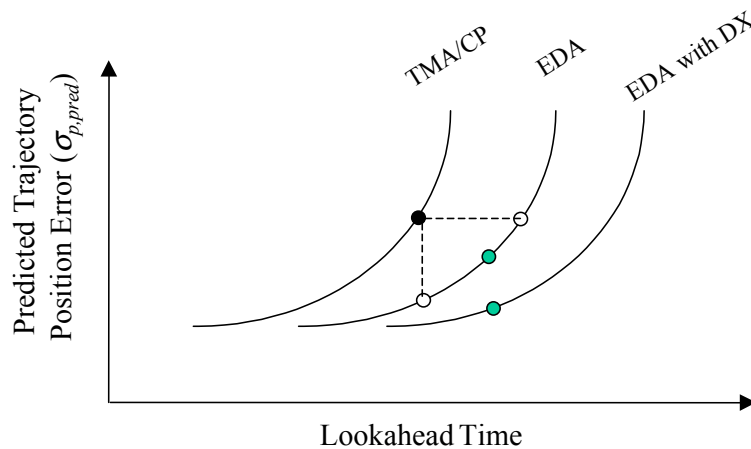


**Figure 21 Trajectory Prediction Accuracy Initial Position Accuracy & Time Horizon Relationship**

This report assumes a particular time horizon/predicted trajectory position error combination to represent the conflict probe technology of each case. The values of trajectory uncertainty are then used to derive other ATM perception attributes including the acceptable controller spacing, perceived miss distance and probability of conflict.

### Trajectory Prediction Accuracy

Trajectory Prediction Accuracy is defined as the accuracy of a flight trajectory predicted at a specific future location or set time horizon. This can be specified either in terms of (a) position uncertainty at a fixed future time point; or (b) timing uncertainty as to when the aircraft crosses a future range or altitude point. The Separation Assurance ATM Interruptions benefits analysis incorporates 12-minute trajectory prediction accuracy of all flight modes (arrival, departure, over-flight), representing ATM conflict probe accuracy. The assumption is that the conflict probe is looking ahead to where the aircraft will be 12 minutes into the future.

### Calculating Timing Error at the End of Climb/Descent Flight Segments

We begin by defining the quantitative expression for the timing error ( $\sigma_{t,M}$ ) for climb and descent flight segments. That is the uncertainty in timing of the trajectory crossing a

certain point at the end of a climb or descent phase of flight. The variance of the climb/descent maneuver timing error was modeled using the following equation:<sup>6</sup>

$$\sigma_{t,M} = \sqrt{\sum_{\forall i} A_i^2 \sigma_i^2} \quad (3)$$

Where:  $\sigma_{t,M}$  = Total time delay error uncertainty (e.g., metering fix crossing time error)  
 $A_i$  = Sensitivity of timing error to the error in parameter  $i$  (e.g., surveillance error)  
 $\sigma_i$  = Set of 10 parameters defining the progress, or characteristics, of a trajectory that are subject to error

Each  $A_i$  coefficient can be interpreted as the sensitivity of parameter  $i$  to the overall maneuver timing error. When combined with the assumed contributing parameter error values ( $\sigma_i$ ), the maneuver timing can be calculated. The  $A_i$  coefficients can be estimated using field and simulated data in Equation (6) and estimating the unknown coefficients. Alternatively, sensitivities can be derived independently and combined in the Equation (6) format. Both methods are employed here.

Baseline estimates of the 10  $A_i$  coefficients for the corresponding 10 contributing error parameters are summarized in Table 4 for the climb and descent flight segments. Descent coefficients were derived in reference [33], which estimated the Equation (3) coefficients based on high-fidelity aircraft simulation results. Climb coefficients were primarily arrived at by evaluating individual parameter sensitivities using a CTAS stand-alone (trajectory synthesizer) system with field data, as discussed in reference [31]. For several parameters, climb sensitivities were unknown. In these cases (as noted in the table) the descent coefficient values were also used for climbs, as a first-cut approximation.

**Table 4 Climb and Descent Model Sensitivity Coefficients**

Flight Phase Timing Error Sensitivity Coefficients			
Parameter	Units	Climb	Descent
Initial Weight	sec/%	24.2	0.88
(Thrust – Drag)	sec/%	4.08*	1.39
TOD Placement	sec/nm	N/A	4.08
Speed. Adherence	sec/kt	11.1*	1.46
X-Track Wander	sec/nm	1.77**	1.77
Aircraft Navigation Bias	sec/deg	1.94**	1.94
Turn Dynamics	sec/sec	1.11**	1.11
Wind Forecast	sec/kt	3.7*	0.95
Temperature Forecast	sec/°C	8.7*	4.62
Surveillance	sec/kt	0.26**	0.26

\* Path distance errors at TOC converted to time error based on speed of 415 kts at TOC

\*\* Climb coefficients set equal to descent coefficients, due to lack of climb data.

Table 5 presents the contributing error parameter values required to calculate ATM trajectory prediction timing accuracy using Equation (3). The error statistics in Table 5 are presented in the form of a root-sum-square (rss) error. Appendix D provides supporting detail on the component mean and standard deviation ( $\sigma$ ) of the error used to

<sup>6</sup> This formulation assumes that the parameters have small correlation, the typical assumption if the correlation coefficients are unknown. More study would be required to determine if the correlation is truly negligible.

derive the rss for each parameter and ATM DST technology case. Here, values are presented for the FFP1 Baseline, EDA and EDX cases. Shading indicates improvement from prior case. These values draw extensively from the literature, current research, and supplemented by discussions with NASA conflict probe experts to quantitatively differentiate the various proposed technology cases by flight mode. In all cases, these error parameter values assume jet aircraft with an onboard FMS flight control (LNAV and VNAV) in the en route airspace. In general, prediction of descent flight segments is naturally stabilizing as it is a closed loop system ending at the arrival fix merge point. In contrast, climbs are naturally unstable as they diverge from the departure fix to the top of climb location.

A key Baseline limitation in predicting climb and descent timing is the lack of common ATM-aircraft knowledge of speed profile and top of climb/descent location. This leads to large errors in speed adherence and estimated TOD placement. These errors are reduced for metered descents with the EDA-calculated maneuver advisories, where the pilot is expected to be targeting the controller-cleared EDA descent advisory. The EDA improvement is reflected in the two shaded cells in Table 5.

**Table 5 Trajectory Prediction Contributing Error values (Jet with FMS)**

Error		Passive Baseline			Active Baseline											
		FFP1			EDA			EDX1 (Wx)			EDX2 (Wt,Thr/Dg)			EDX3 (Spd Intent)		
Parameter	Unit	Cl	Cr	D	Cl	Cr	D	Cl	Cr	D	Cl	Cr	D	Cl	Cr	D
Initial Weight	%	9.2	N/A	7.8	9.2	N/A	7.8	9.2	N/A	7.8	7.6	N/A	5.6	7.6	N/A	5.6
(Thrust – Drag)	%	5.9	N/A	5.9	5.9	N/A	5.9	5.9	N/A	5.9	2.1	N/A	2.1	2.1	N/A	2.1
TOD Placement	nm	N/A	N/A	20	N/A	N/A	0.25	N/A	N/A	0.25	N/A	N/A	0.25	N/A	N/A	0.25
Speed Adherence <sup>(1)</sup> ( $\sigma_{V,FTE}$ )	kt	15	15	15	15	15	4.0	15	15	4.0	15	15	4.0	4.0	15	4.0
X-Track Wander	nm	0.14	N/A	0.14	0.14	N/A	0.14	0.14	N/A	0.14	0.14	N/A	0.14	0.14	N/A	0.14
AC Navigation Bias	deg.	0.15	N/A	0.15	0.15	N/A	0.15	0.15	N/A	0.15	0.15	N/A	0.15	0.15	N/A	0.15
Turn Dynamics	Sec	2.3	N/A	2.3	2.3	N/A	2.3	2.3	N/A	2.3	2.3	N/A	2.3	2.3	N/A	2.3
Wind Forecast ( $\sigma_{V,W}$ )	kt	12.0	13.4	12.0	12.0	13.4	12.0	8.9	10.5	8.9	8.9	10.5	8.9	8.9	10.5	8.9
Temperature Forecast	°C	1.0	N/A	1.0	1.0	N/A	1.0	0.5	N/A	0.5	0.5	N/A	0.5	0.5	N/A	0.5
Surveillance-Speed ( $\sigma_{V,S}$ )	kt	13.1	12.5	13.1	13.1	12.5	13.1	13.1	12.5	13.1	13.1	12.5	13.1	13.1	12.5	13.1
Surveillance-Position	nm	N/A	0.87	N/A	N/A	0.87	N/A	N/A	0.87	N/A	N/A	0.87	N/A	N/A	0.87	N/A

(1) Includes components of mismatched CTAS-FMS speed targets and aircraft Flight technical error.

Key Error Sources/References (also see Appendix D):

**Initial Weight** – Baseline rss and EDX2 sigma error of airline fleet data.[8]

**Thrust & Drag** – Baseline rss and EDX2 sigma error only of NASA TSRV test results.[34]

**TOD Placement** – Baseline CTAS-FMS mismatch, EDA FMS typical RNAV error rss of 0.25 nm.

**Speed Adherence** – Baseline CTAS-FMS mismatch & FTE, EDA improves arrival target and EDX3 improves climb/descent target to strictly reflect FMS flight technical error [34]

**X-Track Wander** – Baseline rss [35]

**AC Navigation Error** – Baseline FMS GPS/INS Guidance system error of 0.14 degrees.

**Turn Dynamics** – Baseline FMS-guided rss error [36]

**Wind Forecast** – Baseline RUC 3-hour forecast, EDX1 improves to ITWS/TW rss error [37]

**Temperature Forecast** – Baseline RUC 3-hour forecast, EDX1 improve assumed to be nowcast rss error [38]

**Radar Surveillance** – Baseline along-track position and ground speed error of SSR [34]

The following paragraphs describe the choice of parameter accuracy values used to defining each case. Further detail is included in Appendix D.

**FFP1** – All FFP1 parameters were based on current system errors as defined in various sources. Additionally, FFP1 descent parameters were calibrated to the 90 second arrival fix delivery accuracy observed in the 1997 DFW prototype TMA field tests [39].<sup>7</sup> The lack of common ATM-aircraft knowledge of speed profile and top of climb/descent location, prior to EDA, is a key limitation of climbs and descents in this case, leading to large errors in speed adherence and TOD placement.

<sup>7</sup> Based on recent observations [55], arrival metering fix delivery accuracy is suspected to be better than the 90 sec (1-sigma) error found in earlier prototype field tests, but no quantitative data is available.

**EDA** –The EDA case assumes that the EDA-calculated maneuver advisories given to pilots by controllers, reduces the adherence and actuation of TOD placement and speed adherence descent parameters relative to the FFP1 case. In EDA, the pilot is assumed to be targeting the controller-cleared EDA-calculated descent advisory. Thus, the residual error reflects FMS flight technical error, under FMS flight control, in meeting this target. EDA advisories were assumed to improve both the cruise and descent phase of flight of metered arrivals. Unmetered arrivals, departure cruise and climb, and overflight cruise flight segments remain unimproved from FFP1 values. As with the FFP1 case, EDA descent parameters were calibrated to match observed 1992-1995 EDA prototype field test arrival metering fix delivery error of 15-20 seconds [35].

**EDX1 (EDA with Weather)** – In the prediction of aircraft flight trajectories, forecast winds and temperatures are major causes of uncertainty. This case assumes improvement in weather accuracy assuming all pilots downlink onboard wind and temperature measurements, which then refine National Oceanic and Atmospheric Administration (NOAA) Rapid Update Cycle (RUC) 3-hour weather forecasts used by CTAS. This localized Terminal Winds model is under development as part of the Integrated Terminal Weather System (ITWS/TW) [40], which will incorporate the downlinked meteorological data and provide 30-minute updates of the 3-hour RUC forecast. Only negligible improvement is expected with ITWS/TW in the high-altitude cruise phase of flight. Further improvement results as these updated forecasts are uplinked and used by the aircraft's FMS trajectory prediction models. Although the weather may differ significantly from these forecasts, the FMS and CTAS trajectory predictions, based on a common forecast, will react similarly, greatly enhancing predicted position accuracy.

**EDX2 (EDA with Weather, Weight & Thrust/ Drag Coefficients Data Exchange)** – This case assumes that EDA is provided an improved estimate of each aircraft's weight, either from the airline AOC computer system or directly from the aircraft's FMS. Additionally thrust and drag coefficients are also assumed to be downlinked. All these parameters improve upon static aircraft-specific values current used by CTAS. Cruise flight predictions are assumed to not benefit from these parameters, reflecting a low sensitivity of these errors to cruise flight predictions. The value of the improved weight estimates is derived from a previous study of actual weights of an airlines DFW flights [8]. Thrust/drag estimates are taken from a prior study using the NASA Transport Systems Research Vehicle (TSRV), a converted B737 [34].

### **EDX3 (EDA with Weather, Weight, Thrust/Drag, and Speed Intent Data Exchange)**

This case assumes the receipt of aircraft speed intent from all aircraft within the target en route airspace. Under arrival metering conditions, EDA is assumed to try to accommodate this speed preference in the EDA-calculated descent speed advisories [2, 41]. Assuming an FMS-guided aircraft and a common EDA-FMS speed target, the speed adherence errors of metered arrival aircraft are very small and the benefit of downlinking the speed intent appears to be negligible [34]. However, for non-metered arrivals as well as departures (without EDA advisories) the speed preference represents a best estimate of the pilot's speed target, and leads to significant error reduction. In calculating the EDX3 speed errors, it was assumed that the mean error component of the baseline rss speed adherence error is negated.

#### **Calculation of Position Error at the End of Climb, Cruise or Descent Flight Segments**

We next define a quantitative expression for trajectory position prediction accuracy at the ends of climb, cruise and descent phases of flight. Here it is assumed that the climb phase ends with a cruise segment, the descent phase begins with a cruise segment, and the cruise phase is at a constant altitude. In each case, a fixed time horizon is used to define the end point of the particular phase. More detail on the equation derivations can be found in Appendix C.

A convenient mathematical model for determining the along-track position error of a single aircraft at a certain time horizon into the future can be described by the following equation. This equation allows for improved prediction accuracy if key parameters are provided in a more-timely manner from more accurate sources:

$$\sigma_{P, Pred}(\tau) = \sqrt{\sigma_P^2 + \tau^2 \sigma_V^2} \quad (4)$$

Where:  $\sigma_{P, Pred}$  = Predicted trajectory position error  
 $\sigma_P, \sigma_V$  = Position and velocity error terms  
 $\tau$  = Time period of flight cruise segment subject to velocity errors

This equation assumes that trajectory prediction error results only from along-track position error, which is reasonable since we assume an FMS-equipped fleet. The first variance term in Equation (4) represents either the initial or intermediate position error contribution of the trajectory. For a climb trajectory consisting of a climb segment followed by a cruise segment, it represents the position error at the end (top) of the climb segment. For a descent trajectory consisting of cruise and descent segments, it represents the contribution to position error due to the descent segment alone (i.e., at the end of the descent segment.) Thus, this position error term is directly related to the climb or descent timing error described previously by Equation (3) for those trajectories that have climb or descent segments. That is, if we use some average trajectory ground speed  $V_M$ , then:

$$\sigma_P = \sqrt{\sigma_{t,M}^2 V_M^2} \quad (5)$$

Where:  $V_M$  = Average velocity during the climb or descent segment

In this study, an average climb or descent ground speed of 350 kts was used. This is the rough average of arrival/departure meter fix crossing speed of 280 kts and TOD/TOC speed of 415 kts.

For a cruise trajectory, the first term in Equation (4) represents the uncertainty in position of the aircraft at the beginning of that trajectory. This is simply the error in the surveillance system position measurement at that time (see Table 5).

In Equation (4),  $\sigma_v$  represents the velocity-related error contribution that accrues during the cruise segment of the trajectory with a particular time horizon. This term is expanded as:

$$\sigma_v = \sqrt{\sigma_{V,S}^2 + \sigma_{V,W}^2 + \sigma_{V,FTE}^2} \quad (6)$$

Where:  $\sigma_{V,S}$ ,  $\sigma_{V,W}$ ,  $\sigma_{V,FTE}$  = Surveillance, wind, and speed adherence error terms from Table 5.

### **Time Horizon and $\tau$ for Climb, Cruise, and Descent Trajectories**

The final attribute in calculating trajectory prediction accuracy is the conflict probe time horizon. This is important to the overall predicted position, as suggested earlier in Figure 21. Conflict probe tools typically have a time horizon of 20-minutes, with the controller alerted to potential conflicts 20 minutes prior to their first loss of separation. If the conflict probe tool provides resolution advisories, the advisory is provided at this time and is continually updated until the controller issues a clearance resolving the conflict.

Similarly, this study defines conflict probe time horizon as the time between the initiation of the resolution maneuver and the initial loss of separation. Typically, this time is quite variable and at the controller's discretion. At a minimum, some time is needed to procedurally issue the clearance and for aircraft to initiate the maneuver. If the tool supplies no conflict resolution advisory, the controller will need more time to develop or use the conflict probe tool to trial-plan several options until a satisfactory resolution is found. For most conflict situations, a trained controller can complete trial planning, with the CTAS Conflict Probe Trial Planner (CPTP) tool, in approximately 10 seconds per alternative [42]. Additionally, controllers may monitor a conflict weighting the benefit of lower resolution costs with early intervention, against the probability that the conflict will not materialize due to uncertainties, which reduce with time.

In this study, advisories are assumed to be provided to controllers at 20 minutes, with a 8-minute controller/pilot lag, resulting in a 12-minute time horizon. This lag covers the issuance (plus development under FFP1 operations), and pilot initiation of the resolution. Although a technology-specific time horizon would likely be chosen to trade-off high false/missed alerts with cost of conflict resolution, a common time horizon was chosen to represent all cases and focus on the conflict prediction accuracy benefit of EDX.

In Equation (4), for the climb trajectory, the parameter  $\tau$  is set to the portion of the trajectory that is assumed to remain in the conflict probe time horizon after the climb segment is complete. For the descent trajectory,  $\tau$  is set to the time period of the cruise segment that precedes the descent segment during the time horizon. For the cruise trajectory,  $\tau$  is set to the entire length of the trajectory time horizon.

Thus, for conflicts predicted to occur during cruise flight, only cruise trajectory prediction errors contribute. In this case, the value of  $\tau$  in Equation (4) is set at 12

minutes. For conflicts identified to occur during either climb or descent flight, the conflict probe time horizon is assumed to nominally encompass half the climb or descent segment error, with the remaining time period accruing cruise accuracy errors. A 20-minute climb (10,000 ft to the TOC) [31] and 15-minute descent (TOD to 10,000 ft) [32] were assumed. Thus, for a climb trajectory, it is assumed that 10 minutes of the trajectory is from the climb segment, and  $\tau$  is set at 2 minutes to cover the remaining cruise segment. For a descent trajectory, it is assumed that 7.5 minutes of the trajectory is from the descent segment, and  $\tau$  is set to 4.5 minutes to cover the preceding cruise segment.

This approximate trajectory model is illustrated in Figure 22 for arrivals. In Figure 22, the prediction accuracy of a conflict predicted to involve a descending aircraft (at conflict PCA), but predicted while that aircraft was in cruise would include error contributions from both descent (half of 15-minute descent duration) and cruise (remaining 4.5 minutes) flight segments. Conversely, the prediction accuracy of a conflict predicted to involve a cruising arrival flight (PCA occurs prior to descent) would include only cruise error contributions. As a result, the EDA metering conformance advisories lead to better prediction of metered arrivals during both the cruise and descent arrival flight segments. Parallel situations apply to trajectory accuracy of departure climb and cruise flight segments.

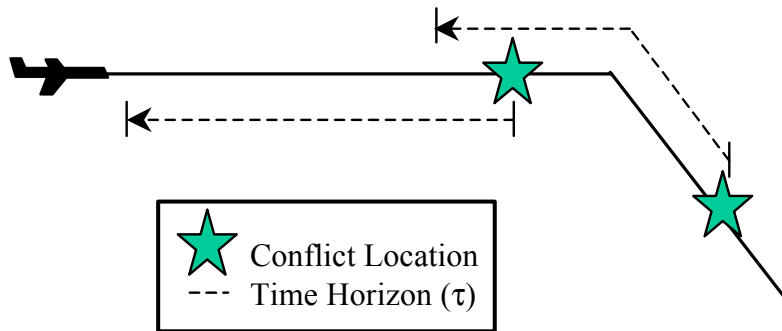


**Figure 22 Arrival Conflict Time Horizon**

**Estimated Trajectory Prediction Accuracy**

Trajectory prediction accuracies in both timing and position are estimated using Table 5 error parameter values in Equations (3) through (6), along with Table 4 climb/descent timing sensitivity coefficients and the common 12-minute time horizon value. Table 6 shows the error contributions and resulting 12-minute trajectory prediction error in climb, cruise and descent segments for arrival, overflight, and departure operations. The first row presents the timing error from Equation (3) for each case. Note that EDA is assumed to reduce the timing error at end of the arrival descent segment from 86.1 sec to 17.9 sec, with further improvement under EDX. The second and third rows represent the position and velocity terms for Equation (4). For the climb and descent segments, the position error term is derived from the corresponding timing error term using Equation (5). The last row of Table 6 shows composite predicted position error resulting from these calculations for the various flight phases. In the case of arrival-descent and departure-

climb conflicts, the 12-minute trajectory prediction error includes a combination of climb or descent segment and cruise segment errors. Note that the FFP1 Baseline descent maneuver timing error was calibrated to approximate the 90 second arrival fix delivery accuracy observed in the 1997 DFW prototype TMA field tests [30]. The EDA case was similarly calibrated to the 15-20 second error observed in the 1992-1995 EDA prototype field tests [10]. Note that shading of a cell indicates improvement from the previous case.

Essentially, EDA is assumed to improve metered arrival flight trajectory prediction accuracy and EDX cases primarily improve the non-metered arrival, departure, and overflight operations. For overflight cruise operations EDX1 weather downlink had negligible improvement at cruise altitudes, cruise flights were assumed insensitive to EDX2 weight error. EDX5 does not improve on-flight plan trajectory prediction error.

**Table 6 Assumed ATM Trajectory Prediction Accuracy**

	FFP1 Baseline					EDA					
	DEP		OVR	ARR		DEP		OVR	ARR*		
	CL	CR	CR	CR	D	CL	CR	CR	CR	D	
<b>Error Components</b>											
Maneuver $\sigma_{t,M}$	sec	283	NA	NA	NA	86.1	283	NA	NA	NA	17.9
Position $\sigma_p$	nm	13.7	0.87	0.87	0.87	4.18	13.7	0.87	0.87	0.87	0.87
Velocity $\sigma_v$	nm/m in	0.39	0.39	0.39	0.39	0.39	0.39	0.39	0.39	0.30	0.30
<b>12-minute Trajectory Prediction Accuracy</b>											
Predicted Position Error $\sigma_{p,pred}(\tau)$	nm	13.8	4.7	4.7	4.7	4.5	13.8	4.7	4.7	3.7	1.6
	<b>EDX1 (Weather)</b>					<b>EDX2 (Aircraft Weight)</b>					
	DEP		OVR	ARR*		DEP		OVR	ARR*		
	CL	CR	CR	CR	D	CL	CR	CR	CR	D	
<b>Error Components</b>											
Maneuver $\sigma_{t,M}$	sec	281	NA	NA	NA	15.6	251	NA	NA	NA	12.8
Position $\sigma_p$	nm	13.7	0.87	0.87	0.87	0.76	12.2	0.87	0.87	0.87	0.62
Velocity $\sigma_v$	nm/m in	0.36	0.39	0.38	0.29	0.27	0.36	0.39	0.38	0.29	0.27
<b>12-minute Trajectory Prediction Accuracy</b>											
Predicted Position Error $\sigma_{p,pred}(\tau)$	nm	13.7	4.7	4.6	3.6	1.4	12.2	4.7	4.6	3.6	1.4
	<b>EDX3 (Speed Intent)</b>					<b>EDX5 (Next 2 Waypoints)</b>					
	DEP		OVR	ARR*		DEP		OVR	ARR		
	CL	CR	CR	CR	D	CL	CR	CR	CR	D	
<b>Error Components</b>											
Maneuver $\sigma_{t,M}$	sec	192	NA	NA	NA	12.8	192	NA	NA	NA	12.8
Position $\sigma_p$	nm	9.4	0.87	0.87	0.87	0.62	9.4	0.87	0.87	0.87	0.62
Velocity $\sigma_v$	nm/m in	0.27	0.29	0.29	0.30	0.27	0.27	0.29	0.29	0.30	0.27
<b>12-minute Trajectory Prediction Accuracy</b>											
Predicted Position Error $\sigma_{p,pred}(\tau)$	nm	9.4	3.6	3.6	3.6	1.4	9.4	3.6	3.6	3.6	1.4

Note: Bold values are calibrated to CTAS TMA [39] and EDA [35] field test results.

\* Applies to metered arrivals only.

For future analysis, it is recommended that the assumed error parameter and position accuracy values be continually updated, as new research identifies better estimates of trajectory prediction accuracy. Such reviews could be complimented by a comprehensive sensitivity study to determine the accuracy under the expected range of operational conditions. The importance of these parameters to the model results suggests they should be periodically refined to keep abreast with ongoing research efforts.

### Acceptable Controller Spacing

Observations of air traffic operations show that actual spacing between aircraft, as implemented by air traffic controllers, are generally larger than the FAA separation requirements [22]. Controllers have been observed to intervene in trajectories that exceed and nearly double the en route legal separation value of 5 nm. This intentional buffer protects against errors in the execution of the resolution trajectory, including trajectory prediction errors. Acceptable Controller Spacing (ACS) in this report is assumed to be a function of the required minimum separation and the intentional controller excess spacing buffer. This concept is displayed in Figure 23 for the lateral dimension. As trajectory uncertainties are reduced and controllers become confident in the consistency of more accurate trajectory predictions, this buffer is assumed to shrink, in both the horizontal and vertical dimensions, while maintaining the current level of safety. Additionally, although controllers may wish to continue to be alerted of conflicts using the existing safety criteria, it is assumed that the separation assurance interruption rate will reflect the reduced ACS under improved trajectory prediction accuracy.

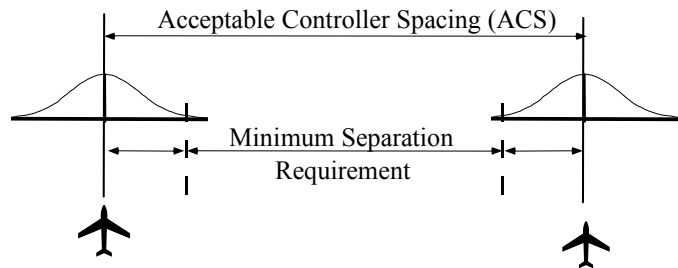


**Figure 23 Acceptable Controller Separation (ACS) Results from Predicted Position Accuracy**

To be in conflict, aircraft must violate Acceptable Controller Spacing (ACS) in either the horizontal or vertical dimensions. FAA horizontal separation minimum in en route airspace is 5 nm. FAA vertical separation minimums between aircraft of opposing headings are 2,000 ft above FL290 and 1,000 ft at or below. The hemispherical rule defines the altitudes assigned for various aircraft headings. The en route surveillance radar allows a tolerance of 200 ft above/below the cleared altitude to allow for nominal flight deviations.

The assumed FFP1 Baseline horizontal and vertical ACS values are shown in Table 7. These values concur with CTAS conflict probe field test observations in en route airspace where the conflict probe tool was typically set to alert controllers of conflicts falling below these values [44-45]. A separate en route analysis [46] indicates that controllers

without a conflict probe tool interrupted trajectories with an uninterrupted miss distance averaging 9 nm. Moreover, 50 percent and 60 percent (of the 57 studied incidents) were expected to have a minimum separation distances of 8 nm or less, respectively [42]. This threshold is an upper bound on the ACS, as controllers may not act on all the displayed incidents, but will begin to monitor the conflict thereby impacting controller workload. Finally, note that a significantly larger safety buffer is applied to vertical ACS for transitioning (climb/descent) flights, due to the larger uncertainty in predicting these flight modes.

Future study cases assume reductions in the FFP1 Baseline ACS values, as a function of predicted horizontal position accuracy. Equation (7) has been used in prior studies to relate *timing* accuracy to in-trail ACS at the *runway threshold*. [33] Equation (7) is used here to relate *position* accuracy to *en route* horizontal and vertical ACS, assuming zero-mean Gaussian accuracies.

$$ACS = n\sigma_{p.pred} + Rule \quad (7)$$

where: *Rule* = En route minimum separation requirement [22]  
 = 5 nm horizontally, 2000/1000 ft vertically >FL290/≤FL290  
 $\sigma_{p.pred}$  = Trajectory prediction position accuracy (Table 5)  
 $n$  = Minimum separation fraction  
 = (0.22, 0.67, 0.60) horizontal and (72.5, 0.0, 200.0) vertical for (climb, cruise, descent) flight segments

The minimum separation fraction values of Equation (7) are estimated based on current system ACS values [30]. That is, the assumed current system (FFP1 case) horizontal and vertical ACS values (bolded in Table 7) are combined with FFP1 trajectory prediction position accuracy values of Table 6 and FAA minimum en route separation (*Rule*) to derive the minimum separation fraction ( $n$ ). Using these minimum separation fractions (one for each flight mode in both the horizontal and vertical dimension), EDA and EDX ACS values (Table 7) are generated reflecting the Table 6 improvements in trajectory prediction accuracy.

Table 7 shows the baseline and improvement in ACS assumed with the FFP1, EDA and EDX cases. Again, bold values identify model inputs based on expert judgement and previous CTAS conflict probe operations [44]. Shaded cells indicate improvement due to EDA and data exchange when compared to the previous case. Note that vertical ACS does not improve, since it is already at the FAA minimum and EDX5 does not impact ACS.

**Table 7 Acceptable Controller Spacing**

		FFPI Baseline					EDA				
		DEP		OVR	ARR*		DEP		OVR	ARR*	
		CL	CR	CR	CR	D	CL	CR	CR	CR	D
<b>Horizontal ACS</b>											
En Route	nm	<b>8.00</b>	<b>8.00</b>	<b>8.00</b>	<b>8.00</b>	<b>8.00</b>	8.00	8.00	8.00	7.37	6.07
<b>Vertical ACS</b>											
>FL290	Ft	<b>3000</b>	<b>2000</b>	<b>2000</b>	<b>2000</b>	<b>3000</b>	3000	2000	2000	2000	2357
<=FL290	Ft	<b>2000</b>	<b>1000</b>	<b>1000</b>	<b>1000</b>	<b>2000</b>	2000	1000	1000	1000	1357
		EDX1 (Weather)					EDX2 (Aircraft Weight)				
		DEP		OVR	ARR*		DEP		OVR	ARR*	
		CL	CR	CR	C	D	CL	CR	CR	CR	D
<b>Horizontal ACS</b>											
En Route	nm	7.98	7.91	7.91	7.26	5.95	7.66	7.91	7.91	7.26	5.91
<b>Vertical ACS</b>											
>FL290	Ft	2994	2000	2000	2000	2318	2886	2000	2000	2000	2303
<=FL290	Ft	1994	1000	1000	1000	1318	1886	1000	1000	1000	1303
		EDX3 (Speed Intent)					EDX5 (Next 2 Waypoints)				
		DEP		OVR	ARR*		DEP		OVR	ARR	
		CL	CR	CR	CR*	D	CL	CR	CR	CR*	D
<b>Horizontal ACS</b>											
En Route	nm	7.04	7.26	7.26	7.26	5.91	7.04	7.26	7.26	7.26	5.91
<b>Vertical ACS</b>											
>FL290	Ft	2680	2000	2000	2000	2303	2680	2000	2000	2000	2303
<=FL290	Ft	1680	1000	1000	1000	1303	1680	1000	1000	1000	1303

Note: Bold values assumed to reflect current system operations [44].

\* Applies to metered arrivals only.

### 5.2.2 Perceived Miss Distance

A large component of ATM perception is the accuracy at which ATM perceives the extent and degree of the potential conflict. Inaccurate perception may lead to false or missed interventions because the conflict may be perceived as more or less severe than in actuality. Perceived miss distance is the metric used to define ATM perception of potential incident time, location, and geometry. The incident database, defined in Section 5.1, determines the actual incident time, location, and miss distance. We use prior research to determine the corruption of these facts, based on the inaccuracies inherent in the ATM conflict probe tool. This concept is illustrated in Figure 24 where actual aircraft tracks and miss distance ( $r_f$ ) are shown with bold (—) lines. Dashed (--) lines show inaccurately predicted flight tracks due to ATM prediction errors in heading and speed. These errors result in a range of perceived conflict miss distances which may be more or less severe than the actual miss distance.

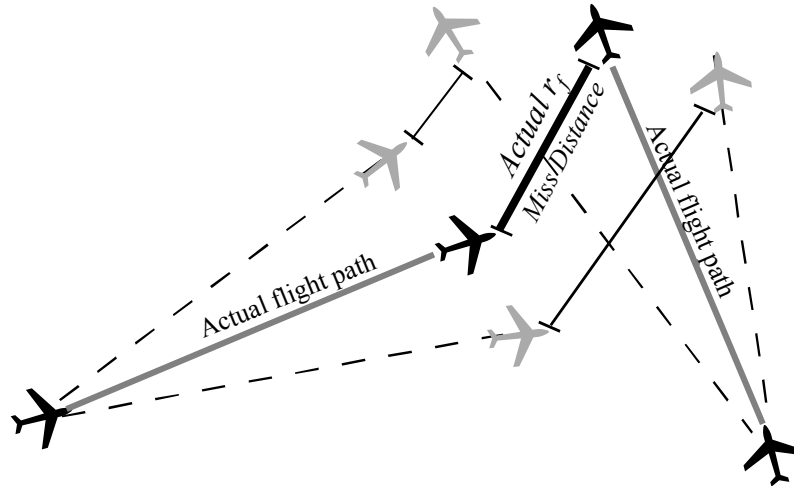


**Figure 24 Perceived Miss Distance results from Actual Miss Distance ( $r_f$ ) and Prediction Accuracy**

Equation (8) describes the variation in miss distance at point of closest approach as a function of the technology-specific trajectory prediction accuracies of the conflicting aircraft pair. The full derivation can be found in [47-48]. A two-dimensional model is used, as all potential incidents were previously filtered by vertical separation criteria (vertical ACS of Table 7):

$$\sigma_{r_f} = \sqrt{\sigma_{p,pred,acj}^2 + \sigma_{p,pred,acj}^2} \quad (8)$$

where:  $\sigma_{p,pred,acj}$  = Predicted trajectory position accuracy at point of closest approach for aircraft  $j$  (nm)

Equation (8) is applied to each incident in the Incident Database using the technology-specific trajectory prediction accuracies (Table 5) associated with the conflicting aircraft, and a time horizon of 12 minutes. The result is a Gaussian distribution of miss distance, with a mean equivalent to the actual uninterrupted Incident Database miss distance. This distribution is compared with horizontal ACS to determine the ATM's probability of perceived conflict and subsequent intervention.

### 5.2.3 Probability of Conflict

A Probability of Conflict, or probability of ATM interruption, is calculated by comparing the ACS with the conflict probe perceived attributes and actual Incident Database attributes for each incident. This probability indicates the likelihood that a controller would perceive the incident as a conflict requiring intervention. Because the Perceived Miss Distance is stochastic in nature, this comparison takes the form shown in Figure 25.

In Figure 25, the Perceived Miss Distance is shown as a Gaussian distribution with a mean value equal to the actual miss distance. The ACS bounds ( $\pm$ ACS) are overlaid onto the perceived miss distance curves. The shaded region between  $\pm$ ACS is the probability that ATM would perceive this incident as equal or less than the ACS, and intervene to

resolve the perceived conflict. The unshaded region represents the probability that no conflict was perceived nor intervention made at the strategic conflict probe time horizon. This mean value assumption implies that the aircraft is following the DST assumed flight plan route intent. Off flight plan intent is discussed later in this chapter. Figure 25 shows three examples representing the three possible outcomes for a particular incident. These include incidents where the actual miss distance ( $r_f$ ) is:

- less than the minimum separation requirement ( $\pm M$ );
- larger than  $M$  but less than the Acceptable Controller Spacing ( $\pm ACS$ ); and
- larger than ACS.

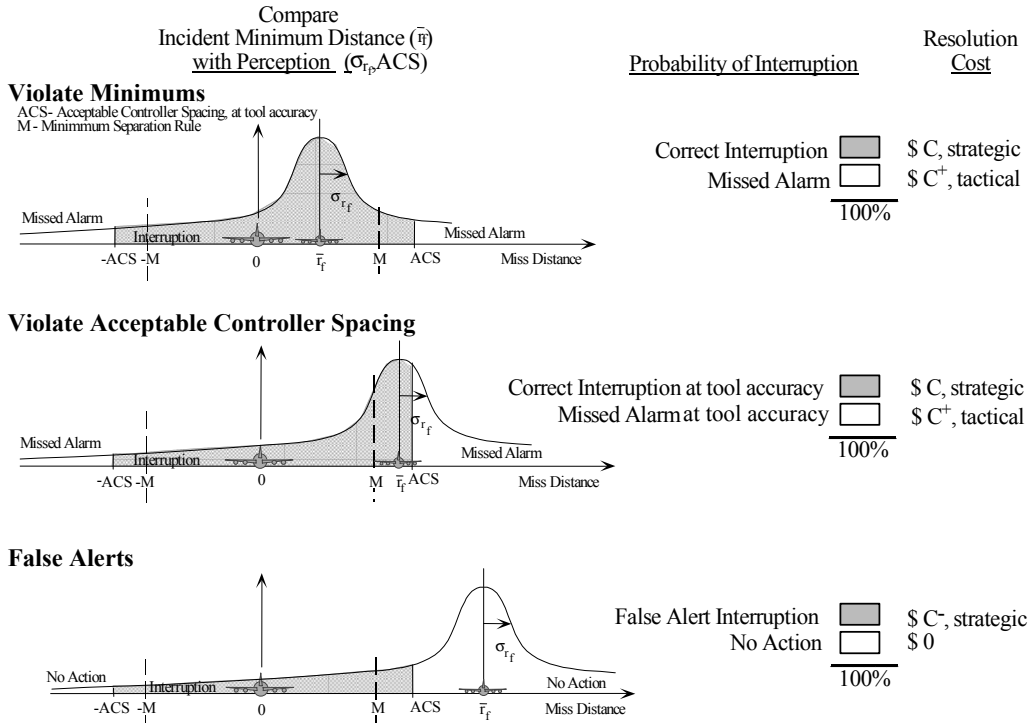


**Figure 25 Comparison of Perceived Miss Distance Curves and Acceptable Controller Spacing (ACS) results in Probability of Conflict and Resolution Costs for Each Type of Incident**

In Figure 25, intervention is the correct course of action in the top two scenarios because the actual miss distance (between aircraft symbols) is less than the ACS. In these cases, a missed alert would result if no 12-minute intervention were made. Once ATM *did* perceive these incidents, a tactical intervention would be required with a shorter time horizon and a higher cost. Conversely, intervention in the last scenario of Figure 25 would be a false alert, and would lead to an unnecessary ATM interruption and its associated costs. Improved accuracy of the conflict probe tool would lead to a tightening of the Perceived Miss Distance curve about the mean value. As a result, the shaded region would be modified, reducing the number of false and missed alerts.

The probability of perceived conflict, which determines the likelihood of ATM interruption of an incident, is equivalent to the area under the perceived miss distance

curve between  $\pm$ ACS, calculated using Equation (9), derived in previous research [47-48]:

$$P(\text{conflict}) = \frac{1}{2} \operatorname{erf}\left(\frac{R+r_f}{\sqrt{2}\sigma_{r_f}}\right) + \frac{1}{2} \operatorname{erf}\left(\frac{R-r_f}{\sqrt{2}\sigma_{r_f}}\right) \quad (9)$$

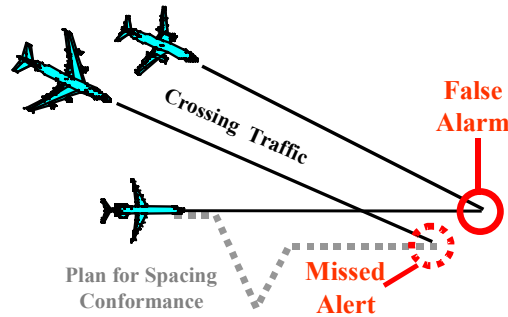
where:  $r_f$  = Actual miss distance at point of closest approach  
 $R$  = Acceptable controller spacing (ACS) (Table 7)  
 $\sigma_{r_f}$  = Miss distance error from Equation (8)  
 $\operatorname{erf}(x)$  = Integral of the standardized Gaussian distribution function from(0,  $x$ )  
 $\operatorname{erf}(x) = \frac{2}{\sqrt{\pi}} \int_0^x e^{-u^2} du$  and  $\frac{1}{2} \operatorname{erf}\left(\frac{x}{\sqrt{2}}\right)$  = Integral of the normal probability distribution function

This probability determines the likelihood of ATM interruption of this incident. When action on both the shaded and unshaded probabilities of Figure 25 are tied to resolution costs, a weighted resolution cost of each incident can be identified. The costs of the shaded/unshaded actions are noted in Figure 25. In general, correct alerts are assigned the strategic cost at the technology's expected time horizon. Missed alerts are assigned costs based on a more expensive tactical resolution maneuver at a shorter time horizon, and false alerts are assigned a small cost tied to strategically resolving a conflict that would not actually have occurred. The resolution costs are discussed in more detail in a later section.

#### Impact of Off Flight Plan/Bad Intent

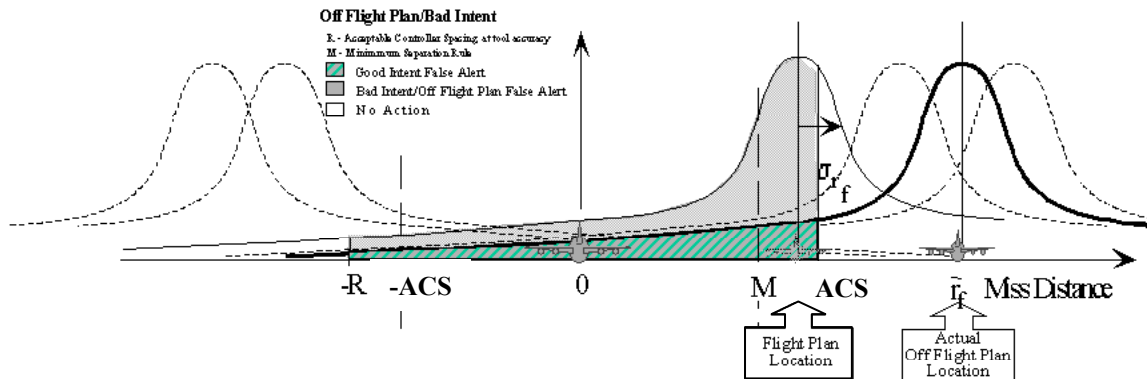
In the current system, flights are frequently diverted off the filed flight plan for a variety of reasons including metering conformance, conflict avoidance, and accommodation of requests for direct routes. If these deviations are not recorded as a flight path amendment, CTAS is unaware of the changed aircraft intent. The lack of updated intent degrades conflict probe trajectory prediction, frequently resulting in a false alert for the original conflict, and/or a missed alert on the new route. Future integrated conflict probe, direct routing, and metering conformance tools (i.e., EDA) will assist controllers in recording these intent changes for use by other ATM DSTs. Alternatively, aircraft downlink of its next few waypoints (i.e., the EDX5 case) can automatically correct DST aircraft intent errors. In both cases, the improved knowledge of aircraft intent leads to conflict probe performance benefits. Thus, it is important that the modeling effort be sensitive to unrecorded off-flight plan impacts on conflict probe functions.

Figure 26 illustrates a situation where an eastbound aircraft's filed flight plan route supposedly conflicts with a southeast flight (actually a false alarm). To avoid this, the controller vectors the eastbound aircraft for spacing conformance but fails to record this change as a flight plan amendment. As a result, the initial presumed conflict is avoided (false alert), but is replaced by a new undetected conflict (missed alert) with a second southeast flight.



**Figure 26 Off-flight Plan Effect on ATM Perception**

The analysis accounted for inaccurate intent information as part of ATM perception. If an aircraft is off its filed flight plan, the inaccurate intent data changes the ATM perception attributes of Figure 25 slightly, as shown in Figure 27. The key change is the shift of the second aircraft’s actual location, reflecting a gap between the perceived (flight plan) and actual (off-flight plan) miss distance. Thus, the perceived miss distance curve is still centered about the flight plan intent, which no longer matches the actual intent of the aircraft. Per the scenario of Figure 27, inaccurate intent results in a significantly higher probability (larger area below miss distance error curve between  $\pm ACS$ ) for the indicated false alert than would occur with good intent information.



**Figure 27 Off-Flight-Plan Probability of Conflict Estimation**

The actual unrecorded off-flight plan location of the second aircraft would depend on the direction and magnitude of the off-flight plan route change, as shown by the various dashed curves in Figure 27. However, the specific undocumented route given by the controller is unknown, and the scope of this effort precludes us from identifying likely routings from the flight geometry. Thus, for this study it is assumed that a controller would clear the aircraft to a route that would avoid any original flight plan-based conflict, while not creating any new conflicts. This approach implies that the off-flight plan route would avoid the flight-plan-based conflict, converting the incident into a false alert.

Additionally, the off-flight plan location of the second aircraft was assumed to be outside the ACS ( $\pm ACS$ ) by a distance equal to the horizontal ACS safety buffer ( $ACS - FAA$

minimum Rule). This results in the solid off-flight plan curve of Figure 27 (regardless of the original miss distance attributes). Thus, under erroneous intent, ATM’s perceived probability of conflict would not change, implied by the area under the original flight plan-based location between the ACS bounds, but it would now represent a false alert, as the off-flight plan route avoided the conflict and thus no intervention is necessary.

Using this approach, a lack of accurate intent data will result in a higher frequency of false alerts. Probability of conflict is calculated for both accurate and inaccurate intent situations and combined based on the weighted frequency of inaccurate intent information. Good intent data leads to a mix of correct, missed, and false alert probabilities of Figure 25, while bad intent is assumed to represent false alerts, as discussed above and shown in Figure 27.

The frequency of aircraft off-flight plan intent errors is assumed to vary by case, as shown in Table 8. In the FFP1 case, full intent errors are assumed in all flight modes, reflecting the lack of integration of the metering and the conflict probe tools and no downlink of aircraft intent. The frequency of inaccurate intent was assumed to be 15 percent for all flight modes, based on discussions with conflict probe experts [44] and Indianapolis Center observations that only 18 percent of all route clearances are documented [49]. This baseline assumption essentially assumes 15 percent of all FFP1 conflicts involve an aircraft that is off-flight plan, but perceived to be on flight plan. With the integration of arrival metering/conflict probe in the EDA case, metered arrival intent errors are assumed to be removed, while non-metered arrivals, departures, and overflight intent inaccuracy remains unchanged. Under EDX5, the aircraft is assumed to automatically downlink the next two waypoints, improving intent for all flights. Thus, EDX5 is assumed to remove aircraft intent errors on all flight modes.

Overall, use of the above modeling approach to account for undocumented off-flight plan routing is felt to be a conservative simplification of real-world operations. Further investigation of likely off-flight plan routes as well as better estimates of assumed frequency of bad intent are recommended.

**Table 8 Frequency of Off-Flight-Plan Route Intent Error**

		FFP1			EDA			EDX1, EDX2, EDX3			EDX5		
	Units	CL	CR	D	CL	CR	D	CL	CR	D	CL	CR	D
Bad Intent	%	15%	15%	15%	15%	15%	0%	15%	15%	0%	0%	0%	0%
Good Intent	%	85%	85%	85%	85%	85%	100%	85%	85%	100%	100%	100%	100%

### FFP1 Perception Limitations

Additional processing was performed on the FFP1 Incident database to account for its unique ATM perception limitations. As discussed previously, the conflict probe tool assumed in the FFP1 case, has access only to the originally filed aircraft flight plans. As such, it's ATM perception is hindered, increasing the missed and false alerts that either are avoided or encountered when the flights are delayed to meet the TMA arrival metering schedule. Because the EDA conflict probe tool has access to the CTAS-developed advisories supplied to the controllers to meet the TMA schedule, these misperceptions are removed.

To reflect the degraded FFP1 Perception, Incident Databases were developed from both the original (filed flight plan) and TMA-metered trajectories. These two Incident Databases were then combined, by adjusting the probability of conflict and resolution costs, as appropriate. This adjustment is defined below for incidents that occurred in the original and/or metered Incident Database:

- **Incidents appearing in both Incident Databases** – Correctly detected conflicts, but with incorrect attributes. The original database ATM perception was used with the metered database conflict attributes and resolution costs.
- **Incidents appearing in only the Original (filed flight plan) Incident Database** – These are false alerts. The original database ATM perception is used with the original database conflict attributes and resolution costs.
- **Incidents appearing in only the Metered Incident Database** – These are missed alerts if the metered database identifies the conflict PCA as less than the ACS. Zero ATM perception for this conflict was assumed (set Probability of Conflict to 0 percent) combined with the metered database conflict attributes and resolution costs.

### 5.3 Conflict Resolution and Costs

ATM separation assurance intervention costs were identified for each incident in the Incident Database. The development of these costs used a conflict resolution algorithm sensitive to the specific aircraft involved and their flight geometry. Only heading change conflict resolutions were modeled. Additionally, three types of ATM intervention costs were identified: correct alerts, false alerts, and missed alerts. The resolution cost of each type differs in its assumed time horizon and conflict severity.

The trajectories were not changed to implement the ATM separation assurance intervention action; rather, the intervention was used to identify a representative cost penalty for the interruption. Three types of ATM separation assurance intervention costs were identified: correct, false, and missed alerts. As previously discussed, the resolution cost of each type differs in its time horizon and conflict severity. The resolution costs are expected to decline with fewer and less severe ATM interruptions, as technology improves.

### 5.3.1 Resolution Strategies

Conflict resolution advisories provided by conflict probe tools supply information to a human controller who retains full authority and responsibility for safe separation of air traffic. Controllers typically consider three fundamental methods, alone or in combination, to resolve traffic conflicts: heading, speed, and/or altitude changes. Additionally heading maneuvers can include either direct routing to the next waypoint or various out-and-back or S-turn vectoring from the nominal trajectory. These strategies are listed with their frequency of use, both with and without use of the CTAS CPTP trial planner in Table 9, based on field observations made during the CPTP tests September 1997 at the Denver ARTCC [42] and November 1998 at Ft. Worth ARTCC [50].

**Table 9 Resolution Strategies both with and without the CPTP Tool**

<u>Resolution Type</u>	ZDV97	ZDV97	ZFW98	ZFW98
	<u>Manual</u>	<u>CPTP</u>	<u>Manual</u>	<u>CPTP</u>
Vectoring	38%	27%	16%	14%
Altitude	26%	27%	54%	48%
Direct-to	11%	36%	18%	31%
Speed	0%	3%	6%	2%
Multiple	7%	3%	4%	2%
No-Action	18%	4%	4%	3%

Note: No-action refers to cases where the CPTP planning tool was employed but no aircraft clearances were issued.

In this study, only symmetric heading change resolutions that return aircraft to their original flight plans were considered. Correctly estimating the full cost of altitude maneuvers and identifying when direct-to maneuvers were more advantageous than symmetric heading maneuvers, were beyond the resources of this study.

The possible geometry of the modeled heading resolutions includes backside and frontside maneuvers. These maneuvers are performed in the horizontal plane with standard turn rates (with a maximum turn angle of 60 degrees). Speed is assumed to be fixed during the heading maneuver. The resolution algorithm identifies the heading change necessary to just clear the second aircraft's Protected Airspace Zone (PAZ). As discussed previously (Table 7), the PAZ assumes an intentional safety margin, in addition to the FAA minimum separation requirement. A heading maneuver is chosen that just averts one aircraft from piercing the other aircraft's PAZ. The recovery maneuver is symmetric to the resolution maneuver, returning both aircraft to their original flight paths. For all separation assurance interruptions, the conflict resolution increased path distance at constant speed. A sample heading change resolution strategy is shown in Figure 28 [47-48]. The figure shows the relative motion of aircraft B with respect to aircraft A during a symmetric backside heading maneuver.

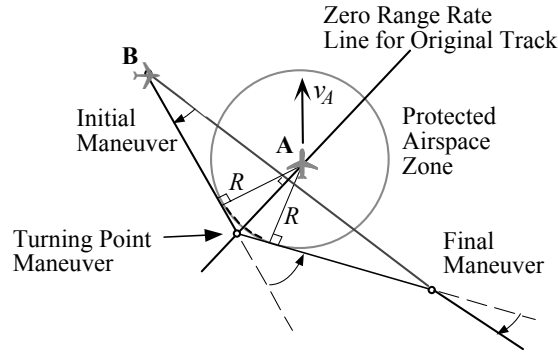


**Figure 28 Heading (Backside) Resolution Maneuver**

The algorithm evaluates both a frontside and backside resolution for each conflict pair's initial conditions. The minimum cost solution, either frontside or backside, is chosen, as shown in Figure 29.

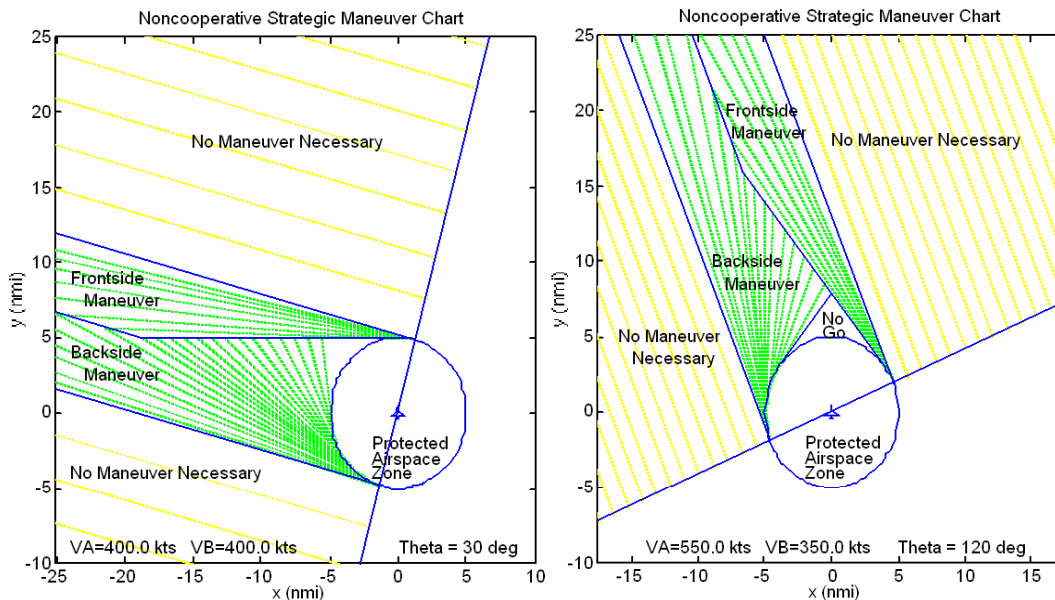


**Figure 29 Minimum Cost Resolution between Backside and Frontside Options**

In the heading resolution strategies, the cost of resolution is assumed to be shared by both aircraft of the conflicting aircraft pair. Such cooperative resolutions tend to be less costly than non-cooperative solutions where one maneuvering aircraft bears the total cost with a more extensive maneuver. However, because of differing aircraft operating costs, cooperative resolutions may neither minimize overall nor individual resolution costs. Although non-cooperative resolutions may be operationally favored because of reduced workload (only one aircraft requires intervention), many conflicts could not be resolved by interruption of only one of the conflicting aircraft. Thus, the cooperative resolution strategy was used in all cases.

Additionally, when the conflict resolution algorithm could not calculate a valid separation assurance conflict resolution cost, the average cost of that conflict type (i.e.,

pairwise operations type for Arrival-Departure conflicts), as determined from valid resolutions of that same type, was employed.

It is assumed that these resolution strategies and associated fuel penalties will provide sufficient degrees of freedom for ATM to avoid the identified conflict as well as subsequent incidents caused by its resolution. Additional costs may be incurred if neighboring traffic are impacted by the resolution maneuver. As we only tabulate a fuel penalty for the resolution, without altering the flight's actual trajectory, the impact on neighboring aircraft is unknown, and is not accounted for in this analysis. Also, we do not consider the case where a resolution maneuver is blundered, decreasing the separation between the aircraft, or other extenuating circumstances such as Special Use Airspace (SUA), turbulence, terrain, or weather avoidance.

### **Resolution Code Input Parameters**

The resolution code used in the ATM Interruptions Model requires the input of initial aircraft state information and the aircraft's PAZ dimensions. Additionally, the model assumes that the aircraft is in steady-state from its initial position through resolution recovery.

In our conflict resolution logic, three categories are considered: (i) near-term *tactical* conflicts (Missed Alerts) which cannot be avoided without immediate action; (ii) far-term *strategic* conflicts (Correct Alerts) which can be smoothly resolved so they never become near-term threats; and (iii) *falsely* perceive conflicts (false alerts), where the conflict perceived by ATM did not really exist. Although these resolutions would require the same initial aircraft state, the PAZ size and the maneuver initiation time are adjusted as appropriate.

### **PAZ Size and Time Horizon**

The PAZ dimensions used in the conflict resolution code reflect the Acceptable Controller Spacing (ACS) values of Table 7. Strategic resolutions assume the common time horizon of 12 minutes before conflict start. For missed alerts, the initiation time was reduced to 5 minutes in all cases to reflect a more tactical, and therefore more expensive maneuver. For false alerts, a conflict was forced by increasing the PAZ size to be just larger than the conflict's Point of Closest Approach (PCA) attributes. The strategic resolution of such conflicts, assumed to represent false alert fuel penalties, was always less than or equal to the correct alerts resolution cost.

### **Initial Aircraft State**

The initial state of the aircraft prior to the separation assurance conflict resolution was developed by extrapolating backwards linearly from the aircraft state at the PCA. This PCA-based pseudo-initial state was used rather than the actual state at this time because the resolution strategy required both aircraft to be in steady-state throughout the resolution maneuver. To produce the pseudo-initial state, the PCA aircraft heading, speed, and altitude change rate, were held constant while the aircraft's flight was reversed by the appropriate 12 minute time horizon before the beginning of conflict.

### 5.3.2 Resolution Costs

Once the resolution geometry was defined, a cost penalty function identified the expected resolution costs. Only the fuel cost of the resolution maneuver was considered, assuming that any time penalty could be made up at a later point in the flight

The resolution maneuver is represented by flight segment components of heading changes and steady level flight. The fuel cost of executing these flight segments in each resolution strategy is summed and compared to the cost of performing no maneuver. For all maneuvers, the resolution code produced an increase in path distance at a constant speed. Equation (10) was used to estimate the fuel cost of the resolution's increased path distance:

$$\text{Resolution Fuel Cost} = (\Delta S / V) \times FB \times C_{fuel} \quad (10)$$

where:  $\Delta S$  = Increase path distance with heading maneuver (nm)  
 $V$  = Aircraft ground speed, held constant during maneuver (kt)  
 $FB$  = Fuelburn rate by altitude and aircraft class (lb/hour)  
 $C_{fuel}$  = Fuel cost (\$0.10/lb)

In Equation (10), the change in path distance is converted to a time value, based on the aircraft speed, multiplied by a fuelburn rate (per unit time), and the cost of fuel. The fuelburn rates were based on Eurocontrol BADA [21] performance data, sensitive to altitude, flight mode (climb, cruise, and descent), and aircraft class. The fuelburn tables used in the analysis are provided in Appendix B.

## 6. ATM Interruptions Benefits

---

This chapter summarizes the number, type, resolution strategy and cost of ATM interruptions for each technology case under study. Both Metering Conformance and Separation Assurance ATM interruptions are covered. Controllers impose Metering Conformance interruptions upon arrival or departure traffic to meet airport flow-rate restrictions. In contrast, controllers make Separation Assurance interruptions to resolve conflicts between aircraft pairs of various types including arrivals, departures, and overflights (both satellite airport operations and true overflights) that operate in the studied en route airspace. Simulated daily interruptions and costs are presented and then extrapolated to annual and NAS-wide benefit estimates.

### 6.1 Simulated DFW Daily Interruptions

In general, ATM interruptions fall into three categories: correct, missed, and false alerts. Correct and missed alerts correspond to valid conflicts, based on ATM's perception, while false alerts are predicted conflicts perceived by the conflict probe tool as an incident requiring intervention, although the two aircraft are never actually in conflict.

These categories are defined further below:

- **Correct Alert (CA)** - Conflicts correctly perceived by ATM (i.e., minimum aircraft separation falls below the Acceptable Controller Spacing). As a result of the correct perception, ATM is able to resolve the impending conflict at the strategic time horizon.
- **Missed Alert (MA)** - Conflicts *not* correctly perceived by ATM. Due to conflict probe inaccuracies, the tool identified no projected conflict. However, these aircraft will eventually drop below acceptable separation, requiring ATM resolution. Thus, as a result of ATM misperception, conflict detection, and the initiation of a conflict resolution maneuver are delayed, resulting in a tactical resolution at an economic penalty. A tactical maneuver is more severe and costly than if started earlier as a strategic maneuver.
- **False Alert (FA)** - Erroneous conflicts detected by the conflict probe tool despite an acceptable miss distance. As with missed alerts, false alerts result from conflict probe trajectory prediction errors, and result in extra workload for controllers and pilots, and add additional flight costs for deviations that are unnecessary.

#### Metering Conformance ATM Interruptions

As arrival and departure aircraft are metered at the Center/TRACON boundary, they must be separated to meet TRACON flow-rate restrictions. A scheduling algorithm was used to determine the arrival/departure metering fix crossing time (STA) and the associated amount of delay required to comply with airport flow rate restrictions, common for all study cases. All metering conformance interruptions are assumed to be correct alerts

(CA). Additionally, these trajectories may also require separation assurance interruptions, as discussed later in this chapter.

Departure metering conformance interruptions were assumed to employ ground holds to absorb the necessary metering delay using the time-shift method. This timeshift method was applied to meter departure under all cases, so no benefits accrued.

Arrival metering conformance interruptions delayed aircraft with a mix of case-specific altitude, speed, and vectoring/time-shift delay strategies. The number of metering conformance interruptions and case-specific share of total delay absorbed by each method is shown in Table 10. Two delay strategy breakdowns are shown in the table. The first shows the frequency of employing each method. The second identifies the share of total delay absorbed by each method. The table does not show the EDX cases, as these cases were not assumed to improve over EDA, employing the same delay strategy, parameters, and time horizon. Additionally, despite the different trajectories in the two EDA cases (arrivals on STAR or direct routing), there was no significant difference in metering conformance results. The EDA direct and STAR arrival routes are subject to the same arrival fix crossing schedule and resulting metering delays, but differ in the time the trajectories enter the en route ARTCC. Because of the similar results, the following discussion will address them jointly as EDA results. Note that the similar results imply that direct routing does not inhibit EDA metering conformance efficiency.

**Table 10 Metering Conformance Delay Methods**

	No. Delayed Arrivals	Delay (min)		Method Frequency (%)*			Share of Total Delay (%)		
		Ave.	Total	Altitude	Speed	Vect/TS	Alt/Spd	Vector	TimeShift
FFP1									
Arrivals	662	4.0	2,682	41.2%	38.4%	84.9%	16.2%	47.2%	36.6%
Departures	796	5.35	4,256	NA	NA	100%	NA	NA	100%
EDA-STAR									
Arrivals	662	4.0	2,654	47.0%	74.0%	65.9%	31.8%	34.4%	33.8%
Departures	796	5.35	4,256	NA	NA	100%	NA	NA	100%
EDA-Direct Arrivals									
Arrivals	662	4.0	2,653	46.8%	74.0%	65.9%	31.8%	34.4%	33.8%
Departures	796	5.35	4,256	NA	NA	100%	NA	NA	100%

\* Because multiple methods were applied to each flight, these columns sum to over 100 percent

Table 10 shows the common departure metering conformance interrupts, delays and delay absorption methods applied under all cases. In contrast, despite common metering restrictions and number of interruptions, EDA absorbs the delay using more fuel-efficient speed and altitude methods. The frequency breakdown and Figure 30 clearly show that EDA replaces the Baseline’s use of vectoring with less intrusive and more cost-effective speed control and altitude arrival delay methods. Additionally, because of the lower aircraft-specific speeds afforded by EDA-automation, more delay can be absorbed in nominal vectoring methods, before employing the alternate time-shift method, a vectoring surrogate.

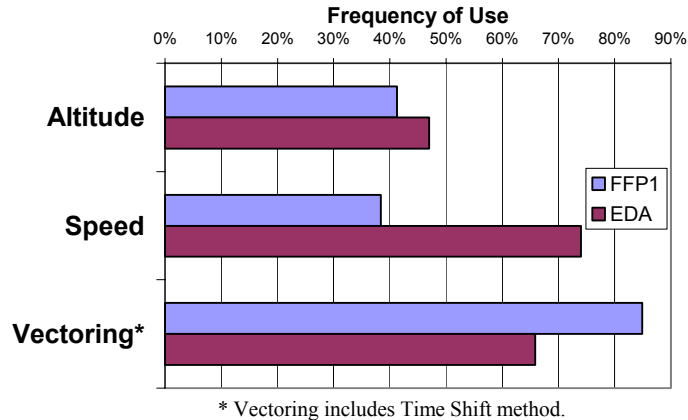


**Figure 30 Comparison of Employed Metered Arrival Delay Strategy**

As previously shown in Table 10 and Figure 16 (Chapter 4), the metered flights were delayed typically 3-5 minutes, with an average of 4.0 minutes for arrivals and 5.4 minutes for departures. The range of arrival delay absorbed with each method is shown in Table 11. The table compares the varying effectiveness of the delay absorption methods employed in both the Baseline and EDA cases. Additionally, these values compare favorably with the expected range of delay absorption, based on observations of controller practices [35].

**Table 11 Metered Arrival Delay Comparison**

	NASA Estimate	Delay (minutes)								
		FFP1			EDA – STAR**			EDA – Direct Arrivals**		
		Range	Ave	Total	Range	Ave	Total	Range	Ave	Total
Altitude	1-4	0-2.5	0.2	160	0-10.2	1.3	845	0-10.2	1.3	845
Speed	1-3	0-4.6	0.4	275						
Vectoring*	8+	0-18.1	3.4	2,247	2.8-17.9	2.7	1,808	2.8-17.9	2.7	1,808

\* Vectoring includes Time Shift method.

\*\* CTAS EDA cases combine speed and altitude methods.

Table 12 compares the resulting arrival metering conformance fuel cost tied to the FFP1 Baseline and EDA cases. The table points out the fuel efficiency of speed delays, where delays absorbed with speed control can actually reduce the overall flight cost (i.e., note negative values in Table 12). Additionally, EDA with direct arrival routes (i.e., those marked “Direct Arrivals”) was found to have slightly lower altitude/speed interruption costs than those that followed the STAR routes, resulting in overall lower delay fuel costs under the direct case. This implies that direct routing does not inhibit EDA metering conformance efficiency. Overall, EDA saved approximately \$4000 worth of fuel (at \$0.10 per lb) in the daily simulation. These benefits reflect a more efficient delay strategy, which are separate from the benefits of direct routing (e.g., time/path savings), calculated in other studies [2,11].

**Table 12 Simulated Metered Arrival Fuelburn Comparison**

	FFP1			EDA-STAR			EDA-Direct Arrivals		
	Fuel (lbs)								
	Range	Ave	Total	Range	Ave	Total	Range	Ave	Total
Altitude/Speed	(168)-579	14	9,502	(533)-590	17	11,494	(753)-483	13	8,645
Vectoring*	0-2,659	244	161,422	0-2,440	182	120,205	0-2440	183	120,866
Total	(133)-2,793	258	170,924	(533)-2,773	199	131,700	(533)-1,870	196	129,511
Total Fuel Cost (\$) **									
Total	\$(13)-279	\$25.82	\$17,092	\$(53)-277	\$19.89	\$13,170	\$(53)-187	\$19.56	\$12,951

\* Vectoring includes Time Shift method.  
 \*\* Assumes \$0.10 per lb of fuel.

As both cases used the same traffic scenario and flow-rate constraints, each flight was subject to the same time delays in the Baseline FFP1 and EDA cases. As a result, EDA savings primarily reflect improved fuel efficiency in absorbing the common metering delay. However, a vectoring turn back error was applied which, in some cases, increased the flight time to the arrival fix. Less error was applied in the EDA case, based on prototype EDA observations [24]. This increased the overall FFP1 time by 1 percent (see Table 10), increasing EDA daily cost savings by \$500 (\$740 with direct route case), for daily savings of \$4,499 for EDA-STAR and \$4,739 for EDA-Direct Arrivals. Figure 31 graphically shows the distribution of total (time and fuel) per operation EDA metering conformance fuel savings.

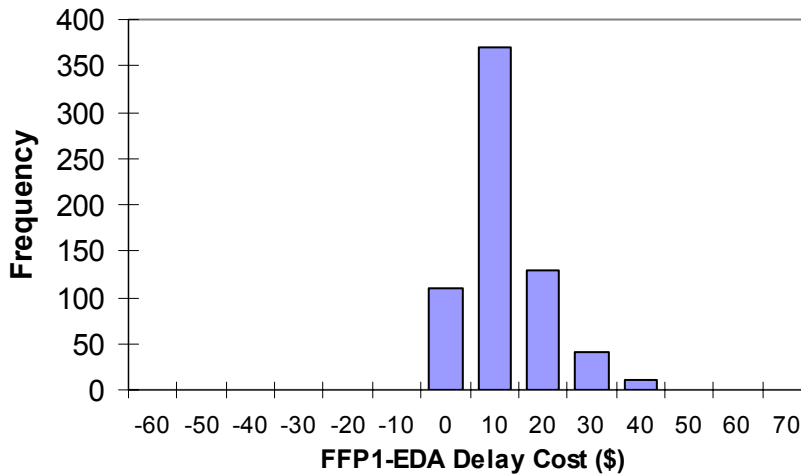


**Figure 31 EDA Metering Conformance Savings Per Operation**

**Separation Assurance ATM Interruptions**

Separation Assurance ATM interruptions can occur as correct, missed, or false alerts. Table 13 summarizes the number and type of ATM perceived separation assurance conflicts simulated under each case, categorized as correct (CA), missed (MA), and false (FA) alerts. Each conflict implies interrupting one or both flights to maintain separation. These ATM interruptions resolve conflicts between aircraft pairs of various types including DFW arrivals (ARR), DFW departures (DEP), and overflights (OVR, including satellite airport operations) within the DFW en route/transition airspace. Arrival-Arrival and Departure-Departure alerts with PCAs larger than the FAA minimum separation rule

(5 nm) were not included (NAs in Table 13). Because controllers closely monitor these streams at tight in-trail spacing during rush periods (assumed to be 5.5 nm for this study), conflict alerts between these aircraft can be a nuisance and is frequently deactivated [44]. Additionally, it should be noted that although EDA metering conformance maneuver advisories are designed to be conflict-free, where possible with all other traffic, this de-confliction was not fully accounted for in the modeling of EDA trajectories. Thus, EDA conflict alerts involving metered arrivals (over 80 percent of all identified arrival conflicts) would likely be significantly lower than identified in Table 13

Table 13 includes two metrics defining the proportion of missed and false alerts. The missed alert rate ( $R_{MA}$ ) is defined as the ratio of the number of overall missed alerts to the total number of admissible conflicts. The false alert rate ( $R_{FA}$ ) is defined as the ratio of the number of false alerts to the total number of admissible predicted conflicts. These values are expected to be approximately 35 percent and 45 percent for missed and false alert rates, respectively, based on previous analysis for the CTAS CPTP conflict probe at a 20 minute time horizon. [43] These metrics are defined as follows:

$$R_{MA} = N_{MA}/(N_{CA} + N_{MA}) \quad (11)$$

$$R_{FA} = N_{FA}/(N_{CA} + N_{MA}) \quad (12)$$

Where:  $N_i$  = Number of conflicts of type i

The alert rates include all conflicts displayed to the controller at the common 12-minute time horizon. Most conflict probe tools include a probability-based color coding that may limit controller action on low probability false alerts, especially at the longer time horizon (e.g. CTAS CPTP displays only conflicts above 50 percent probability). However, to account for the small false alerts resulting from the off-flight plan bad intent modeling approach, these conflicts (at their low probability) are included in Table 13. Although missed alerts would also be filtered, they are also included as it is assumed that the conflict probe at some point prior to the impending conflict will pick them up. The interruption costs of missed alerts reflect this shorter time horizon (5 minutes before initial loss of separation).

**Table 13a Number and Category of EDA Separation Assurance ATM Interruptions**

	Number of ATM Resolutions						Metrics	
	PCA<Rule		Rule<PCA<ACS		PCA >ACS	Total	$R_{MA}$	$R_{FA}$
	CA	MA	CA	MA	FA			
<b>FFPI Baseline</b>								
OVR-OVR	122	86	170	180	291	848	48%	52%
OVR-ARR	39	44	62	119	185	449	62%	70%
OVR-DEP	26	56	47	142	227	498	73%	84%
ARR-DEP	4	9	7	34	55	110	80%	102%
DEP-DEP	13	24	NA	NA	NA	37	NA	NA
ARR-ARR	58	87	NA	NA	NA	145	NA	NA
Total	263	307	286	474	758	2,087	59%	67%
<b>EDA – STAR Arrivals</b>								
OVR-OVR	131	77	156	159	259	782	45%	50%
OVR-ARR	64	27	93	72	124	380	39%	48%
OVR-DEP	48	35	79	93	161	416	50%	63%
ARR-DEP	7	8	18	23	54	110	56%	98%
DEP-DEP	18	20	NA	NA	NA	37	NA	NA
ARR-ARR	173	32	NA	NA	NA	205	NA	NA
Total	440	198	346	347	599	1,930	46%	56%
<b>EDA – Direct Arrivals</b>								
OVR-OVR	131	77	156	159	259	782	45%	50%
OVR-ARR	67	30	94	82	120	392	41%	44%
OVR-DEP	48	35	79	93	161	416	50%	63%
ARR-DEP	15	19	34	50	76	195	58%	65%
DEP-DEP	18	20	NA	NA	NA	37	NA	NA
ARR-ARR	142	25	NA	NA	NA	167	NA	NA
Total	421	205	364	383	617	1,989	47%	53%

PCA = Point of Closest Approach distance, Rule = FAA minima, ACS = Acceptable Controller Spacing  
ARR = DFW Arrival, DEP = DFW Departure, OVR = Overflight/Satellite

**Table 13b DFW EDA Arrival Separation Assurance Conflicts Detail**

	Number of ATM Resolutions						Metrics	
	PCA<Rule		PCA<ACS		PCA >ACS	Total	$R_{MA}$	$R_{FA}$
	CA	MA	CA	MA	FA			
<b>FFPI Baseline</b>								
OVR-ARR	39	44	62	119	185	449	62%	70%
ARR-DEP	4	9	7	34	55	110	80%	102%
ARR-ARR	58	87	86	124	172	527	59%	48%
Total	101	140	156	277	412	1,086	62%	61%
<b>EDA – STAR Arrivals</b>								
OVR-ARR	64	27	93	72	124	380	39%	48%
ARR-DEP	7	8	18	23	54	110	59%	98%
ARR-ARR	173	32	143	57	90	494	22%	22%
Total	244	67	254	152	268	984	31%	37%

**Table 13c Number and Category of EDX Separation Assurance ATM Interruptions**

	Number of ATM Resolutions						Metrics	
	PCA< Rule		Rule<PCA<ACS		PCA>ACS	Total	$R_{MA}$	$R_{FA}$
	CA	MA	CA	MA	FA			
<b>EDA – Direct Arrivals Baseline</b>								
OVR-OVR	131	77	156	159	259	782	45%	50%
OVR-ARR	67	30	94	82	120	392	41%	44%
OVR-DEP	48	35	79	93	161	416	50%	63%
ARR-DEP	15	19	34	50	76	195	58%	65%
DEP-DEP	18	20	NA	NA	NA	37	NA	NA
ARR-ARR	142	25	NA	NA	NA	167	NA	NA
Total	421	205	364	383	617	1,989	47%	53%
<b>EDX1 (Weather)</b>								
OVR-OVR	132	76	152	154	259	773	45%	50%
OVR-ARR	67	29	92	80	117	386	41%	44%
OVR-DEP	48	34	79	92	161	414	50%	63%
ARR-DEP	15	19	34	49	76	193	58%	66%
DEP-DEP	18	19	NA	NA	NA	37	NA	NA
ARR-ARR	144	23	NA	NA	NA	167	NA	NA
Total	425	200	357	375	613	1,971	46%	54%
<b>EDX2 (Weight, Thrust/Drag Coefficients, Weather)</b>								
OVR-OVR	135	73	150	139	259	756	43%	52%
OVR-ARR	68	28	91	74	117	379	39%	45%
OVR-DEP	50	33	79	86	161	409	48%	65%
ARR-DEP	16	18	33	42	76	185	55%	70%
DEP-DEP	19	19	NA	NA	NA	37	NA	NA
ARR-ARR	144	23	NA	NA	NA	167	NA	NA
Total	432	194	353	342	613	1,934	45%	55%
<b>EDX3 (Speed Intent, Weight, Thrust/Drag Coefficients, Weather)</b>								
OVR-OVR	145	64	141	110	253	713	38%	55%
OVR-ARR	71	25	82	58	117	354	35%	50%
OVR-DEP	54	29	75	67	157	382	43%	70%
ARR-DEP	18	16	32	34	76	175	50%	76%
DEP-DEP	21	16	NA	NA	NA	37	NA	NA
ARR-ARR	145	23	NA	NA	NA	167	NA	NA
Total	454	172	330	269	604	1,829	40%	60%
<b>EDX5 (Next 2 Waypoints, Speed Intent, Weight, Thrust/Drag Coefficients, Weather)</b>								
OVR-OVR	145	64	141	110	234	694	38%	51%
OVR-ARR	71	25	82	58	117	354	35%	50%
OVR-DEP	54	29	75	67	150	375	43%	67%
ARR-DEP	18	16	32	34	75	175	50%	76%
DEP-DEP	21	16	NA	NA	NA	37	NA	NA
ARR-ARR	145	23	NA	NA	NA	167	NA	NA
Total	454	172	330	269	577	1,802	40%	57%

Note: Number of false alerts was assumed to be equal or less than prior case.

PCA = Point of Closest Approach distance, Rule = FAA minima, ACS = Acceptable Controller Spacing

ARR = DFW Arrival, DEP = DFW Departure, OVR = Overflight/Satellite

As comparison of the cases in Tables 13a, 13b, and 13c shows, the total number of conflicts declines with improved technology. For example, in all cases, the number of unavoidable conflicts, where the Minimum Horizontal Separation (MHS) is less than the Rule, remains relatively constant, with increased share of correct vs. missed alerts. An exception to this occurs with the change to direct arrival trajectory routing beginning in the EDA-Direct Arrivals case. Additionally the proportion of false and missed alert rates declines, a key controller workload benefit.

Differences between the FFP1 and EDA cases in Tables 13a, reflect: (i) integration with arrival route intent (e.g. metering conformance clearances), (ii) trajectory prediction accuracy, including time horizon, and (iii) changed arrival delay strategy. The EDA integration of conflict probe-metering conformance functions and improved arrival trajectory prediction accuracy, is assumed to be largely responsible for the 24-30 percent improvement for missed, 19-21 percent for false alerts, and 5-7 percent overall reduction in conflict alerts, key controller workload benefits. Indeed, the excessive FFP1 false and missed alert rates would give controllers little confidence in a conflict probe tool's ability to correctly predict actual incidents. This may be exacerbated with our analysis, as we do not filter out conflicts lower than a certain threshold of probability. A comparison of EDA-STAR and EDA-Direct cases in Table 13a shows that either EDA case provides significant improvement over the FFP1 Baseline. Under the EDA-Direct Arrivals case, the results show a slightly smaller number of conflicts less than the FAA minima (PCA < Rule), but slightly more missed and false alerts. With the exception of the arrival-departure conflicts, the missed alert and false alert rates remained nearly the same as the EDA-STAR case.

Table 13b looks in detail at the FFP1 and EDA arrival conflicts. Unlike Table 13a, it includes conflicts exceeding FAA minimums (PCA > Rule). The changes between scenarios reflect the differences in arrival metering conformance flight changes under Baseline and EDA operations, the EDA integration of these flight changes with conflict probe, and the EDA reduction in the ACS. Despite this complex interplay of changes, the overall picture is a reduction in arrival conflicts by 9 percent and a halving of the missed and false alert rates, signaling significant controller workload savings. The number of conflicts above FAA minimums but below ACS declines, and in both categories EDA shows a significant shift from missed to correct alerts. Additionally, the number of arrival missed and false alerts are reduced by 62 and 35 percent, respectively. These changes all contribute to sharp fall in missed/false alert rates from 62/61 percent to 31/37 percent.

It should be noted that the EDA benefits appear to be diluted by the fact that the *modeled* EDA arrival metering conformance flight changes lead to more arrival conflicts than Baseline metering strategies, as shown by the EDA increase of 70 conflicts below FAA minimums (PCA < Rule). In fact, a more accurate modeling of EDA metering conformance flight changes would show a reduction in conflicts, since EDA attempts to advise conflict-free metering conformance maneuvers [61]. Despite the EDA modeling limitation, the Table 13b results indicate that the EDA improvements in Arrival-Arrival conflict rates (59/48 to 22/22 for missed and false alerts respectively) may allow controllers to better utilize the conflict probe for such conflicts. Under existing

uncertainties, the conflict probe is generally de-activated for high-density arrival flows due to excessive workload issues related to conflict probe errors [44].

In Table 13c, the total number of conflicts is shown to decline with EDX enhancement, a reduction of almost 10 percent (187 conflicts) in EDX5. Additionally the number of false and missed alert conflicts decline, particularly the missed alerts. For example, in all cases the number of unavoidable conflicts where the point of closest approach (PCA) separation is less than the FAA minima ( $PCA < Rule$ ), remains relatively constant, with increased share of correct vs. missed alerts. In contrast, conflicts above FAA minimums but below Acceptable Controller Spacing ( $Rule < PCA < ACS$ ) decline with the EDX reductions in ACS safety buffers. Rather than shift to a correct alert, these conflicts seem to become false alerts. Improved cases should allow false alerts to be averted, but additional false alerts may result from the reduction in ACS.

The number of missed alerts declines by 25 percent under EDX, with the largest benefits resulting from the ACS improvements of aircraft weight (EDX2) and speed intent (EDX3). The false alerts decline by almost 2 percent through EDX3 and by an additional 5 percent with the EDX5 downlink of the next two waypoints. Because these improvements may not keep up with the reduction in overall conflicts, the benefit is less apparent from the missed and false alert rate metrics ( $R_{MA}$  and  $R_{FA}$ ), where the false alert actually increase as a proportion of overall conflicts. It should be noted that the assumptions for undocumented off-flight plan routing, fully corrected under EDX5, is reflected only as an improvement in the low-cost false alerts. Additional benefit would be expected in identifying new missed alerts or changed correct alert geometries, resulting from the inaccurate intent. Finally, recall that EDA arrival metering conformance integration captured some of the intent improvement benefits, leaving EDX5 to strictly reflect improvements in non-metered arrivals, overflight, and departure intent.

The share of all ATM separation assurance interruptions by operations type is compared with recent CTAS conflict probe and Boeing Simulation resolutions in Table 14 [42, 51]. The CTAS field test results are also from the ZFW ARTCC airspace, albeit with a much small sample size. The simulated interruptions compare favorably with CTAS observations, although the simulation gave a slightly larger share of overflight-overflight and fewer arrival-arrival interruptions. The Boeing results in the Cleveland ARTCC show how these results might differ for other ARTCCs with different traffic patterns and mix of arrival, departure, satellite, and overflight operations.

**Table 14 Comparison of ATM Interruptions by Operations Type**

	ZFW ARTCC		CLE ARTCC
	FFP1	CTAS[42]	Boeing[51]
OVR-OVR	41%	33%	17%
OVR-ARR	22%	23%	32%
OVR-DEP	24%	24%	24%
ARR-DEP	5%	6%	13%
DEP-DEP	2%	3%	8%
ARR-ARR	7%	11%	5%
Total	100%	100%	100%
No. Interrupts	2,087	204	965

Note: The Boeing study assumes climb, cruise, and descent rather than DEP, OVR, and ARR.

## 6.2 ATM Interruptions Costs

The cost of all ATM interruptions for the FFP1 baseline and EDA/EDX cases is shown in Table 15. Both metering conformance and separation assurance interruptions are included in the table. In general, both per operation and daily costs are reduced with the enhanced technology cases.

For metering conformance ATM interruptions, the departure costs reflect ground-holding delay absorption, while arrival costs reflect speed, altitude, heading or time shift delay absorption mechanisms. The metering conformance costs are considerably higher than the separation assurance ATM interruptions, as they include the cost of time in addition to fuel, even though time costs are not the primary benefit. As previously stated, no improvement was modeled to the departure metering conformance interruptions. The EDA arrival delay strategy, emphasizing the more efficient speed control methods, was found to reduce fuel cost per operation on average, assuming STAR arrival routes, by over almost \$7, leading to a total daily cost savings of nearly \$4,500. Under the alternate direct arrival case, EDA saved an additional \$241 per day. EDX, as modeled, shows no change from EDA because common metering conformance delay strategy and time horizon values were used.

**Table 15a DFW ATM Interruptions Costs**

	Number of Interruptions	Resolution Cost (\$/op)		Total	Daily Total
		Fuel	Time		
<b>FFP1</b>					
Arrival Metering	662	\$25.82	\$78.84	\$104.66	\$69,283
Departure Metering	796	\$15.22	\$94.01	\$109.23	\$86,950
Separation Assurance	2,087	\$1.98	\$0.00	\$1.98	\$4,123
Total	3,545	\$9.40	\$35.83	\$45.24	\$160,356
<b>EDA-STAR</b>					
Arrival Metering	662	\$19.89	\$77.97	\$97.86	\$64,784
Departure Metering	796	\$15.22	\$94.01	\$109.23	\$86,950
Separation Assurance	1,930	\$1.90	\$0.00	\$1.90	\$3,660
Total	3,388	\$8.54	\$37.32	\$45.87	\$155,394
<b>EDA-Direct Arrivals</b>					
Arrival Metering	662	\$19.56	\$77.93	\$97.50	\$64,543
Departure Metering	796	\$15.22	\$94.01	\$109.23	\$86,950
Separation Assurance	1,989	\$1.79	\$0.00	\$1.79	\$3,552
Total	3,447	\$8.30	\$36.68	\$44.98	\$155,045

**Table 15b DFW EDX ATM Interruptions Costs**

	Number of <u>Resolution Cost (\$/op)</u>			<u>Total</u>	Daily <u>Total</u>
	<u>Interrupts</u>	<u>Fuel</u>	<u>Time</u>		
<b>EDA-Direct Arrivals</b>					
Arrival Metering	662	\$19.56	\$77.93	\$97.50	\$64,543
Departure Metering	796	\$15.22	\$94.01	\$109.23	\$86,950
Separation Assurance	1,989	\$1.79	\$0.00	\$1.79	\$3,552
Total	3,447	\$8.30	\$36.68	\$44.98	\$155,045
<b>EDX1 (Weather)</b>					
Arrival Metering	662	\$19.56	\$77.93	\$97.50	\$64,543
Departure Metering	796	\$15.22	\$94.01	\$109.23	\$86,950
Separation Assurance	1,971	\$1.77	\$0.00	\$1.77	\$3,482
Total	3,429	\$8.33	\$36.87	\$45.20	\$154,975
<b>EDX2 (Weight, Thrust/Drag Coefficients, Weather)</b>					
Arrival Metering	662	\$19.56	\$77.93	\$97.50	\$64,543
Departure Metering	796	\$15.22	\$94.01	\$109.23	\$86,950
Separation Assurance	1,934	\$1.74	\$0.00	\$1.74	\$3,374
Total	3,392	\$8.38	\$37.27	\$45.65	\$154,867
<b>EDX3 (Speed Intent, Weight, Thrust/Drag Coefficients, Weather)</b>					
Arrival Metering	662	\$19.56	\$77.93	\$97.50	\$64,543
Departure Metering	796	\$15.22	\$94.01	\$109.23	\$86,950
Separation Assurance	1,829	\$1.58	\$0.00	\$1.58	\$2,882
Total	3,287	\$8.50	\$38.46	\$46.97	\$154,375
<b>EDX5 (Next 2 Waypoints, Speed Intent, Weight, Thrust/Drag Coefficients,</b>					
Arrival Metering	662	\$19.56	\$77.93	\$97.50	\$64,543
Departure Metering	796	\$15.22	\$94.01	\$109.23	\$86,950
Separation Assurance	1,802	\$1.58*	\$0.00	\$1.58	\$2,830
Total	3,260	\$8.56	\$38.78	\$47.34	\$154,323

The separation assurance ATM interruptions costs reflect only the fuelburn of resolving the conflicts perceived by ATM, under the given technology. This includes correct and false alerts resolved strategically, and tactical missed alert resolutions. In general, the average and total costs are reduced with EDA and EDX technologies. The range of average costs for the scenarios is identified in Table 16.

**Table 16 Average Separation Assurance Resolution Costs by Incident Type**

	Average Resolution Cost (\$)		
	<u>CA</u>	<u>MA</u>	<u>FA</u>
OVR-OVR	\$0.94-1.05	\$1.74-2.15	\$0.67-0.73
OVR-ARR	\$0.59-1.23	\$1.29-2.76	\$0.69-0.88
OVR-DEP	\$0.65-0.79	\$1.36-1.66	\$0.44-0.58
ARR-DEP	\$0.16-0.24	\$0.37-0.54	\$0.20-0.24
DEP-DEP	\$4.88-6.50	NA	NA
ARR-ARR	\$0.79-1.75	NA	NA

As expected, the missed alert costs are largest, reflecting the tactical interruption, five minutes before conflict start. The false alerts are always smallest reflecting the fact that no actual conflict existed and thus interruption deviations should be lower. The range in correct alert costs are highest for the FFP1 case and decline with EDA and EDX enhancements. The high cost of the departure-departure case reflects the significantly higher fuelburn rates during climb, compounded with the heavier departure weight and

increased drag at lower altitudes. Conversely, the arrival-departure cost is very low, likely reflecting a reduced conflict duration as one aircraft climbs and the other descends from the point-of-closest approach.

### 6.3 ATM Interruptions Savings

#### 1996 DFW Daily Savings

Typical 1996 daily savings at DFW due to reduced frequency and expense of ATM interruptions, are found by taking the difference between the total costs of each case relative to a baseline case. FFP1 was used as the baseline for the EDA cases, while EDA-Direct Arrivals was used as the EDX baseline. The resulting daily savings are shown in Table 17a and 17b.

**Table 17a EDA ATM Interruptions Savings, relative to FFP1 Baseline**

	EDA-SID/STAR		EDA-Direct Arrivals	
	<u>Interrupts</u>	<u>Daily Cost</u>	<u>Interrupts</u>	<u>Daily Cost</u>
Arrival Metering	0	\$4,499	0	\$4,740
Departure Metering	0	\$0	0	\$0
Separation assurance	157	\$ 463	98	\$ 571
Total	157	\$4,962	98	\$5,311

**Table 17b EDX ATM Interruptions Savings, relative to EDA-Direct Arrivals Baseline**

	EDX1		EDX2		EDX3		EDX5	
	<u>Interrupts</u>	<u>Daily Cost</u>						
Arrival Metering	0	\$0	0	\$0	0	\$0	0	\$0
Departure Metering	0	\$0	0	\$0	0	\$0	0	\$0
Separation assurance	18	\$ 22	55	\$ 161	160	\$ 293	187	\$ 380
Total	18	\$ 22	55	\$ 161	160	\$ 293	187	\$ 380

EDA shows a nearly \$5,000 daily improvement in metering conformance interruptions, with a 5 percent savings found with EDA-Direct Route trajectories. The EDA cases also show reduction in the number of separation assurance interruptions amounting to \$571 daily. This is the result of the reduction in conflicts (98 to 157 less) as well as the lower missed and false alert rates, largely due the improved arrival intent with integrated EDA metering conformance and conflict probe functionalities.

EDX does not show any improvement in metering conformance interruptions because it was assumed to employ the same metering conformance criteria as EDA. However, the various EDX cases do show reduction in the number and cost of separation assurance ATM interruptions. This is the result of fewer conflicts and the lower missed and false alert rates with data exchange of aircraft attributes and intent. The largest benefit occurs with the improvements, primarily to climb accuracy, when aircraft weight (EDX2) and speed intent (EDX3) is downlinked. It should be noted that the small cost savings of reducing missed, and particularly false alerts, does not reflect the workload benefits associated with these improvements.

### 1996 NAS-wide Annual Savings

These daily DFW savings can be extrapolated to an annual level by accounting for the total number of 1996 DFW operations. This same method can be used at other candidate airports across the country to estimate NAS Benefits. NAS benefits are calculated based on deployment of EDA and EDX in the en route airspace of 37 candidate airport sites. This set was chosen to represent high-demand NAS airports, include FAA FFP1 and Phase 2 deployment locations.

The simple extrapolation used here employs Equations (11) and (12) to estimate annual ATM Interruptions Benefits. This is similar to the extrapolation method employed in other studies [1-2, 52]. An alternate method might employ pairwise factors to relate conflict frequency to traffic volume:

$$\text{Annual Costs} = (\text{Annual Ops}) \times (\text{Interrupt Rate}) \times (\text{Cost Per Interrupt}) \quad (11)$$

$$\text{Annual Savings} = \text{Annual Cost}_{\text{BL}} - \text{Annual Cost}_{\text{EDA/X}} \quad (12)$$

where: *Annual Ops* = Annual airport operations (00s) (for Metering Conformance Interruptions)  
 = Annual ARTCC operations (00s) (for Separation Assurance Interruptions)  
*Interrupt Rate* = Number of interruptions per 100 operations (Table 18)  
 = *Interrupt Rate* x *Airport Factor* (for Metering Conformance Interruptions)  
*Apt Factor* = Factor accounting for local airport rush arrival frequency relative to DFW, based on  
 FAA delay data (Appendix E)  
*Cost Per Interrupt* = Average cost per interruption (Table 18)

The daily interruption rates and costs observed in the simulation and used in Equation (11), assuming a conservative fuel cost of \$0.10 per pound, are summarized in Table 18. The interruption rate is based on 2,176 airport and 8,003 ARTCC operations in the daily simulation. Note that the metering conformance interruptions rate in Table 18 are given per daily *airport* operation, which includes both arrivals and departures. Thus, a rate of 50 per 100 operations is assumed to represent all arrival operations. The metering conformance interruptions impacts all rush arrivals. The simulated DFW rush arrival rate was adjusted by an *Airport Factor* to account for variations in congestion at each facility. Airports with less overall delays are assumed to require disproportionately fewer metering conformance interruptions. Thus, airports with less demand-capacity congestion are assumed to delay fewer en route arrival and departure aircraft to meet airport-scheduling constraints. An individual airport's assumed delayed arrival rate is adjusted from the nominal DFW value of Table 18, using FAA delay data [50]. These data record delays at each airport in excess of 15 minutes in CY1996, including both arrivals and departures. This metric hides the significant number of smaller delays during an arrival rush period and includes delayed departures, making it a gross indicator of the airport's level of delayed arrival flights. Using these data, the airports are broken into five delay categories. Engineering judgement was used to assign each category a rush arrival rate relative to DFW. Simulated rates (Table 4) of 130%, 115%, 100%, 80%, and 60% for airport delay classes 1, 2, 3, 4, and 5 were used, as shown in Table 2.6. The FAA delay data and criteria used to assign delay classes are included in Appendix E. These values are used in Equation (11) to estimate the interruption rate as part of the annual benefits calculation.

**Table 18 DFW Daily Simulation Interruption Rates and Costs**

ATM Interruption Type	Ops Basis	FFP1	EDA-SS	EDA-DR	EDX1	EDX2	EDX3	EDX5
		Interrupt Rate (per 100 ops)						
Arrival Metering	Apt Arr/Dep	30.4	30.4	30.4	30.4	30.4	30.4	30.4
Departure Metering	Apt Arr/Dep	36.5	36.5	36.5	36.5	36.5	36.5	36.5
Separation assurance	ARTCC	26.1	24.1	24.9	24.6	24.2	22.9	22.5
		Cost Per Interrupt (\$/op)						
Arrival Metering	Apt Arr/Dep	\$104.66	\$97.86	\$97.50	\$97.50	\$97.50	\$97.50	\$97.50
Departure Metering	Apt Arr/Dep	\$109.23	\$109.23	\$109.23	\$109.23	\$109.23	\$109.23	\$109.23
Separation assurance	ARTCC	\$1.98	\$1.90	\$1.79	\$1.77	\$1.74	\$1.58	\$1.58*

\* EDX3 cost rates applied to EDX5

**Annual Benefits Summary**

The annual benefits by airport are shown in Table 19a for EDA, relative to the FFP1 Baseline, and Table 19b for EDX, relative to an EDA-Direct Arrivals Baseline. Annual savings are the difference between the annual ATM interruptions cost of the baseline and future cases, as calculated using Equations (11) and (12). Although all interruptions are shown by airport, the totals reflect only a single instance of each ARTCC. The annual savings are plotted graphically by airport in Figures 32a and 32b for EDA and EDX, respectively.

The annual EDA benefits at any single airport ranges from \$0.28M at BDL to nearly \$2.1M at ORD. Over 90 percent of the EDA cost savings are derived from metering conformance improvements. Thus, the large hub airports, ORD, DFW, ATL, and LAX, saved the most, with a total of over \$1.5M annually. Benefits at all 37 airports, representing NAS-wide deployment, totaled over \$27M, after accounting for overlapping ARTCC airspace. Total EDA benefits increased by 7 percent under EDA with arrival direct routing. It should be noted that the EDA-Direct Arrivals metering conformance benefits reflect a more efficient delay strategy, which are separate from the benefits of direct routing time/path savings, calculated in a separate study [2,11].

It should be noted that the similar EDA benefits estimated for STAR and direct arrival routing implies that direct routing does not inhibit EDA metering conformance efficiency or separation assurance interruption improvements. Indeed, the results indicate that automation may allow aircraft to file for their user-preferred direct routes with ATM DST-assisted management and monitoring interrupting these routes only as required for metering conformance and separation assurance. Such direct arrival routing benefits are enabled by EDA automation, allowing controllers to dynamically adhere to metering constraints without restricting aircraft to common arrival paths. During non-rush periods, user-preferred direct arrival routes would save both time and fuel. During metering, no time savings would accrue due to delays but, as the metering conformance results of this report show, the direct arrival route actions have a slight fuel advantage without adversely impacting metering conformance workload. Separation assurance conflicts are also reduced relative to the FFP1 Baseline under direct arrival routes. Despite a slightly higher interrupt rate in the EDA-Direct Arrivals case, the smaller per operation resolution cost resulted in larger overall annual/NAS-wide benefits. Such direct arrival routing

benefits are enabled by EDA automation, allowing controllers to dynamically adhere to metering constraints without restricting aircraft to common arrival paths.

The EDX benefits strictly represent separation assurance interruption improvements. Because the per operation cost savings of the separation assurance benefits is so much smaller, the annual benefits are much less than the EDA cases. The total EDX5 benefits at any one ARTCC ranges from \$125,000 at ZOA to \$264,000 at ZAU, with all 37 airports having an annual benefit of \$3.6 million, when accounting for overlapping ARTCC airspace. The primary benefit resulted from the EDX5 waypoint intent (44 percent) and EDX3 speed intent (40 percent), which impacted all flight modes. EDX2 aircraft weight (12 percent) and EDX1 weather (4 percent) resulted in smaller share of the overall savings. Note that these results are highly sensitive to the order in which these incremental improvements were made.

It should be noted that these benefit estimates do not account for the significant controller workload improvements. In all separation assurance cases, safety improves with enhanced surveillance under EDA and EDX metered arrival trajectory prediction.

Under EDA, controller workload is enhanced by EDA assistance in strategic planning to meet the dual objectives of separation assurance and compliance with flow-rate restrictions. EDA maneuver advisories embody an efficient inter-sector approach to metering restrictions, easing controller strategy and clearance development. By identifying an appropriate strategy as well as magnitude, EDA reduces controller workload. Indeed, in early EDA testing, over two-thirds of the EDA clearances provided to controllers required no modification, being acceptable in both method (speed, heading, altitude) and magnitude [54]. Additionally, the use of a high-fidelity model to develop the EDA maneuver advisories improves their accuracy over cognitively-developed interruptions, reducing the need for additional corrective interruptions closer to the restriction, and limiting vectoring which requires two clearances (i.e., turnout and turn back).

**Table 19a EDA ATM Interruptions Benefits**

Airport	Annual Operations (000s)						Rush Arr	Annual Savings (\$M. 1998)			
	Airport	ARTCC	Apt Delay Delays/Categor y	Rate (/100 Ops)	EDA-STAR		EDA-Direct				
					Metering Conformanc	Separation Assurance	Metering Conformanc	Separation Assurance			
Atlanta	ATL	773	ZTL 2,453	23.88	3	30.4	1.41	0.14	1.49	0.18	
Nashville	BNA	226	ZBW 1,727	1.36	5	18.2	0.18	0.10	0.19	0.12	
Boston	BOS	463	ZME 1,978	0.73	2	18.2	0.25	0.11	0.26	0.14	
Bradley	BDL	161	ZBW 1,727	26.37	5	34.9	0.97	0.10	1.03	0.12	
Baltimore	BWI	270	ZDC 2,331	3.67	5	18.2	0.30	0.14	0.31	0.17	
Cleveland	CLE	291	ZOB 2,870	4.68	5	18.2	0.32	0.17	0.34	0.21	
Charlotte	CLT	457	ZTL 2,453	6.55	4	24.3	0.67	0.14	0.71	0.18	
Cincinnati	CVG	394	ZID 2,222	10.38	4	24.3	0.57	0.13	0.61	0.16	
Washington National	DCA	310	ZDC 2,331	6.53	4	24.3	0.45	0.14	0.48	0.17	
Denver	DEN	454	ZDV 1,527	1.90	5	18.2	0.50	0.09	0.53	0.11	
Dallas – Ft. Worth	DFW	870	ZFW 2,118	19.59	3	30.4	1.58	0.12	1.68	0.15	
Detroit	DTW	531	ZOB 2,870	9.10	4	24.3	0.77	0.17	0.82	0.21	
Newark	EWL	443	ZNY 2,040	65.25	1	39.5	1.05	0.12	1.11	0.15	
Ft. Lauderdale	FLL	236	ZMA 1,542	1.53	5	18.2	0.26	0.09	0.27	0.11	
Houston Hobby	HOU	252	ZHU 1,853	2.57	5	18.2	0.28	0.11	0.29	0.13	
Washington Dulles	IAD	330	ZDC 2,331	6.81	4	24.3	0.48	0.14	0.51	0.17	
Houston – Intercontinental	IAH	392	ZHU 1,853	11.45	4	24.3	0.57	0.11	0.61	0.13	
N.Y. Kennedy	JFK	361	ZNY 2,040	29.53	2	34.9	0.76	0.12	0.80	0.15	
Las Vegas	LAS	480	ZLA 1,981	3.68	5	18.2	0.52	0.12	0.56	0.14	
Los Angeles	LAX	764	ZLA 1,981	24.13	3	30.4	1.39	0.12	1.47	0.14	
N.Y. LaGuardia	LGA	343	ZNY 2,040	46.22	1	39.5	0.81	0.12	0.86	0.15	
Orlando	MCO	342	ZJX 1,878	4.59	5	18.2	0.37	0.11	0.40	0.13	
Chicago Midway	MD W	254	ZAU 2,894	6.70	4	24.3	0.37	0.17	0.39	0.21	
Memphis	MEM	364	ZME 1,978	NA	5	18.2	0.40	0.11	0.42	0.14	
Miami	MIA	546	ZMA 1,542	6.79	4	24.3	0.80	0.09	0.84	0.11	
Minneapolis	MSP	484	ZMP 2,027	9.29	4	24.3	0.70	0.12	0.75	0.14	
Oakland	OAK	516	ZOA 1,368	NA	5	18.2	0.56	0.08	0.60	0.10	
Chicago O’Hare	ORD	909	ZAU 2,894	34.46	2	34.9	1.90	0.17	2.02	0.21	
Portland	PDX	306	ZSE 1,393	2.41	5	18.2	0.33	0.08	0.35	0.10	
Philadelphia	PHL	406	ZNY 2,040	17.95	3	30.4	0.74	0.12	0.78	0.15	
Phoenix	PHX	544	ZAB 1,505	7.25	4	24.3	0.79	0.09	0.84	0.11	
Pittsburgh	PIT	447	ZOB 2,870	6.60	4	24.3	0.65	0.17	0.69	0.21	
San Diego	SAN	244	ZLA 1,981	3.31	5	18.2	0.27	0.12	0.28	0.14	
Seattle	SEA	398	ZSE 1,393	6.37	4	24.3	0.58	0.08	0.61	0.10	
San Francisco	SFO	442	ZOA 1,368	56.57	1	39.5	1.05	0.08	1.11	0.10	
Salt Lake City	SLC	374	ZLC 1,509	3.53	5	18.2	0.41	0.09	0.43	0.11	
St. Louis	STL	517	ZKC 1,986	34.04	2	34.9	1.08	0.12	1.15	0.14	
37-Airport Total	---	430	---	39.2M	---	---	25.09	2.28	26.59	2.80	

• Totals include only one instance of each ARTCC, excluding the shaded ARTCC operations separation assurance operations.

**Table 19b EDX ATM Interruptions Benefits**

<u>Airport</u>	<u>ARTC</u>	Annual ARTCC Ops (000s)	Separation Assurance Interruptions Annual Savings (\$000s, 1998)			
			<u>EDX1</u>	<u>EDX2</u>	<u>EDX3</u>	<u>EDX5</u>
	<u>C</u>					
Atlanta (ATL)	ZTL	2,453	22.0	59.8	205.5	224.1
Nashville (BNA)	ZBW	1,727	15.5	42.1	144.7	157.8
Boston (BOS)	ZME	1,978	17.7	48.2	165.7	180.7
Bradley (BDL)	ZBW	1,727	15.5	42.1	144.7	157.8
Baltimore (BWI)	ZDC	2,331	20.9	56.8	195.3	213.0
Cleveland (CLE)	ZOB	2,870	25.7	70.0	240.5	262.2
Charlotte (CLT)	ZTL		22.0	59.8	205.5	224.1
Cincinnati (CVG)	ZID	2,222	19.9	54.2	186.1	203.0
Washington National (DCA)	ZDC	2,331	20.9	56.8	195.3	213.0
Denver (DEN)	ZDV	1,527	13.7	37.2	128.0	139.5
Dallas – Ft. Worth (DFW)	ZFW	2,118	19.0	51.6	177.4	193.5
Detroit (DTW)	ZOB	2,870	25.7	70.0	240.5	262.2
Newark (EWR)	ZNY	2,040	18.3	49.7	170.9	186.4
Ft. Lauderdale (FLL)	ZMA	1,542	13.8	37.6	129.2	140.9
Houston Hobby (HOU)	ZHU	1,853	16.6	45.2	155.2	169.3
Washington Dulles (IAD)	ZDC	2,331	20.9	56.8	195.3	213.0
Houston–Intercontinental (IAH)	ZHU	1,853	16.6	45.2	155.2	169.3
N.Y. Kennedy (JFK)	ZNY	2,040	18.3	49.7	170.9	186.4
Las Vegas (LAS)	ZLA	1,981	17.7	48.3	165.9	181.0
Los Angeles (LAX)	ZLA	1,981	17.7	48.3	165.9	181.0
N.Y. LaGuardia (LGA)	ZNY	2,040	18.3	49.7	170.9	186.4
Orlando (MCO)	ZJX	1,878	16.8	45.8	157.4	171.6
Chicago Midway (MDW)	ZAU	2,894	25.9	70.6	242.5	264.4
Memphis (MEM)	ZME	1,978	17.7	48.2	165.7	180.7
Miami (MIA)	ZMA	1,542	13.8	37.6	129.2	140.9
Minneapolis (MSP)	ZMP	2,027	18.1	49.4	169.9	185.2
Oakland (OAK)	ZOA	1,368	12.2	33.4	114.6	125.0
Chicago O’Hare (ORD)	ZAU	2,894	25.9	70.6	242.5	264.4
Portland (PDX)	ZSE	1,393	12.5	34.0	116.7	127.2
Philadelphia (PHL)	ZNY	2,040	18.3	49.7	170.9	186.4
Phoenix (PHX)	ZAB	1,505	13.5	36.7	126.1	137.5
Pittsburgh (PIT)	ZOB	2,870	25.7	70.0	240.5	262.2
San Diego (SAN)	ZLA	1,981	17.7	48.3	165.9	181.0
Seattle (SEA)	ZSE	1,393	12.5	34.0	116.7	127.2
San Francisco (SFO)	ZOA	1,368	12.2	33.4	114.6	125.0
Salt Lake City (SLC)	ZLC	1,509	13.5	36.8	126.4	137.9
St. Louis (STL)	ZKC	1,986	17.8	48.4	166.4	181.5
37-Airport Total/Average	---	39,202	350.9	955.9	3,284.4	3,581.6

\* Totals include only one instance of each ARTCC, excluding the shaded ARTCC operations separation assurance operations.

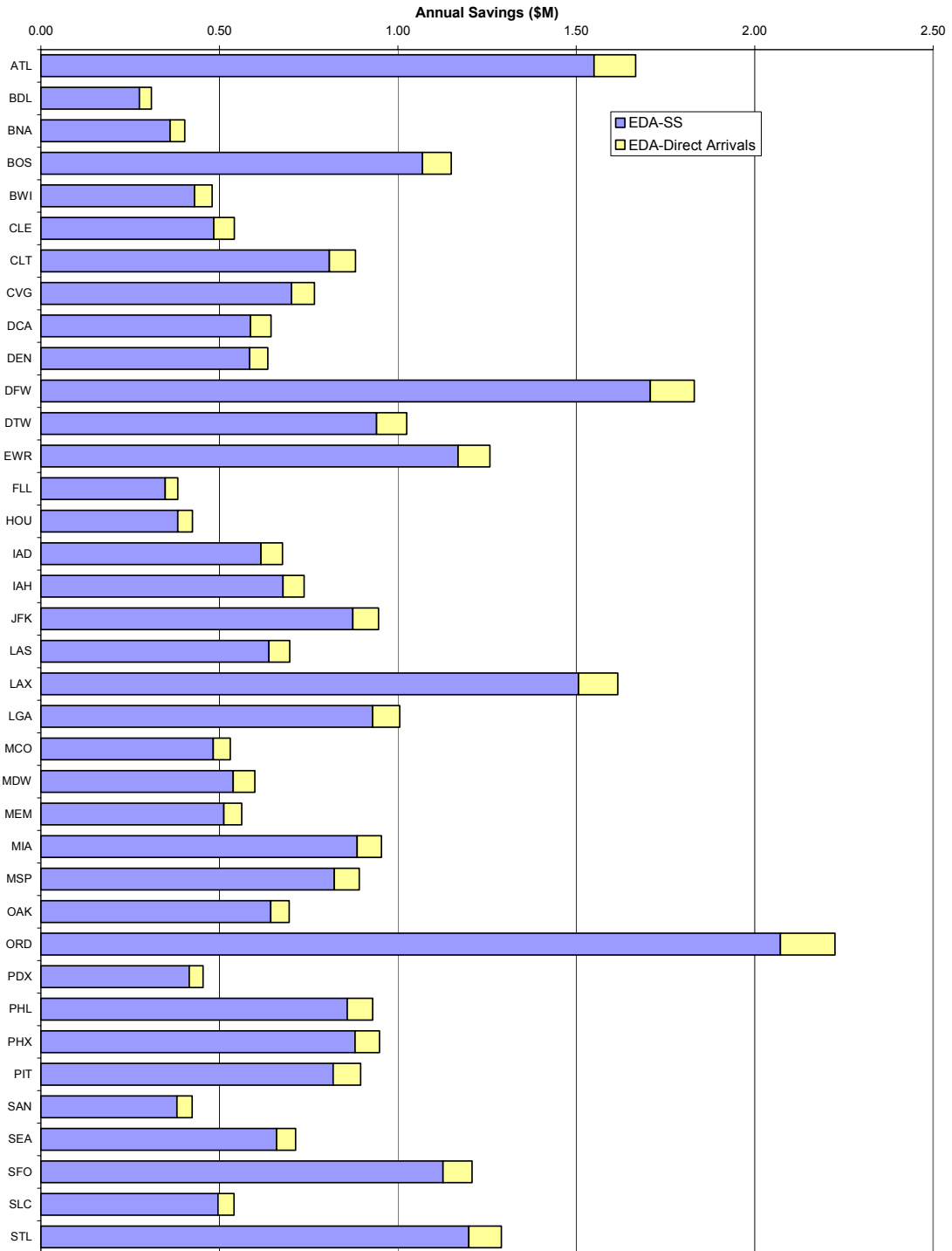


**Figure 32a EDA Annual Savings by Airport Site**

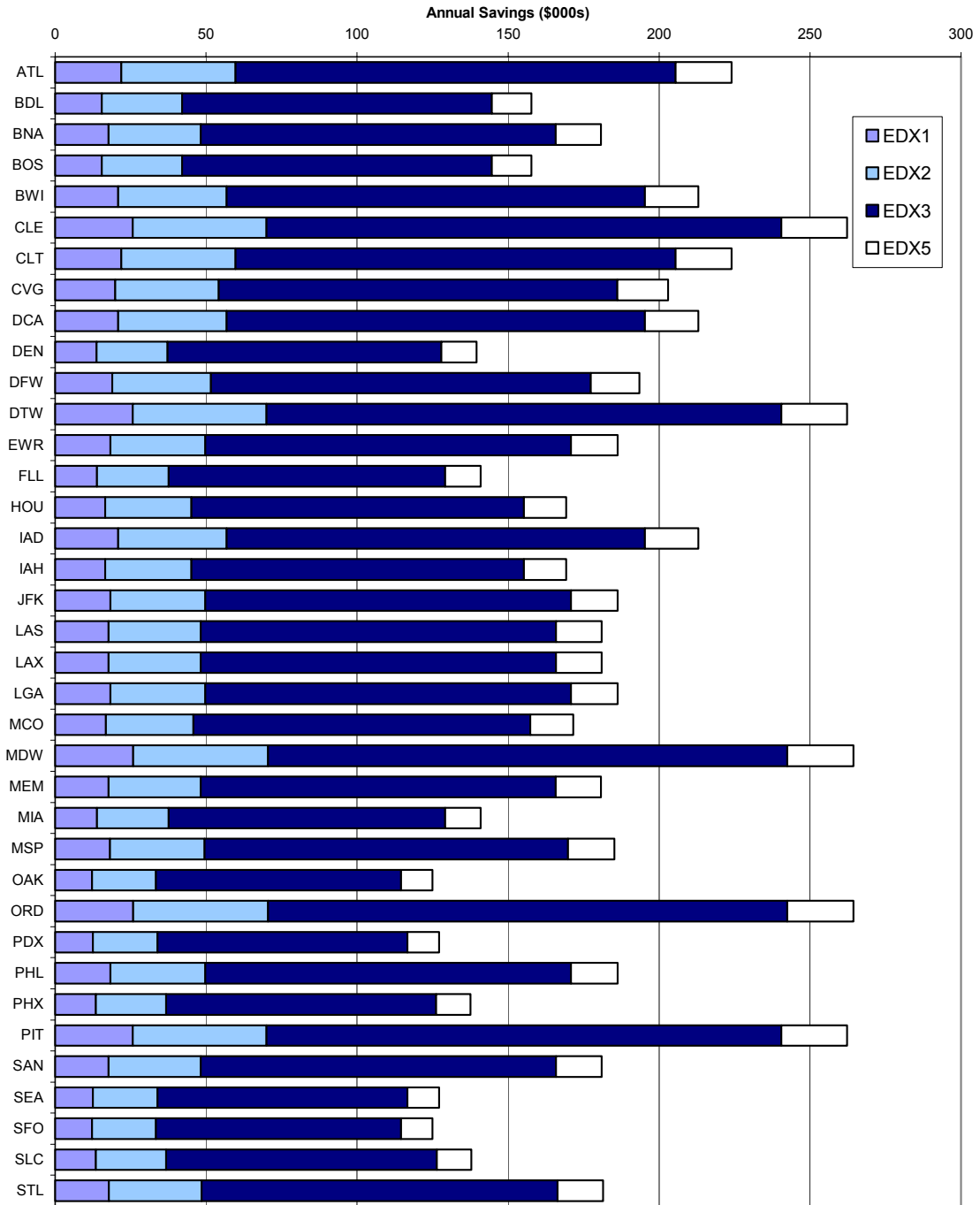


Figure 32b EDX Annual Savings by Airport Site

Current TMA-based arrival metering conformance procedures typically include the following clearances [55]:

**Clearance 1:** Altitude, speed, and vectoring heading change to conform to arrival metering schedule. This clearance may split into two under busy conditions with an initial altitude clearance, followed later by a vectoring/speed clearance. Additionally, multiple altitude clearances may be given to step descend aircraft in order to de-conflict merging arrival streams that have been vectored, or to avoid crossing traffic streams.

**Clearance 2:** Heading change to turn back aircraft towards a Fix or Navaid. The timing of this clearance is assisted by the TMA delay count-down. That is, TMA displays a dynamic delay value for each metered aircraft, indicating its conformance to the metering schedule, if turned back now.

**Clearance 3:** Appraise pilot of arrival metering fix crossing restrictions and instruct pilot to begin descent (typically at pilot discretion).

EDA poses several advantages to this Baseline metering conformance procedure:

- Clearance 1 will more frequently not be split into multiple clearances, due to the EDA ability to provide initial conflict-free advisories that conform to arrival metering constraints;
- Clearance 2 turn back, may be required less frequently, with the EDA replacement of vectoring with speed and altitude methods for smaller delays.
- Arrival metering fix delivery accuracy will improve with more accurate Clearance 2 vector turn back under EDA, and the ability of EDA to fine-tune descent speeds in Clearance 3.

EDA maneuver advisories are set-up to autoload into a datalink message format for uplink to pilots. This will speed up clearance delivery/readback, enhancing controller workload.

In terms of separation assurance controller workload, the improved EDA metered arrival prediction and integration of flow-rate conformance flight changes with conflict probe functions, greatly reduces the probability of missed or nuisance (false) conflict alerts. Indeed, the analysis identified a halving of the arrival missed and false alert rates under EDA, in addition to the EDA reduction in overall detected conflicts. EDX also enhances separation assurance controller workload by further improving conflict probe trajectory prediction accuracy, through better knowledge of actual aircraft state, weather and atmospheric conditions, and future intent. The improved trajectory prediction, especially the EDX5 downlink of next two waypoint intent, greatly reduces the probability of missed or nuisance (false) conflict alerts. Indeed, the analysis identified a 25 percent reduction in the number of missed and 7 percent reduction in false alerts under EDX, in addition to a 10 percent reduction in overall detected conflicts. Safety also benefits with enhanced surveillance under improved EDX trajectory prediction capabilities.

## **7. Conclusions and Recommendations**

---

This report has assessed the performance of en route DST technologies for reducing the frequency and impact of ATM-based deviations to the user's preferred trajectories, namely the CTAS En Route Descent Advisor (EDA) and EDA enhanced with user-CTAS data exchange (EDX). This work estimated both metering conformance and separation assurance ATM interruptions benefits. This work was conducted in cooperation with related NASA AATT efforts summarizing EDA [1] and EDX [2] benefits, and reflects modeling and input parameter improvements over previous efforts [7-8].

The ATM Interruptions model used in this effort provides an approach to evaluating the trajectory costs of en route ATM interruptions by modeling specific controller metering and conflict resolution actions, aided by automated DST technology. The metering conformance modeling is sensitive to the complex interactions of time horizon, controller delay strategy ordering and accuracy used to absorb arrival metering delays. Additionally, the importance of integrating metering conformance and separation assurance (e.g., conflict probe) functions was evaluated. The separation assurance interruptions modeling is sensitive to the complex interactions of ATM conflict detection and resolution (including the relationship among false, missed, and correct alerts), a conflict probe tool's stochastic position accuracy as a function of time horizon, and controller perception and safety margins in resolving potential conflicts.

This effort quantified EDA metering conformance and EDA/EDX separation assurance ATM interruption savings. Metering conformance interruptions delay aircraft to meet airport capacity constraints. EDA maneuver advisories assist controllers in formulating and executing a traffic delay strategy to meet arrival metering fix crossing schedule. EDA allows controllers to quickly and accurately assess the impact of various delay strategies, and more effectively use fuel-efficient strategies, such as speed control, resulting in lower cost metering conformance interruptions. It was found that EDA saved an average of 59 lbs and 2.6 seconds or \$6.80 per arrival metering conformance interruption, for a total saving of \$25.09M annually assuming NAS-wide deployment at 37-airports. In addition, the EDA metering conformance procedures are more strategic and require less overall workload than those currently used by the FFP1 Baseline

For separation assurance interruptions, ATM relies on accurate predictions of flight trajectories within its conflict probe tool to accurately identify the location and nature of pending separation violations. With more accurate trajectory predictions (e.g., EDA advisories and EDA/EDX updated state/intent) ATM perception would improve, resulting in fewer ATM flight interventions and associated resolution fuel penalties. Additionally, improved traffic conflict prediction will include more accurate estimation of conflict geometry and speeds, leading to more efficient resolution maneuvers. It was found that EDA reduced separation assurance interruptions by 7.7 percent with each interruption savings an average of 0.8 lbs or \$0.08 per interruption, for a total saving of \$2.80M annually assuming NAS-wide deployment at 37-airports. More significantly, the EDA separation assurance conflicts required less overall workload primarily because of

the integration with metering conformance flight intent, reducing missed and false alert rates by 50 and 40 percent, respectively.

Relative to an the EDA-Direct Arrivals baseline, it was found that EDX reduced separation assurance interruptions by 10 percent with each interruption savings an average of 2 lbs or \$0.21 per interruption, for a total savings of \$3.6M annually assuming NAS-wide deployment at 37-airports. More significantly, the EDX separation assurance conflicts required less overall workload primarily because of the downlink of aircraft state and flight intent, reducing the number of missed and false alerts by 25 and 7 percent, respectively. Additionally other benefits are noted but not quantified, including EDA and EDX enhancement to overall safety, strategic controller planning across multiple sectors, and reduced nuisance conflict alerts.

## Recommendations

The remainder of this chapter discusses recommendations for future work to increase the fidelity of the ATM Interruptions Model (AIM) employed in this effort and the accuracy of the associated benefit estimates. Implementation of these recommendations would reinforce the ATM Interruptions Modeling approach as a powerful and efficient mechanism for evaluating a variety of en route operational impacts at the level of specific air traffic controller clearances.

### Metering Conformance Analysis

The following improvements are suggested to refine the metering conformance model and analysis parameters.

- **Improve metering conformance strategy parameter assumptions** – Assumed actuation parameters, such as speed error, speed increment, and vectoring turn back error can be regarded as pilot actuation or controller advisory errors. In this report these values were based on expert judgement. It would be useful to support these assumptions with field data or tie their value to DST technology attributes, such as trajectory prediction accuracy. This would also facilitate modeling EDX improvements, separate from EDA.
- **Model EDX metering conformance strategy improvement** - No improvement is modeled with EDX over EDA delay strategy. Further model development could capture the benefits of the more accurate EDA metering advisories as CTAS trajectory prediction accuracy is improved through user-CTAS data exchange.
- **Improved best endurance speed estimates** – BADA “low” cruise values were used in the Metering Conformance ATM Interruptions model component to approximate best endurance speeds. A suggested improvement is to generate best endurance speeds directly for a range of aircraft. This could be done through selected high-fidelity simulation runs for multiple aircraft at multiple altitudes to augment the BADA speeds. Alternatively, a more analytical calculation of best endurance speeds for various aircraft could be employed.

- **Allow non-jets to employ altitude delay method** - This study assumed altitude delay absorption would only be fuel-efficient for jet aircraft. This is reflective of existing conditions which are restricted by cognitive limitations in assessing such a case. An analysis is suggested to identify whether EDA should use the altitude method for non-jets, given its fuel-efficiency for these aircraft types at their lower altitude routes.
- **Incorporate vectoring error and TOD shift in delayed trajectories**– Vector turn back is the final maneuver clearance given by a controller before the flight reaches the arrival metering fix. As such, this turn back maneuver is critical to the ability to deliver aircraft accurately to the TRACON boundary. Additionally, with metering conformance changes in speed, the TOD location shifts. Although the metering conformance interruption cost of the vectoring turn back error and shift in TOD was accounted for in the cost of the interruption, additional effort is required to implement these elements geometrically in the metered (delayed) 4D trajectories used by the conflict probe.
- **Model ATM interruptions coupling** – Currently, little interaction other than aircraft intent, links the metering conformance and separation assurance ATM interruptions functions in the ATM Interruptions Model. Possible coupling could entail modeling metering conformance arrival metering fix delivery errors, assumed to improve with technology. This would also allow the model to address the metering cost of not meeting the metering fix STA. Currently all scenarios used a 15-second tolerance relative to the scheduled metering fix crossing time. Additionally, when vectoring turn back error caused the flight to arrive late to the metering fix, no penalty, other than excessive path length, was imposed despite the obvious impact on inefficient metering fix throughput.
- **Improve rush arrival extrapolation** – In this effort, detailed information on the number and magnitude of DFW rush arrivals was evaluated and extrapolated to other airports based simply on FAA delay data. However, rush attributes are likely to vary significantly by airport in both the number and magnitude of delays necessary to balance airport demand and capacity restrictions. Additionally, the employed method relies on readily available data that is only a gross estimator of arrival metering delay. Because of the high sensitivity of the metering conformance benefits to the rush assumptions, improvements to the rush arrival extrapolation methodology would be beneficial.

#### **Separation Assurance Analysis**

The following improvements are suggested to refine the ATM Interruptions Model separation assurance model and analysis parameters.

- **Enhanced off-flight plan modeling**– This study developed a first-cut methodology to evaluate the impact of off-flight plan erroneous intent data on separation assurance conflicts. This conservative simplification of real-world operations assumed a set (not flight-specific) geometry for the off-flight plan conflict and implies that no new missed alerts are created with this routing. Additionally, the frequency of such routing, estimated by expert judgement, was not assumed to vary by flight mode.

This modeling approach and associated parameter assumptions should be reevaluated in future efforts.

- **Improve conflict counting method** - In this analysis, all conflicts perceived to fall below controller acceptable controller spacing (ACS) at the strategic time horizon were tallied. Additionally, no conflicts were filtered out as having a probability of conflict below a given threshold, as done by operating conflict probe DSTs. This was largely due to retain the off-flight plan intent error impact. Additionally, as ACS shrinks, controllers may wish to continue to be alerted of conflicts using the original larger ACS safety buffers, even if these flights are not interrupted. Also, evaluating conflicts at the strategic time horizon does not reflect false alerts that are not acted on and missed alerts that are interrupted more fuel-efficiently before our assumed tactical 5-minute horizon. Thus it is recommended that the methodology used to identify and count separation assurance conflicts be reevaluated.
- **Enhance resolution strategies** – As presented here, only vectoring resolutions were considered for separation assurance conflicts. Alternate strategies including altitude and direct-to resolutions, may want to be considered, since observations of actual conflict resolution strategies indicates that vectoring, altitude, and direct-to resolutions constitute the majority of conflict resolutions [42, 50]. For future analyses, direct-to resolution could be included as a modification of the vectoring resolution, by reducing the path distance on appropriate flights. In addition to saving path distance, direct-to resolutions reduce controller workload by avoiding the second turn back clearance returning the aircraft back on course. Additionally, the resolution methodology could be extended to analyze potential conflicts that involve more than two aircraft and to understand the impact of other proximate aircraft on the degrees of conflict resolution freedom.

### General Analysis Recommendations

The following recommendations are suggested to improve the robustness of the model and resulting benefits estimates.

- **Evaluate multiple initial conditions.** Because the ATM Interruptions benefit estimates depend on both the number and geometry of conflicts, it is suggested that the analysis be enhanced to account for variations in the initial conditions and thus variations in the number, location, type, and cost of subsequent conflict set. Initial conditions that may be altered include the specific arrival/departure times and airport capacities, represented by airport acceptance rates. In addition to variations on a single day, multiple days could be studied to determine the variability of the ATM interruption results to different demand levels, weather, and other important parameters (e.g., traffic flow management actions, special use airspace restrictions, etc.).
- **Evaluate additional en route ARTCCs** - Aircraft trajectories and potential conflicts for different en route airspaces should be studied to better understand the major factors governing the extrapolation of both metering conformance and separation assurance conflicts in a single ARTCCs (ZFW) on a single day to NAS-wide annual levels.

- **Calibrate FFP1 Baseline**– The FFP1 Baseline metering conformance and separation assurance interruption frequency and attributes count be verified against field data to ensure valid modeling of these problem domains. Adjustments could be made to the modeling methodology to better concur with field observations.
- **Improve trajectory parameter accuracy values** - The values of the trajectory parameter accuracies used in the report to represent EDA and EDX case ATM perception were arrived at using a mix of analytical models, field data, and engineering judgment. It is suggested that these models and parameter assumption be reviewed and continually updated with ongoing research in this area. In particular, climb accuracy estimates are less robustly supported by modeling and field data. The estimate of the various user-CTAS data exchange parameter errors could be improved by analyzing representative airline-provided data. There may also be a desire to include other EDX data exchange parameters. The importance of these parameters to the model results suggests they should be stringently modeled and continuously refined to keep abreast of ongoing research efforts.
- **Perform sensitivity analyses** - Several parameters in the model could be studied in terms of their sensitivity to the resulting benefits estimates. For example, the assumption of cooperative separation assurance resolutions severely reduces the resolution fuel cost and may not reflect actual controller clearances. Additionally, the assumption of perfect inter-sector coordination could be removed in the FFP1 case to more accurately reflect ATM time horizon limitations without EDA. Optimal time horizon and probability thresholds could also be computed from the model.



## Acronyms

---

AATT	Advanced Air Transportation Technologies
ACS	Acceptable Controller Spacing
AOC	Airline Operational Control Center
ARR	Arrival Operation
ARTCC	Air Route Traffic Control Center, also known as a Center
ATC	Air Traffic Control
ATL	Atlanta Hartsfield International Airport
ATM	Air Traffic Management
BADA	Eurocontrol Base of Aircraft Data
BOD	Bottom of Descent
BOS	Boston Logan International Airport
BWI	Baltimore-Washington International Airport
CA	Conflict Probe Correct Alert
CAS	Calibrated Airspeed
Center	Air Route Traffic Control Center (ARTCC)
cl	Climb flight mode
CLE	Cleveland Hopkins International Airport
CLT	Charlotte-Douglas International Airport
CPTP	CTAS EDA Conflict Prediction and Trial Planning
cr	Cruise flight mode
CTAS	Center/TRACON Automation System
CVG	Cincinnati/Northern Kentucky International Airport
d	Descent flight mode
DCA	Washington National Airport
DEN	Denver International Airport
DEP	Departure Operation
DFW	Dallas-Ft. Worth International Airport
DIR	Direct Routing
DST	Decision Support Tool
DSR	Display System Replacement

DTW	Detroit International Airport
EDA	CTAS En Route/Descent Advisor
EDX	En Route/Descent Advisor with Data Exchange
ETMS	Enhanced Traffic Management System
EWR	Newark International Airport
FA	Conflict Probe False Alert
FAA	Federal Aviation Administration
FANG	FMS-ATM Next Generation
FAR	Federal Aviation Regulations
FLL	Ft. Lauderdale-Hollywood International Airport
FFP1	FAA's Free Flight Phase 1 Program
FMS	Flight Management System
ft	feet
HOU	Houston Hobby International Airport
IAD	Washington Dulles International Airport
IAH	Houston-Intercontinental Airport
IFR	Instrument Flight Rules
ITWS	Integrated Terminal Weather Service
JFK	N.Y. Kennedy International Airport
kt	knot, nautical mile per hour
LAS	Las Vegas McCarran International Airport
LAX	Los Angeles International Airport
LGA	N.Y. LaGuardia Airport
LNAV	Lateral Navigation
MA	Conflict Probe Missed Alert
MCO	Orlando International Airport
MDW	Chicago Midway Airport
MEM	Memphis International Airport
MF	Metering Fix
MIA	Miami International Airport
MSP	Minneapolis-St. Paul International Airport
NAS	National Airspace System

NASA	National Aeronautics and Space Administration
nm	nautical mile
NOAA	National Oceanic and Atmospheric Administration
NRA	NASA Research Announcement
nm	nautical mile
OAK	Oakland International Airport
ORD	Chicago O'Hare International Airport
OVR	Overflight Operation
PAZ	Protected Airspace Zone
PCA	Point of Closest Approach
PDX	Portland International Airport
PHL	Philadelphia International Airport
PHX	Phoenix Sky Harbor International Airport
PIT	Greater Pittsburgh International Airport
RTA	Required Time of Arrival
rms	Root-Mean-Squared
rss	Root-Sum-Squared
RTO	Research Task Order
RUC	Rapid Update Cycle
SAN	San Diego International Airport
SEA	Seattle-Tacoma International Airport
SFO	San Francisco International Airport
SID	Standard Instrument Departure
SLC	Salt Lake City International Airport
SRC	System Resources Corporation
STA	Scheduled Time of Arrival
STAR	Standard Terminal Arrival Route
STL	St. Louis-Lambert International Airport
TMA	CTAS Traffic Management Advisor
TOD	Top of Descent
TRACON	Terminal Radar Approach Control
TS	CTAS Trajectory Synthesizer

TW	ITWS Terminal Winds Program
URET CCLD	User-Request Evaluation Tool, Core Capabilities Limited Deployment
VNAV	Vertical Navigation
Wx	Weather
ZAB	Albuquerque, NM ARTCC
ZAU	Chicago, IL ARTCC
ZBW	Nashau, NH ARTCC
ZDC	Leesburg, VA ARTCC
ZDV	Denver, CO ARTCC
ZFW	Ft. Worth, TX ARTCC
ZHU	Houston, TX ARTCC
ZID	Indianapolis, IN ARTCC
ZJX	Jacksonville, FL ARTCC
ZKC	Kansas City, KS ARTCC
ZLA	Los Angeles, CA ARTCC
ZLC	Salt Lake City, UT ARTCC
ZMA	Miami, FL ARTCC
ZME	Memphis, TN ARTCC
ZMP	Minneapolis, MN ARTCC
ZNY	New York, NY ARTCC
ZOA	Oakland, CA ARTCC
ZOB	Cleveland, OH ARTCC
ZSE	Seattle, WA ARTCC
ZTL	Atlanta, GA ARTCC

## Appendix A Modified Arrival Input Trajectories

---

In past studies [7-8] NASA-provided daily traffic sample of DFW, derived from NAS Enhanced Traffic Management System (ETMS) flight plans. In this study, the input undelayed DFW arrival trajectories were modified to represent more realistic profiles. This was motivated by long descents of the original data, which precluded the delay absorption strategies that primarily occur prior to TOD.

The trajectories were modified using a two-step process. Initially, a small sample of May 1997 ZFW radar track data [56] was analyzed to identify descent rates for four aircraft categories. These descent rates are shown in Table A.1. These rates were rounded, based on engineering judgement and sample size, and applied to the original input arrival trajectories. In applying the new descent rates to the arrival trajectories, the original flight waypoints and their times were not changed. Starting at the arrival metering fix (MF) or bottom of descent (BOD) waypoint, the descent rates were applied to determine the new waypoint altitudes, until the original cruise altitude was reached. This resulted in a new TOD location. Ground speed was then calculated for each segment based on the path distance between waypoints and waypoint crossing times. In validating the application method, the resulting speeds were assessed for reasonableness.

**Table A.1 DFW Radar-based Descent Rates**

Aircraft Category	MF* Altitude (ft)	Sample Size	Radar Descent Rate Range (ft/min)	Applied Descent Rate (ft/min)
Heavy Jets (B747)	10,000'	1	4064 ft/min	3000 ft/min
Large Jets ( MD80)	10,000'	5	2303 ft/min	2300 ft/min
Turboprops (E120)	7,000'	5	1938 ft/min	2000 ft/min
Piston Props (BE33)	3,000'	2	1188 ft/min	1200 ft/min

\* Altitudes were assigned at a point crossing a 40 nm ring around the airport, actual DFW arrival fixes vary from 28 (TACKE) to 46 (BAMBE/FEVER) nm.

As expected, the resulting modified arrival trajectories were found to have steeper descents and shorter descent times, as exhibited in Figures A.1 and A.2, respectively. Although the average modified descent time is slightly smaller than the 10-11 min descent cited by CTAS experts familiar with the ZFW airspace, Figure A.1 shows a spike of 10 minute descents. [23]

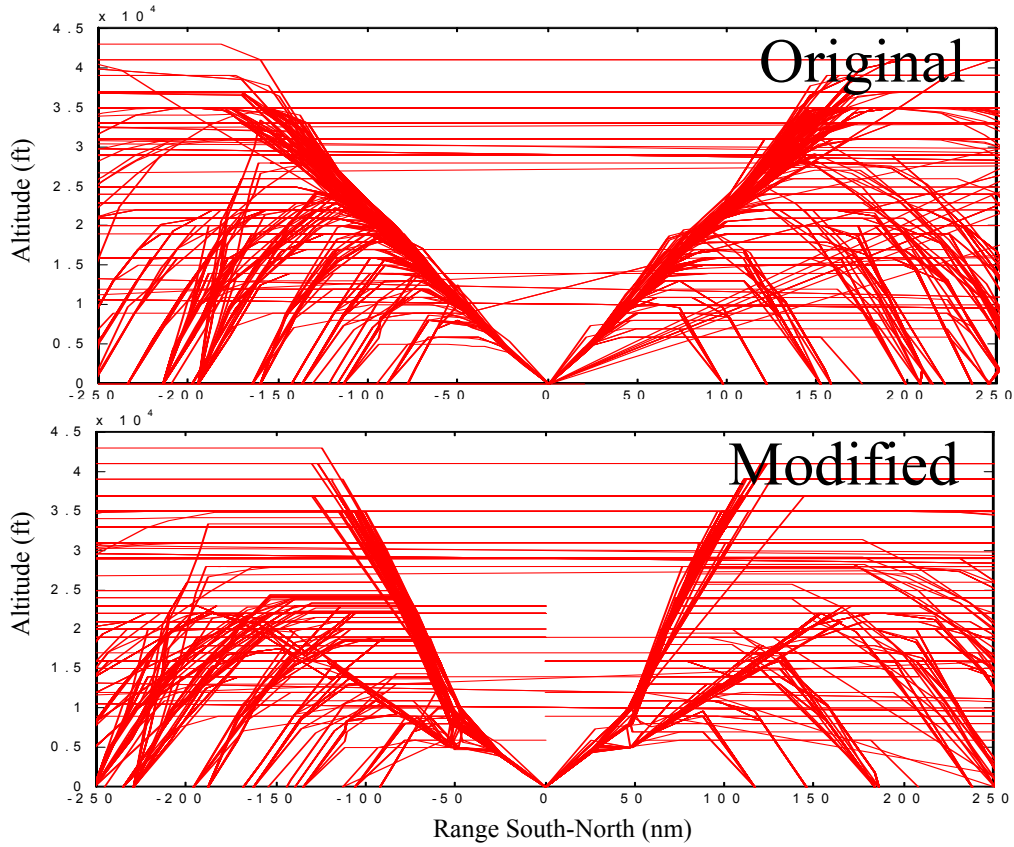


Figure A.1 Original and Modified DFW Arrival Trajectories

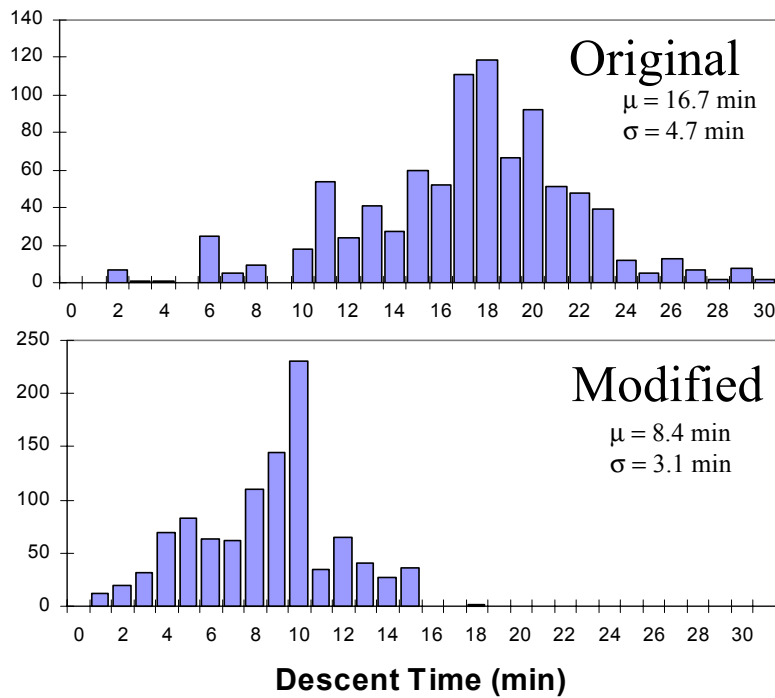


Figure A.2 Original and Modified DFW Arrival Descent Times

## Appendix B Aircraft Cost Rates and Fuelburn Rates

**Table B.1 Time and Fuelburn Rates by Aircraft Class**

Engine Type	Engine Num	A/C Size	A/C Class	FAA-Based Cost Rates (\$/hr)					Fuelburn* (lbs/min) Gd Hold (1)
				Time Cost			Fuel & Oil Cost		
				Crew	Maint.	Subtotal	Airborne	Ground**	
J	4	H	4JH	2,488	1,699	4,187	2,703	901	150
J	4	L	4JL	582	990	1,572	829	276	46
J	3	H	3JH	1,981	1,459	3,440	1,827	609	102
J	3	L	3JL	1,188	712	1,900	1,025	342	57
J	3	S+	3JS+	280	596	876	626	209	35
J	2	H	2JH	1,489	780	2,269	1,152	384	64
J	2	LH	2JLH	1,164	493	1,657	754	251	42
J	2	L	2JL	851	531	1,382	651	217	36
J	0	L	JL	701	527	1,228	593	198	33
J	2	LS	2JLS	551	523	1,074	535	178	30
J	2	S+	2JS+	251	515	766	420	140	23
J	0	S+	JS+	238	438	676	335	112	19
J	2	S	2JS	225	361	586	249	83	14
J	1	L	1JL	240	400	640	300	110	18
J	1	S+	1JS+	175	250	425	210	80	13
J	1	S	1JS	110	180	290	130	50	8
T	4	L	4TL	672	998	1,670	571	190	32
T	3	L	3TL	439	671	1,110	421	140	23
T	2	L	2TL	205	344	549	270	90	15
T	0	L	TL	203	324	527	226	75	13
T	2	S+	2TS+	201	303	504	181	60	10
T	0	S+	TS+	197	280	477	164	55	9
T	2	S	2TS	193	257	450	147	49	8
T	0	S	TS	155	199	354	128	43	7
T	1	S+	1TS+	117	140	257	109	36	6
T	1	S	1TS	114	110	224	103	34	6
P	4	L	4PL	250	275	525	500	167	28
P	3	S	3PS	220	245	465	445	148	25
P	2	L	2PL	190	215	405	390	130	22
P	2	S+	2PS+	200	204	404	193	64	11
P	0	S+	PS+	136	149	285	131	44	7
P	2	S	2PS	72	93	165	68	23	4
P	0	S	PS	72	77	149	57	19	3
P	1	S+	1PS+	72	60	132	45	15	3
P	1	S	1PS	72	27	99	22	7	1
(Rockwell I	0	0	SST	2,488	1,699	4,187	7,363	2,454	409
J	8	L	8JH	2,488	1,699	4,187	2,703	901	150

Consumer Price Index (CPI)

1982-84 base	100.0
1996	153.0

Oil & Gas Deflator

1992 base	100
1996	104.2

<u>Escalation Factor</u>		<u>Crew</u>	<u>Maint</u>	<u>Subtotal</u>	<u>Airbourne</u>	<u>Ground</u>
1996	1.000	1.000	1.000	1.000	1.000	1.000

Note: Shaded aircraft classes are interpolated/extrapolated from non-shaded values of FAA source.

\* Assumes Fuelcost of \$0.10/lb

\*\* Ground Fuel and oil cost is assumed to be 1/3 of airborne per advice of airline personnel.

Sources: FAA, "Economic Values for Evaluation of Federal Administration Investment and Regulatory Programs," Final Report FAA-APO-98-8, Office of Aviation Policy and Plans. (June 1998)

FAA, "FAA Aviation Forecasts Fiscal Years 1998-2009," Final Report FAA-APO-98-1, Office of Aviation Policy and Plans. (March 1998)

**Table B.2 B737 Fuelburn Rates from High-Fidelity Model Simulations**

Cruise Altitude (ft)	B737 Fuelburn (lbs/min)																			
	100	200	205	210	215	220	225	230	235	240	245	250	255	260	265	270	275			
1000	81.6	81.6	82.6	83.6	84.9	86.2	87.7	89.3	90.9	92.8	94.8	96.9	99.0	101.4	103.9	106.4	109.0			
11000	81.6	81.6	82.6	83.6	84.9	86.2	87.7	89.3	90.9	92.8	94.8	96.9	99.0	101.4	103.9	106.4	109.0			
13000	80.7	80.7	81.6	82.7	84.0	85.3	86.7	88.4	90.0	91.8	93.9	95.9	98.1	100.3	102.8	105.4	108.0			
15000	79.8	79.8	80.8	81.8	83.1	84.4	85.8	87.4	89.1	90.9	92.9	94.9	97.1	99.4	101.9	104.5	107.1			
17000	79.2	79.2	80.1	81.1	82.4	83.6	85.0	86.6	88.3	90.1	92.1	94.2	96.3	98.6	101.1	103.6	106.3			
19000	78.5	78.5	79.5	80.5	81.6	82.9	84.2	85.9	87.6	89.4	91.4	93.5	95.6	97.8	100.2	102.7	105.3			
21000	78.0	78.0	79.0	80.0	81.1	82.4	83.8	85.4	87.1	88.8	90.8	92.9	95.0	97.1	99.6	102.1	104.6			
23000	77.7	77.7	78.6	79.6	80.7	82.0	83.4	85.1	86.7	88.4	90.4	92.5	94.7	96.9	99.2	101.7	104.3			
25000	77.4	77.4	78.2	79.2	80.4	81.7	83.1	84.7	86.5	88.2	90.2	92.3	94.3	96.4	98.8	101.4	104.1			
27000	77.3	77.3	78.2	79.1	80.2	81.5	82.8	84.3	86.0	87.7	89.5	91.6	93.8	96.0	98.4	101.1	103.8			
29000	77.2	77.2	77.9	78.8	79.9	81.2	82.4	83.8	85.5	87.3	89.2	91.4	93.6	96.0	98.4	101.2	104.1			
31000	77.3	77.3	77.9	78.9	79.9	81.1	82.4	83.8	85.6	87.5	89.4	91.6	93.9	96.4	98.9	101.8	105.1			
33000	77.7	77.7	78.2	79.1	80.1	81.4	82.7	84.2	86.0	87.8	89.8	92.2	94.8	97.5	100.8	104.4	110.2			
35000	78.5	78.5	78.8	79.8	80.8	82.1	83.5	85.0	86.9	89.0	91.1	93.9	98.1	102.8	109.4	112.6	112.7			
37000	80.4	80.4	80.7	81.6	82.5	83.8	85.4	87.1	89.1	92.8	97.2	102.7	102.1	102.1	102.2	102.2	102.2			
39000	84.3	84.3	84.3	84.8	86.0	87.2	89.4	91.8	90.2	90.3	90.4	90.4	90.5	90.5	90.5	90.6	90.6			

Cruise Altitude (ft)	CAS Cruise Speed (kts)																			
	280	285	290	295	300	305	310	315	320	325	330	335	340	345	350	400				
1000	111.7	114.6	117.6	120.8	123.9	127.2	130.6	134.1	137.8	141.6	145.4	149.3	153.3	157.6	162.0	162.0				
11000	111.7	114.6	117.6	120.8	123.9	127.2	130.6	134.1	137.8	141.6	145.4	149.3	153.3	157.6	162.0	162.0				
13000	110.7	113.6	116.7	119.8	123.0	126.3	129.6	133.1	136.7	140.4	144.3	148.4	152.6	156.9	161.2	161.2				
15000	109.8	112.7	115.7	118.9	122.1	125.4	128.6	132.0	135.7	139.6	143.6	147.7	151.8	156.1	160.4	160.4				
17000	108.9	111.7	114.7	117.8	120.9	124.2	127.7	131.2	134.9	138.8	142.8	146.9	151.0	155.5	160.1	160.1				
19000	107.9	110.6	113.6	116.8	120.1	123.5	127.0	130.5	134.2	138.1	142.1	146.4	150.9	155.5	160.4	160.4				
21000	107.3	110.1	113.1	116.4	119.6	123.0	126.5	130.1	133.8	137.8	142.1	146.7	151.5	156.3	162.0	162.0				
23000	107.0	109.8	112.8	116.1	119.3	122.8	126.4	130.1	134.1	138.5	142.9	147.8	153.9	161.9	169.2	169.2				
25000	106.7	109.5	112.5	115.8	119.4	123.0	126.9	130.9	134.9	140.0	147.1	155.6	158.6	158.6	158.6	158.6				
27000	106.6	109.7	112.9	116.4	120.1	124.0	128.5	134.3	142.5	150.1	149.5	149.5	149.5	149.6	149.6	149.6				
29000	107.2	110.3	113.9	117.9	123.0	130.5	139.3	140.3	140.4	140.4	140.4	140.4	140.4	140.4	140.5	140.5				
31000	108.8	113.0	119.0	128.2	131.1	131.1	131.2	131.2	131.2	131.2	131.2	131.3	131.3	131.3	131.3	131.3				
33000	118.7	121.6	121.7	121.7	121.7	121.7	121.8	121.8	121.8	121.8	121.8	121.8	121.8	121.8	121.9	121.9				
35000	112.7	112.7	112.7	112.8	112.8	112.8	112.8	112.8	112.9	112.9	112.9	112.9	112.9	112.9	112.9	112.9				
37000	102.3	102.3	102.3	102.3	102.4	102.4	102.4	102.4	102.4	102.4	102.5	102.5	102.5	102.5	102.5	102.5				
39000	90.6	90.7	90.7	90.7	90.7	90.7	90.8	90.8	90.8	90.8	90.8	90.8	90.8	90.9	90.9	90.9				



**Table B.4 Cruise Fuelburn by Altitude and Aircraft Class [21]**

FL	Aircraft Class: Allased Class:																		
	4J/H	4J/L	3J/H	3J/L	3J/S+	2J/H	2J/LH	2J/L	J/L	2J/LS	2J/S+	J/S+	2J/S	1J/L	1J/S+	1J/S	4T/L	3T/L	
0	na	na	na	na	na	na	na	na	na	na	na	na	na	na	na	na	na	na	na
5	na	na	na	na	na	na	na	na	na	na	na	na	na	na	na	na	na	na	na
10	na	na	na	na	na	na	na	na	na	na	na	na	na	na	na	na	na	na	na
15	na	na	na	na	na	na	na	na	na	na	na	na	na	na	na	na	na	na	na
20	na	na	na	na	na	na	na	na	na	na	na	na	na	na	na	na	na	na	na
30	145.5	45.8	80.3	37.1	16.1	86.0	53.1	30.3	30.3	26.0	11.7	11.7	7.1	11.7	7.1	7.1	40.4	10.7	
40	145.5	45.3	80.9	37.4	16.1	86.2	53.2	30.4	30.4	26.0	11.6	11.6	7.2	11.6	7.2	7.2	41.0	10.8	
60	145.4	44.2	82.1	38.0	16.0	86.4	53.5	30.6	30.6	26.0	11.5	11.5	7.4	11.5	7.4	7.4	42.3	10.9	
80	145.4	43.2	83.3	38.6	16.0	86.6	53.7	30.8	30.8	26.1	11.3	11.3	7.6	11.3	7.6	7.6	43.6	11.1	
100	145.3	42.2	84.6	39.2	16.0	86.8	53.9	31.0	31.0	26.1	11.2	11.2	7.8	11.2	7.8	7.8	44.9	11.3	
120	166.2	53.8	115.0	56.4	21.0	100.3	59.8	37.6	37.6	31.2	13.9	13.9	7.9	13.9	7.9	7.9	46.4	11.4	
140	165.7	54.4	116.6	57.1	20.9	100.4	60.0	37.8	37.8	31.1	14.0	14.0	8.2	14.0	8.2	8.2	47.8	11.6	
160	165.2	55.1	118.2	57.9	20.8	100.5	60.3	38.0	38.0	31.1	14.1	14.1	8.4	14.1	8.4	8.4	49.4	11.5	
180	164.6	55.7	119.8	58.8	20.6	100.6	60.5	38.1	38.1	31.1	14.2	14.2	8.6	14.2	8.6	8.6	51.0	11.5	
200	164.0	56.4	121.4	59.6	20.5	100.8	60.7	38.4	38.4	31.1	14.3	14.3	8.8	14.3	8.8	8.8	52.6	11.2	
220	163.4	57.0	123.1	60.5	20.4	100.8	60.9	38.6	38.6	31.1	14.4	14.4	9.0	14.4	9.0	9.0	54.4	10.8	
240	162.7	57.7	124.8	61.3	20.2	100.9	61.1	38.8	38.8	30.9	14.4	14.4	9.3	14.4	9.3	9.3	56.2	10.4	
260	161.9	57.1	126.3	60.7	20.1	100.9	61.4	38.6	38.6	30.0	14.4	14.4	9.5	14.4	9.5	9.5	56.4	10.0	
280	159.3	56.3	124.8	59.8	19.4	101.0	61.6	38.0	38.0	28.9	14.1	14.1	9.8	14.1	9.8	9.8	56.1	9.0	
300	157.0	55.5	122.1	59.1	18.1	100.7	61.8	37.0	37.0	27.5	13.6	13.6	10.1	13.6	10.1	10.1	55.8	8.7	
320	154.1	53.1	119.9	57.4	16.9	98.4	60.9	35.9	35.9	26.4	13.1	13.1	10.3	13.1	10.3	10.3	54.8	6.9	
340	151.3	50.4	116.3	55.0	15.8	96.0	59.5	34.8	34.8	25.4	12.5	12.5	10.1	12.5	10.1	10.1	52.2	6.6	
360	148.0	48.1	113.8	53.0	14.8	93.6	58.6	33.8	33.8	24.7	11.9	11.9	9.7	11.9	9.7	9.7	49.7	5.9	
380	144.8	46.5	112.9	50.3	14.0	92.0	58.4	33.2	33.2	24.2	11.5	11.5	9.4	11.5	9.4	9.4	47.6	4.1	
400	139.1	45.3	111.8	47.8	13.3	91.2	58.8	32.0	32.0	23.9	11.1	11.1	8.7	11.1	8.7	8.7	45.6	4.0	

FL	Aircraft Class: Allased Class:																		
	2T/L	T/L	2T/S+	T/S+	2T/S	T/S	1T/S+	1T/S	4P/L	3P/S	2P/L	2P/S+	2P/S	2P/S	1P/S+	1P/S	4J/H	3J/H	
0	na	na	na	na	na	na	na	na	na	na	na	na	na	na	na	na	na	na	na
5	na	na	na	na	na	na	na	na	na	na	na	na	na	na	na	na	na	na	na
10	na	na	na	na	na	na	na	na	na	na	na	na	na	na	na	na	na	na	na
15	na	na	na	na	na	na	na	na	na	na	na	na	na	na	na	na	na	na	na
20	na	na	na	na	na	na	na	na	na	na	na	na	na	na	na	na	na	na	na
30	10.7	10.7	6.0	6.0	4.3	4.3	4.3	4.3	2.5	2.5	2.5	2.5	2.5	2.5	2.5	2.5	145.5	145.5	
40	10.8	10.8	6.1	6.1	4.3	4.3	4.3	4.3	2.5	2.5	2.5	2.5	2.5	2.5	2.5	2.5	145.5	145.5	
60	10.9	10.9	6.3	6.3	4.4	4.4	4.4	4.4	2.5	2.5	2.5	2.5	2.5	2.5	2.5	2.5	145.4	145.4	
80	11.1	11.1	6.5	6.5	4.4	4.4	4.4	4.4	2.5	2.5	2.5	2.5	2.5	2.5	2.5	2.5	145.4	145.4	
100	11.3	11.3	6.7	6.7	4.4	4.4	4.4	4.4	2.5	2.5	2.5	2.5	2.5	2.5	2.5	2.5	145.3	145.3	
120	11.4	11.4	6.6	6.6	3.9	3.9	3.9	3.9	2.5	2.5	2.5	2.5	2.5	2.5	2.5	2.5	166.2	166.2	
140	11.6	11.6	6.5	6.5	3.9	3.9	3.9	3.9	2.5	2.5	2.5	2.5	2.5	2.5	2.5	2.5	165.7	165.7	
160	11.5	11.5	6.5	6.5	3.9	3.9	3.9	3.9	2.5	2.5	2.5	2.5	2.5	2.5	2.5	2.5	165.2	165.2	
180	11.5	11.5	6.3	6.3	3.8	3.8	3.8	3.8	2.5	2.5	2.5	2.5	2.5	2.5	2.5	2.5	164.6	164.6	
200	11.2	11.2	6.0	6.0	3.6	3.6	3.6	3.6	1.8	1.8	1.8	1.8	1.8	1.8	1.8	1.8	164.0	164.0	
220	10.8	10.8	5.8	5.8	3.5	3.5	3.5	3.5	1.8	1.8	1.8	1.8	1.8	1.8	1.8	1.8	163.4	163.4	
240	10.4	10.4	5.6	5.6	3.3	3.3	3.3	3.3	1.8	1.8	1.8	1.8	1.8	1.8	1.8	1.8	162.7	162.7	
260	10.0	10.0	5.4	5.4	3.2	3.2	3.2	3.2	1.4	1.4	1.4	1.4	1.4	1.4	1.4	1.4	161.9	161.9	
280	9.0	9.0	5.2	5.2	3.1	3.1	3.1	3.1	1.4	1.4	1.4	1.4	1.4	1.4	1.4	1.4	159.3	159.3	
300	8.7	8.7	5.0	5.0	3.0	3.0	3.0	3.0	1.4	1.4	1.4	1.4	1.4	1.4	1.4	1.4	157.0	157.0	
320	6.9	6.9	4.0	4.0	2.9	2.9	2.9	2.9	0.7	0.7	0.7	0.7	0.7	0.7	0.7	0.7	154.1	154.1	
340	6.6	6.6	1.8	1.8	2.8	2.8	2.8	2.8	0.7	0.7	0.7	0.7	0.7	0.7	0.7	0.7	151.3	151.3	
360	5.9	5.9	1.7	1.7	2.7	2.7	2.7	2.7	0.7	0.7	0.7	0.7	0.7	0.7	0.7	0.7	148.0	148.0	
380	4.1	4.1	1.7	1.7	2.6	2.6	2.6	2.6	0.6	0.6	0.6	0.6	0.6	0.6	0.6	0.6	144.8	144.8	
400	4.0	4.0	1.7	1.7	2.2	2.2	2.2	2.2	0.6	0.6	0.6	0.6	0.6	0.6	0.6	0.6	139.1	139.1	

Table B.5 Descent Fuelburn by Altitude and Aircraft Class [21]

FL	Aircraft Class: Allased Class:										Fuel Burn Rate (kg/m in)									
	4J/H	4J/L	3J/H	3J/L	3J/S+	2J/H	2J/LH	2J/L	J/L	2J/LS	2J/S+	J/S+	2J/S	1J/L	1J/S+	1J/S	4T/L	3T/L		
0	40.2	43.5	37.6	22.7	13.9	25.0	18.4	11.9	11.9	15.1	9.8	9.8	4.2	9.8	4.2	4.2	18.1	6.6		
5	39.9	43.2	37.3	22.7	13.7	24.9	18.3	11.9	11.9	15.1	9.7	9.7	4.2	9.7	4.2	4.2	18.0	6.5		
10	39.5	42.9	37.1	22.6	13.5	24.7	18.3	11.9	11.9	15.1	9.6	9.6	4.2	9.6	4.2	4.2	17.8	6.5		
15	39.2	42.6	36.8	22.6	13.3	24.6	18.3	11.9	11.9	15.1	9.5	9.5	4.2	9.5	4.2	4.2	17.7	6.5		
20	38.9	42.2	36.5	22.5	13.1	24.4	18.2	11.9	11.9	15.1	9.4	9.4	4.2	9.4	4.2	4.2	17.6	6.5		
30	38.3	41.5	35.9	22.4	12.7	24.1	18.2	11.8	11.8	15.0	9.2	9.2	4.2	9.2	4.2	4.2	17.3	6.4		
40	37.6	40.9	35.3	22.3	12.3	23.8	18.1	11.8	11.8	14.9	9.1	9.1	4.2	9.1	4.2	4.2	17.1	6.4		
60	36.2	39.6	34.2	22.1	11.5	23.3	18.0	11.8	11.8	14.9	8.7	8.7	4.1	8.7	4.1	4.1	16.6	6.3		
80	34.9	38.2	33.0	21.9	10.7	22.7	17.9	11.7	11.7	14.9	8.3	8.3	4.1	8.3	4.1	4.1	16.1	6.2		
100	33.5	36.9	31.9	21.7	10.0	22.1	17.7	11.7	11.7	14.8	8.0	8.0	4.1	8.0	4.1	4.1	15.6	6.1		
120	32.2	35.6	30.8	21.5	9.2	21.5	17.6	11.7	11.7	14.7	7.6	7.6	4.0	7.6	4.0	4.0	15.1	6.0		
140	30.8	34.3	29.6	21.3	8.4	20.9	17.5	11.6	11.6	14.7	7.2	7.2	4.0	7.2	4.0	4.0	14.6	5.9		
160	29.5	33.0	28.5	21.1	7.6	20.4	17.4	11.6	11.6	14.6	6.8	6.8	4.0	6.8	4.0	4.0	14.1	6.0		
180	28.1	31.7	27.3	20.9	6.9	19.8	17.2	11.5	11.5	14.5	6.5	6.5	4.0	6.5	4.0	4.0	13.6	6.0		
200	25.8	30.4	26.2	20.7	6.5	19.2	17.1	11.5	11.5	14.4	6.1	6.1	3.9	6.1	3.9	3.9	13.1	5.9		
220	24.4	29.0	25.0	20.5	6.2	18.6	17.0	11.5	11.5	14.4	5.9	5.9	3.9	5.9	3.9	3.9	12.6	5.8		
240	23.1	27.7	23.9	20.3	5.9	18.0	16.9	11.4	11.4	14.3	5.6	5.6	3.9	5.6	3.9	3.9	12.1	5.7		
260	21.7	26.4	22.7	20.1	5.6	17.5	16.7	11.3	11.3	14.2	5.3	5.3	5.4	5.3	5.4	5.4	11.6	5.6		
280	20.4	25.1	21.6	19.9	5.4	16.8	16.6	11.2	11.2	14.2	6.6	6.6	5.2	6.6	5.2	5.2	11.1	5.6		
300	40.4	23.7	20.4	19.7	5.1	16.3	16.5	16.4	16.4	14.1	7.9	7.9	4.9	7.9	4.9	4.9	10.6	5.0		
320	37.7	22.4	19.3	19.5	4.9	15.7	16.3	15.8	15.8	17.2	7.7	7.7	4.5	7.7	4.5	4.5	10.1	4.0		
340	35.0	21.1	18.2	19.3	4.6	15.1	16.2	15.2	15.2	16.8	7.3	7.3	4.2	7.3	4.2	4.2	9.6	4.0		
360	52.8	19.8	17.0	19.1	4.4	15.1	16.1	14.6	14.6	16.4	6.9	6.9	3.9	6.9	3.9	3.9	9.1	3.6		
380	48.8	18.5	15.9	18.9	4.2	14.3	16.0	14.1	14.1	16.0	6.6	6.6	3.6	6.6	3.6	3.6	8.6	2.7		
400	44.7	17.1	14.7	18.7	4.0	13.6	15.8	13.6	13.6	15.7	6.4	6.4	3.6	6.4	3.6	3.6	8.1	2.7		

FL	Aircraft Class: Allased Class:										Fuel Burn Rate (kg/m in)									
	2T/L	T/L	2T/S+	T/S+	2T/S	T/S	1T/S+	1T/S	4P/L	3P/S	2P/L	2P/S+	2P/S	2P/S	1P/S+	1P/S	8J/H	SST		
0	6.6	6.6	4.5	4.5	3.2	3.2	3.2	3.2	1.0	1.0	1.0	1.0	1.0	1.0	1.0	0.3	40.2			
5	6.5	6.5	4.5	4.5	3.2	3.2	3.2	3.2	1.0	1.0	1.0	1.0	1.0	1.0	1.0	0.3	39.9			
10	6.5	6.5	4.5	4.5	3.2	3.2	3.2	3.2	1.0	1.0	1.0	1.0	1.0	1.0	1.0	0.3	39.5			
15	6.5	6.5	4.5	4.5	3.2	3.2	3.2	3.2	1.0	1.0	1.0	1.0	1.0	1.0	1.0	0.3	39.2			
20	6.5	6.5	4.4	4.4	3.1	3.1	3.1	3.1	1.0	1.0	1.0	1.0	1.0	1.0	1.0	0.3	38.9			
30	6.4	6.4	4.4	4.4	3.1	3.1	3.1	3.1	1.0	1.0	1.0	1.0	1.0	1.0	1.0	0.3	38.3			
40	6.4	6.4	4.4	4.4	3.0	3.0	3.0	3.0	1.0	1.0	1.0	1.0	1.0	1.0	1.0	0.3	37.6			
60	6.3	6.3	4.3	4.3	2.9	2.9	2.9	2.9	1.0	1.0	1.0	1.0	1.0	1.0	1.0	0.3	36.2			
80	6.2	6.2	4.2	4.2	2.8	2.8	2.8	2.8	1.0	1.0	1.0	1.0	1.0	1.0	1.0	0.3	34.9			
100	6.1	6.1	4.1	4.1	2.7	2.7	2.7	2.7	1.0	1.0	1.0	1.0	1.0	1.0	1.0	0.3	33.5			
120	6.0	6.0	4.1	4.1	2.6	2.6	2.6	2.6	1.0	1.0	1.0	1.0	1.0	1.0	1.0	0.3	32.2			
140	5.9	5.9	4.0	4.0	2.5	2.5	2.5	2.5	1.0	1.0	1.0	1.0	1.0	1.0	1.0	0.3	30.8			
160	6.0	6.0	3.9	3.9	2.4	2.4	2.4	2.4	1.0	1.0	1.0	1.0	1.0	1.0	1.0	0.3	29.5			
180	6.0	6.0	3.9	3.9	2.3	2.3	2.3	2.3	1.0	1.0	1.0	1.0	1.0	1.0	1.0	na	28.1			
200	5.9	5.9	3.8	3.8	2.2	2.2	2.2	2.2	0.7	0.7	0.7	0.7	0.7	0.7	na	25.8				
220	5.8	5.8	3.7	3.7	2.1	2.1	2.1	2.1	0.7	0.7	0.7	0.7	0.7	na	na	24.4				
240	5.7	5.7	3.6	3.6	1.9	1.9	1.9	1.9	0.7	0.7	0.7	0.7	0.7	na	na	23.1				
260	5.6	5.6	3.6	3.6	1.8	1.8	1.8	1.8	0.5	0.5	0.5	0.5	0.5	na	na	21.7				
280	5.0	5.0	3.5	3.5	1.7	1.7	1.7	1.7	0.5	0.5	0.5	0.5	0.5	na	na	20.4				
300	5.0	5.0	3.4	3.4	1.6	1.6	1.6	1.6	0.5	0.5	0.5	0.5	0.5	na	na	40.4				
320	4.0	4.0	2.7	2.7	1.5	1.5	1.5	1.5	0.3	0.3	0.3	0.3	0.3	na	na	37.7				
340	4.0	4.0	1.3	1.3	1.3	1.3	1.3	1.3	0.3	0.3	0.3	0.3	0.3	na	na	35.0				
360	3.6	3.6	1.3	1.3	1.2	1.2	1.2	1.2	0.3	0.3	0.3	0.3	0.3	na	na	52.8				
380	2.7	2.7	1.3	1.3	1.1	1.1	1.1	1.1	na	na	na	na	na	na	na	48.8				
400	2.7	2.7	1.3	1.3	0.9	0.9	0.9	0.9	na	na	na	na	na	na	na	44.7				



## Appendix C ATM Trajectory Accuracy Equations Derivation

---

This appendix details the derivation of the equations to calculate the ATM Trajectory Prediction Accuracy used in the ATM Interruptions Model. This includes the flight-mode specific ATM trajectory prediction equations and an input to these equations, the maneuver timing error. Maneuver timing error model is derived and the source of supporting model coefficients is discussed.

### ATM Trajectory Prediction Accuracy Model

The trajectory prediction accuracy of the Conflict Probe depends on the current position and velocity (initial condition) errors and the uncertainties in the trajectory prediction that occur between the current time and the desired end point. In general, the desired endpoint for cruise is the TOD, for descent it is the (MF), and for climb it is the TOC. For a conflict probe calculation, the endpoint may lie beyond these maneuver completion times.

In addition to the initial condition errors, there are the wind errors, and the speed adherence or so-called Flight Technical Errors (FTE). If the aircraft is maneuvering, such as climbing to its cruise altitude or descending from its cruise altitude to the meter fix, additional prediction errors occur. Finally, the crosstrack errors can in general be ignored as secondary contributors for an FMS-guided aircraft.

A convenient mathematical model for determining the along-track position error of one aircraft at a certain point into the future (look-ahead time) can be described by:

$$\sigma_{P, Pred}(t_{Pred}) = \sqrt{\sigma_P^2(t) + (t_{Pred} - t)^2 \sigma_V^2(t)} \quad (C1)$$

where,

$\sigma_P, \sigma_{P, Pred}$	= standard deviation of current and predicted (relative) position error
$\sigma_V$	= standard deviation of the current velocity error
$t, t_{Pred}$	= current and look-ahead time

For two aircraft (1 and 2), the relative position error, based on equation (C1), at specified look-ahead time is:

$$\sigma_{P, Pred}(t_{Pred}) = \sqrt{[\sigma_{P1}^2(t) + \sigma_{P2}^2(t)] + (t_{Pred} - t)^2 [\sigma_{V1}^2(t) + \sigma_{V2}^2(t)]} \quad (C2)$$

These equations assume that the position and velocity errors of a single aircraft and between aircraft are not correlated. Based on the evaluation of actual aircraft cruise flight pseudo-conflicts, reference [57] established that the relative rms prediction error takes the form:

$$rms_{P, Pred}(t_{Pred}) = (0.333 \text{ nm}) + (t_{Pred} - t)(0.223 \text{ nm/min}) \quad (C3)$$

Equation (C3) suggests that a correlated model is the more correct form for the conflict probe relative position prediction errors. Correlation between the aircraft position and velocity errors may result from use of the same radar to track both aircraft, negligible relative wind error (strongly correlation) and negligible FTE error with FMS-guided aircraft. The unexpected field test results in [57] should be examined further, possibly leading to alternate formulations for Equation (C2). For the present, (C1-C2) will assumed to be the best representation of the errors for one or two aircraft, respectively.

To account for all the errors of one aircraft, Equation (C1) can be modified for three scenarios as follows:

1) No maneuver:

$$\sigma_{P, Pred}(t_{Pred}) = \sqrt{[\sigma_{P,S}^2(t)] + (t_{Pred} - t)^2 [\sigma_{V,S}^2(t) + \sigma_{V,W}^2(t) + \sigma_{V,FTE}^2(t)]} \quad (C4)$$

2) During a maneuver:

$$\sigma_{P, Pred}(t_{Pred}) = \sqrt{[V_M^2(t_{Pred}) \sigma_{t,M}^2(t_{Pred}) - V_M^2(t) \sigma_{t,M}^2(t)]} \quad (C5)$$

3) After a maneuver:

$$\sigma_{P, Pred}(t_{Pred}) = \sqrt{[V_{M,Ave}^2 \sigma_{t,M}^2(t_{M,f})] + (t_{Pred} - t_{M,f})^2 [\sigma_{V,S}^2(t_{M,f}) + \sigma_{V,W}^2(t_{M,f}) + \sigma_{V,FTE}^2(t_{M,f})]} \quad (C6)$$

where,  $\sigma_{P,S}, \sigma_{V,S}$  = standard deviation of the surveillance position and velocity error  
 $V_M, V_{M,Ave}$  = speed during maneuver and average speed during a maneuver  
 $t_{M,f}, \sigma_{t,M}$  = maneuver completion time and standard deviation of maneuver time delay error (e.g.: meter fix crossing time error following descent)  
 $\sigma_{V,M}, \sigma_{V,W}, \sigma_{V,FTE}$  = standard deviation of the maneuver, wind and flight technical (speed adherence) velocity error

For the no maneuver case, the conflict probe position standard deviation at the look-ahead time depends on the surveillance initial position and velocity errors, the wind speed errors, and the FTE speed adherence errors. This was the equation used for the cruise phase of flight.

For the second case the difference between the position errors at the start of the conflict probe calculation and the position errors at the end of the maneuver are the major contributors. Note that the surveillance errors, wind speed errors, and FTE errors are not separately included, since they are included in the maneuver time delay error calculation.

For the position prediction errors occurring after a maneuver, the maneuver time delay errors have to be converted into position error. Since the conflict probe calculation can be performed anytime during this maneuver, it is reasonable to use have the delay error at the midpoint of the maneuver to perform this calculation. This assumes that the error

grows linearly from the start to the end of the maneuver. The time delay error is then converted into a position error using the average speed of the aircraft.

Since the surveillance position error is included in the maneuver time delay error, it is not included in (C6). All the velocity errors are propagated from the midpoint of the maneuver to the look-ahead time. Based on the weight dispersion results presented in [31] for eleven aircraft, the average climb time from the arrival metering fix to the TOC is 20 minutes. A reasonable estimate for the descent from TOD to the departure metering fix is 9 minutes, based on [32]. Equation (C6) was used to determine conflict probe position error for the climb and descent phase. Also, reasonable estimates for the average speed during the climb or descend maneuver is approximately 350 kts. This is based on an average MF crossing speed of 280 kts and a TOD/TOC speed of 415 kts.

### Maneuver Time Error Model

The en route CTAS Decision Support Tools (DSTs) depend heavily on predicting the aircraft time of flight, based on the aircraft's current position and velocity, as measured by the Secondary Surveillance Radar. The DSTs then use simplified models that describe the expected aircraft dynamics for the various phases of flight. These phases include climbing to cruise altitude, the cruise phase prior to descent, and the descent phase to the meter fix crossing. The time of flight can be expressed as a function of all the parameters that determine its value:

$$\tau(t) = f(t, p_1, p_2, \dots, p_N) \quad (C7)$$

where,  $\tau$  = estimated time of arrival (ETA) – at TOC, TOD, or meter fix  
 $t$  = current time  
 $p_i$  =  $i$ 'th parameters that contribute to the ETA, such as weight, thrust, drag, etc.  
 $f$  = non-linear function describing ETA changes with different input parameters

To determine the errors in the ETA, (C7) can be used together with a Taylor Series expansion about the nominal parameters and ETA to obtain:

$$\delta\tau(t) \cong \left( \frac{\partial f(t, p_1, p_2, \dots, p_N)}{\partial p_1} \right) \delta p_1 + \left( \frac{\partial f(t, p_1, p_2, \dots, p_N)}{\partial p_2} \right) \delta p_2 + \dots + \left( \frac{\partial f(t, p_1, p_2, \dots, p_N)}{\partial p_N} \right) \delta p_N \quad (C8)$$

The partial derivatives in (C8) can be determined analytically from the equations of motion that describe the aircraft trajectory and any guidance laws and constraints. Alternately, they can be treated as unknown parameters and determined using an aircraft simulation based on (C7). In the latter case, the simulation would determine the ETA for various nominal and perturbed values of the input parameters,  $p$ . With this latter approach, (C8) would be expressed as:

$$\delta\tau \cong A_1 \delta p_1 + A_2 \delta p_2 + \dots + A_N \delta p_N \quad (C9)$$

The mean ETA error is then:

$$\mu_{\tau} = A_1\mu_{p1} + A_2\mu_{p2} + \dots + A_N\mu_{pN} \tag{C10}$$

The variance of the ETA error is:

$$\sigma_{\tau}^2 = A_1^2\sigma_{p1}^2 + A_2^2\sigma_{p2}^2 + \dots + A_N^2\sigma_{pN}^2 + B_{12}\sigma_{p1}\sigma_{p2} + B_{13}\sigma_{p1}\sigma_{p3} + \dots + B_{N-1,N}\sigma_{pN-1}\sigma_{pN-1} \tag{C11}$$

While the coefficients  $A_i$  are the same in both (C10) and (C11), the  $B_i$  coefficients are a function of the  $A_i$  and the unknown correlation coefficient between the  $\delta p_i$ . For simplicity, the correlation coefficient and  $A_i$  coefficients were combined into a single  $B_i$  coefficient.

If the  $B_i$  coefficients are ignored, then it is assumed that the parameters have small correlation, a typical assumption if the correlation coefficients are unknown. Finally, if the mean and error standard deviation is combined into a root-mean-square (*rms*) error, (C11) can be used by replacing the  $\sigma$  with the *rms* values.

Estimates of the  $A_i$  coefficients for various  $\delta p_i$  parameters are summarized in Table C.1, based on various references. Specifically, the first column summarizes the parameters that have been shown to influence the descent phase of flight. The coefficients are summarized in the remaining columns.

**Table C.1 Dispersion of Trajectory Sensitivities/Partial Derivatives**

Error Parameter ( $p_i$ )	Units	Error Partial Derivatives ( $A_i$ )			
		Descent [33] (sec)	Descent[32] (sec)	Climb[3] (sec/nm)	Climb[58] (sec/nm)
Aircraft Weight	%	0.8837	0.69 sec	39.2 (sec) 4.46 (nm)	16.0 (sec) 1.43 (nm)
Aircraft Thrust	%			0.471 (nm)	
Aircraft Drag	%	-1.3881	-0.96 sec		
TOD Placement	nm	4.0759	2.2 sec	N/A	N/A
Speed Adherence	kts	1.4609	1.4 sec	1.28 (nm)	
Cross-Track Wander	nm	1.7723			
Navigation Bias	deg	-1.9366			
Turn Dynamics	sec	-1.1124			
Wind Forecast	kts	0.9483	3.6 sec		0.425 (nm)
Temperature Forecast	Deg C	4.6186	2.7 sec		6 (sec) or 1 (nm)
Pressure Forecast	In Hg		7.0 sec		
Surveillance	kts	0.2578			

The parameters that determine the aircraft navigation dynamics are the weight, thrust, drag, wind, and temperature. For the descent phase of flight, the weight at the Top of Descent (TOD) is required. The weight for climb generally is the aircraft takeoff weight.

The parameters that determine the aircraft guidance and control are the TOD placement, the speed adherence, the cross-track wander, the navigation bias, and the turn dynamics.

Finally, the principal parameter that initializes the trajectory prediction calculation is the radar surveillance measurement of the current aircraft ground speed.

All of the partial derivatives that are presented in Table C.1 are based on sophisticated simulation of specific aircraft to determine the ETA or position error at either TOC for the climb phase or the metering fix for the descent phase. The relationship between position error and time of flight error can be determined by dividing the resulting TOC position error by the TOC aircraft speed to get the TOC ETA error. The meter fix position error can, in like manner, be converted into a meter fix ETA error by dividing the position error with the meter fix crossing speed.

The difference in sign for some of the coefficients reflects the fact that a positive error in that parameter with a negative coefficient means that the ETA error will be negative. For the  $\sigma$  or rms calculations, the sign does not matter since the coefficients are squared.

Reference [33] provides the most complete set of coefficients, however only for the descent phase. These coefficients were obtained using a generic aircraft model. Reference [32] is based on using a B757 aircraft model. Reference [31] used a collection of eleven aircraft to determine the weight partial derivatives as summarized in Table C.2. For the thrust coefficient, a B727 model was used while for the speed adherence, a B767 model was used.

**Table C.2 TOC Dispersions Due to Jet Aircraft Weight Dispersions3 (%)**

Aircraft	Mean Weight (lb)	Cruise Flight Level	TOC Time Partial* (sec/%)	Mean Speed# (kts)	TOC Path Partial** (nm/%)
B727	159,700	330	14.7	436	1.78
B737	118,500	290	35.5	404	3.98
B747	567,700	270	163.3	399	18.1
B757	192,500	340	24.3	449	3.03
B767	341,800	350	14.6	436	1.77
B777	424,400	340	57.4	433	6.91
DC10	448,100	320	32.9	384	3.51
A319	126,000	350	8.45	409	0.960
F100	87,400	310	24.9	408	2.82
MD11	416,500	320	27.0	400	3.00
MD80	129,900	310	28.6	410	3.26
<b>Fleet-Weighted Average:</b>			<b>24.2</b>	<b>414</b>	<b>2.78</b>

(1) Weighted Average using fleet mix of DFW airline. [8]

# (TOC Path Partial)/(TOC Time Partial/3600 sec)

$$* \left( \frac{\partial t_{TOC}}{\partial w_0} \right) = (t_{TOC,max} - t_{TOC,min}) \left( \frac{0.5(w_{0,max} + w_{0,min})}{100(w_{0,max} - w_{0,min})} \right), \text{ (seconds/percent)} \quad (C12)$$

$$* * \left( \frac{\partial s_{TOC}}{\partial w_0} \right) = (s_{TOC,max} - s_{TOC,min}) \left( \frac{0.5(w_{0,max} + w_{0,min})}{100(w_{0,max} - w_{0,min})} \right), \text{ (nautical miles/percent)} \quad (C13)$$

The weight coefficient from [58] is based on three jet aircraft (EA62, B747, and B767) while the wind coefficient on two aircraft (EA62 and B747), and the temperature

sensitivity is based on one aircraft (EA62). From the collection of partial derivatives in Table C.1, the baseline partial derivatives were selected that are presented in Table C.3 and in the body of the report.

**Table C.3. Assumed Trajectory Sensitivities/Partial Derivatives**

Error Model	Trajectory Error Partial Derivative		
	<u>Units</u>	<u>Climb</u>	<u>Descent</u>
<u>Parameter</u>			
Initial Weight	sec/%	24.2	0.88
(Thrust - Drag)	sec/%	4.08*	1.39
TOD Placement	sec/nm	8.67*	4.08
Speed. Adhere.	sec/kt	11.1*	1.46
X-Track Wander	sec/nm		1.77
A/C Nav. Bias	sec/deg		1.94
Turn Dynamic	sec/sec		1.11
Wind Forecast	sec/kt	3.7*	0.95
Temp. Forecast	sec/°C	8.7*	4.62
Surveillance	sec/kt		0.26

\* Path distance errors at TOC converted to time error based on speed of 415 kts at TOC

## Appendix D ATM Trajectory Prediction Accuracy Errors

---

This Appendix presents the error statistics that are required to determine the ATM trajectory prediction performance of climb, cruise, and descent flight modes. Using these statistics, estimates will be made for the improved performance that can be obtained if key parameters are provided in a more timely manner or from more recent sources, such as the cockpit.

The statistics will be presented in the form of the mean error, the standard deviation ( $\sigma$ ) of the error, and either the root-sum-square (rss) or root-mean-square (rms) error. If the square root is taken of the average sum of the errors squared, the rms is obtained. The same value will be obtained by taking the square root of the sum of the square of the mean and the square of the standard deviation. Hence, the rss and rms will be used interchangeably.

### Weight

Reference [8] provided takeoff weight and TOD weight statistics respectively in Table D.1 and D.2, that was obtained for six different jet aircraft from actual airline fleet. These actual weights were compared to the default values in the CTAS database to derive the weight error statistics of these two tables.

The current weight accuracy can be conveniently represented by the root-sum-square (rss) errors in these two tables. When the weight is downlinked from the cockpit, the mean weight error becomes negligible and only the standard deviation of the weight error is left.

**Table D.1 Aircraft Takeoff Weight Statistics for American Airlines at DFW5**

Aircraft		Actual Takeoff Weight (000lbs)		CTAS Weight Error (%)		
Type	No.	Mean	Sigma	Mean	Sigma	RSS
MD-80	3944	129.2	9.0	2.4	7.0	7.4
F-100	1059	87.0	5.5	-11.0	6.3	12.7
B-757	629	191.9	12.5	7.9	6.5	10.2
B-727	560	159.3	11.0	-2.8	6.9	7.4
B767	91	349.8	51.1	13.2	14.6	19.7
MD-10	81	470.2	88.9	-15.8	18.9	14.6
Weighted Statistics		138.5	10.6	5.1	7.6	9.15

**Table D.2 Aircraft TOD Weight Statistics for American Airlines at DFW5**

Aircraft		Actual TOD Weight (000lbs)		CTAS Weight Error (%)		
Type	No.	Mean	Sigma	Mean	Sigma	RSS
MD-80	3944	115.5	6.4	-4.7	5.6	7.3
F-100	1059	80.0	4.5	-12.5	5.7	13.7
B-757	629	172.4	9.1	1.1	5.3	5.4
B-727	560	140.8	7.8	-0.5	5.5	5.5
B767	91	265.8	13.3	29.6	5.0	30.0
MD-10	81	366.2	33.7	-5.9	9.2	10.9
Weighted Statistics		122.8	6.9	5.5	5.6	7.8

### Thrust and Drag

Reference [34] provides Drag and Thrust minus Drag measurements that were recorded on the NASA Transport Systems Research Vehicle (TSRV) which is a converted B 737 aircraft. The data was collected for descents starting at approximately 34,000 ft altitude and were collected down to about 17,000 ft altitude. The resulting statistics are presented in Table D.3.

As Table D.3 shows, the thrust minus drag data has a smaller  $\sigma$  than the drag  $\sigma$ . This suggests that the thrust and drag statistics are correlated (not independent). For the current DSTs, the thrust minus drag rss error is used. When thrust and drag are downlinked from the cockpit, the  $\sigma$  error remains.

**Table D.3. Thrust and Drag Statistics (%)**

Parameter	Flight Phase	Mean	Sigma	RSS
Drag	Climb/Descent	11.2	2.6	11.5
Drag	Cruise	11.3	1.5	11.4
(Thrust – Drag)	Climb/Descent	5.5	2.1	5.9
(Thrust – Drag)	Cruise	8.4	1.4	8.5

### TOD Placement Error

TOD placement error, when ATM specifies the TOD location with the assistance of CTAS EDA, assumes the accuracy of an FMS-guided aircraft. This is estimated to be 0.25 nm root-mean-square (rms) for a typical area navigation system. For the case where CTAS does not specify the TOD location, the TOD placement error, relative to that modeled by CTAS, is estimated to be as much as 20 nm.

### Speed Adherence

The speed adherence error is a combination of the FMS/CTAS nominal speed profile error and the FMS flight technical error to control the aircraft to the

nominal speed profile. The speed adherence statistics were obtained from [34] for a jet aircraft using an FMS both during cruise and during the descent phase. These statistics are summarized in Table D.4.

**Table D.4 Cruise and Descent Speed Adherence Statistics**

Parameter	Mean	Sigma	RSS
Cruise Mach	0.001	0.0035	0.0036
Cruise CAS (kts)	0.32	1.3	1.3
Descent Mach	0.0025	0.0085	0.089
Descent CAS (kts)	0.05	4.0	4.0

This table assumes that the aircraft is flying a CTAS-specified speed profile. When the FMS speed intent is not known to CTAS, a rss error of 15 kts is assumed.

When the speed intent of the pilot is downlinked from the aircraft, the rss CAS speed error is replaced with the standard deviation of the error. Since the mean CAS speed adherence errors for an FMS-guided aircraft are very small, as shown in Table D.4, the benefit of downlinking the speed intent may be negligible.

**Crosstrack Wander**

The crosstrack wander statistics were obtained from [35] for a jet aircraft using an FMS. For 32 cases, the mean crosstrack error was 0.13 nm and the standard deviation was 0.05 nm. The corresponding rss error is 0.14 nm.

**Navigation Error**

For an FMS-guided aircraft using a GPS/INS guidance system, the heading accuracy is estimated to be 0.15 degrees rss.

**Turn Dynamics**

Turn dynamic statistics that describe the additional distance flown during turns due to not returning to the new course in an optimum fashion were obtained from [36] for an FMS-guided aircraft. The path distance error statistics in [36] were converted to flight time errors assuming an aircraft CAS of 300 kts. The resulting statistics are summarized in Table D.5.

**Table D.5 Path Distance Error Statistics During Turns (sec)**

Turn Angle (deg)	Samples	Mean	Sigma	RSS
20-25	0			
30-35	7	-0.12	0.84	0.85
>40	8	1.56	2.88	3.28
Weighted Total		0.78	2.18	2.32

## Wind and Temperature Errors

Reference [38] provided estimates of the forecast accuracy of winds and temperature using the NOAA Rapid Update Cycle 2 (RUC-2) weather prediction model. The wind forecast accuracy is presented in Table D.6 while the temperature forecast accuracy is presented in Table D.7. These accuracy estimates were obtained by comparing the RUC-2 predictions against rawinsonde measurement data.

**Table D.6 Rapid Update Cycle 2 (RUC-2) Wind Forecast Accuracy (0000 UTC)**

	Forecast Accuracy (rss, kts)		
Flight Phase	0 Hour	1 Hour	3 Hour
Climb/Descent	6.5	9.6	10.2
Cruise	7.5	10.3	11.2

**Table D.7 Rapid Update Cycle 2 (RUC-2) Temperature Forecast Accuracy (0000 UTC)**

	Forecast Accuracy (rss, deg K)		
Flight Phase	0 Hour	1 Hour	3 Hour
Climb/Descent	0.51	1.02	1.09
Cruise	0.56	1.09	1.18

MIT/Lincoln Laboratory has been involved in the development of a wind forecast model for NASA/Ames that takes the RUC wind data and combines it with terminal wind data in the Integrated Weather System (ITWS) Terminal Winds (TW) development model [40]. While the RUC forecasts are generated every 3 hours, the forecast provides hourly forecasts until the next update cycle. The ITWS/TW model provides an update every 30 minutes with a 10 km resolution. This resolution compares to a 60 km resolution for the RUC and 40 km resolution for the RUC-2 forecast models.

To evaluate the performance of the ITWS/TW model as well as the basic RUC model wind forecast accuracy, [13] used pilot reports of winds as collected by the Meteorological Data Collection and Reporting System (MDCRS) to serve as truth. Since this same type of data is used as input into the ITWS/TW model, a different data set was used for the data accuracy evaluation. The result of the wind prediction accuracy both with the basic RUC and with the ITWS/TW that is initialized by the RUC is summarized in Table D.8.

**Table D.8 ITWS Terminal Wind and RUC Wind Forecast Accuracy<sup>11</sup> (kts)**

Flight Phase	RUC			ITWS/TW		
	Mean	Sigma	RSS	Mean	Sigma	RSS
Climb/Descent			12.0	6.4	6.2	8.9
Cruise			13.4	7.8	7.0	10.5
Overall	11.0	7.1	13.1	8.3	5.7	10.1

CTAS has been using the three-hour forecast RUC data for both wind and temperature forecasts. It is anticipated that CTAS will switch to the ITWS/TW wind forecast whose accuracy is summarized in Table D.8. It is further anticipated that CTAS will switch to the one-hour RUC-2 temperature forecast.

The benefit of downlinking the wind data from the cockpit is the ability to regionally update the RUC forecast using a model such as the ITWS/TW. The benefit of downlinking the temperature will result in a net temperature error that is equivalent to the nowcast (0 hour forecast) error of the RUC-2 data in Table D.7.

### Surveillance Errors

Currently, surveillance of the aircraft is provided by the Secondary Surveillance Radars using the Air Traffic Control Beacon Interrogator (ATCBI). With this beacon, the aircraft identity is known and the aircraft altitude is downlinked.

The radar tracking errors are predominantly in the ground speed, since this variable has to be estimated by the tracking software from repeated range and azimuth measurements. Hence, the ground speed accuracy varies depending whether the aircraft is flying a straight course without any changes in speed or whether the aircraft is turning or changing speed. The along track position error, however, is generally maneuver-independent but does increase with the range from the radar.

The along-track position and ground speed errors, obtained from [34], are summarized in Table D.9. This table shows that the position accuracy is higher near the TRACON. The ground speed accuracy, however, degrades progressively from level flight after the aircraft starts performing various maneuvers. In particular, the heading change errors are split into the ground speed errors occurring during the actual heading change and the transient errors that occur right after the maneuver is completed.

**Table D.9 Secondary Surveillance Radar Tracking Accuracy**

Flight Segment	Mean	Sigma	RSS
<u>Along-Track Position Accuracy (nm)</u>			
Top of Descent	0.78	0.39	0.87
Meter Fix	0.50	0.28	0.57
<u>Ground Speed Accuracy (kts)</u>			
Level flight	2.3	12.3	12.5
Altitude change	-2.3	12.9	13.1
Speed change	-35.4	24.4	43.0
Heading change	37.0	58.9	69.6
Post-turn	56.4	55.8	79.3

Since it was not known when these maneuvers occur during the various flight phases, only the level flight and altitude change ground speed accuracy was used to represent the current surveillance accuracy.

## Appendix E 1996 Annual Operations by Airport

**Table E.1 Airport Delays and Assumed Interruption Rates**

Airport	CY1996	CY1996	Delay Category	Rush Arrival Rate	
	Airport (1) Operations	Delays >15 min per 1000 ops (2)		No.	per 100 ops (3) Arr
EWR - Newark	443,431	65.25	1	39.46	47.45
SFO - San Francisco	442,281	56.57	1	39.46	47.45
LGA - N.Y. LaGuardia	342,618	46.22	1	39.46	47.45
ORD - Chicago O'Hare	909,186	34.46	2	34.91	41.97
STL - St. Louis	517,352	34.04	2	34.91	41.97
JFK - N.Y. Kennedy	360,511	29.53	2	34.91	41.97
BOS - Boston	462,507	26.37	2	34.91	41.97
LAX - Los Angeles	764,002	24.13	3	30.35	36.50
ATL - Atlanta	772,597	23.88	3	30.35	36.50
DFW - Dallas-Ft. Worth	869,831	19.59	3		36.50
PHL - Philadelphia	406,121	17.95	3	30.35	36.50
IAH - Houston International	391,939	11.45	4	24.28	29.20
CVG - Cincinnati	393,523	10.38	4	24.28	29.20
MSP - Minneapolis	483,570	9.29	4	24.28	29.20
DTW - Detroit	531,098	9.10	4	24.28	29.20
PHX - Phoenix	544,363	7.25	4	24.28	29.20
IAD - Washington Dulles	330,439	6.81	4	24.28	29.20
MIA - Miami	546,487	6.79	4	24.28	29.20
MDW - Chicago Midway	254,351	6.70	4	24.28	29.20
PIT - Pittsburgh	447,436	6.60	4	24.28	29.20
CLT - Charlotte	457,054	6.55	4	24.28	29.20
DCA - Washington National	309,754	6.53	4	24.28	29.20
SEA - Seattle	397,591	6.37	4	24.28	29.20
CLE - Cleveland	291,029	4.68	5	18.21	21.90
MCO - Orlando	341,942	4.59	5	18.21	21.90
LAS - Las Vegas	479,625	3.68	5	18.21	21.90
BWI - Baltimore-Washington	270,156	3.67	5	18.21	21.90
SLC - Salt Lake City	373,815	3.53	5	18.21	21.90
SAN - San Diego	243,595	3.31	5	18.21	21.90
HOU - Houston Hobby	252,254	2.57	5	18.21	21.90
PDX - Portland	305,964	2.41	5	18.21	21.90
DEN - Denver	454,234	1.90	5	18.21	21.90
FLL - Ft. Lauderdale	236,342	1.53	5	18.21	21.90
BDL - Bradley	160,752	1.36	5	18.21	21.90
BNA - Nashville	226,274	0.73	5	18.21	21.90
MEM - Memphis	363,945	Not Available	5	18.21	21.90
OAK - Oakland	516,498	Not Available	5	18.21	21.90

(1) Source: FAA "1997 Terminal Area Forecast (TAF) System," Office of Aviation Policy and Plans, FAA APO Internet website. (Oct 1998) [59]

(2) Source: FAA "1997 Aviation Capacity Enhancement Plan," Office of System Capacity. (Dec 1997) [53]

(3) Rush Arrival rates assumed to be 130%, 115%, 100%, 80% and 60% of simulated DFW rush arrival rate, based on 1996 FAA delay data and category criteria shown in Table A.3

**Table E.2 Rush Arrival Rate Criteria**

Category No.	CY1996 (1) Delays > 15 minutes Per 1000 Airport Ops	Proportion of DFW (category 3) Rush Arrival Rate	Rush Arrival Rate (Rush Arrivals Per 100 Airport Ops)
1	>35	130%	39.46
2	25-35	115%	34.91
3	15-25	100%	30.35 (2)
4	5-15	80%	24.28
5	<5	60%	18.21

(1) FAA CY1996 Delay Data [53], as shown in Table A.2.

(2) DFW Rush Arrival Rate per ATM Interruptions Model analysis.

**Table E.3 CY1996 Domestic ARTCC Operations**

	ARTCC Facility	ARTCC Departure Ops	ARTCC Overflight Ops	ARTCC Total Ops (1)
ZAB	Albuquerque, NM ARTCC	506,188	493,112	1,505,488
ZAU	Chicago, IL ARTCC	1,180,494	533,343	2,894,331
ZBW	Nashau, NH ARTCC (BOS)	697,875	331,101	1,726,851
ZDC	Leesburg, VA ARTCC (DC)	831,358	668,368	2,331,084
ZDV	Denver, CO ARTCC	434,387	658,530	1,527,304
ZFW	Ft. Worth, TX ARTCC	854,283	409,328	2,117,894
ZHU	Houston, TX ARTCC	825,674	201,509	1,852,857
ZID	Indianapolis, IN ARTCC	669,509	882,649	2,221,667
ZJX	Jacksonville, FL ARTCC	607,723	662,712	1,878,158
ZKC	Kansas City, KS ARTCC	691,746	602,863	1,986,355
ZLA	Los Angeles, CA ARTCC	927,509	125,726	1,980,744
ZLC	Salt Lake City, UT ARTCC	378,163	752,723	1,509,049
ZMA	Miami, FL ARTCC	725,485	90,866	1,541,836
ZME	Memphis, TN ARTCC	575,462	827,193	1,978,117
ZMP	Minneapolis, MN ARTCC	762,151	503,146	2,027,448
ZNY	New York, NY ARTCC	763,938	511,985	2,039,861
ZOA	Oakland, CA ARTCC	616,385	135,186	1,367,956
ZOB	Cleveland, OH ARTCC	967,543	935,158	2,870,244
ZSE	Seattle, WA ARTCC	647,722	97,069	1,392,513
ZTL	Atlanta, GA ARTCC	943,365	565,941	2,452,671
ZAN	Anchorage, A ARTCC	225,034	45,121	495,189
ZUA	Guam CERAP	32,112	8,560	72,784

(1) ARTCC Total Operations is calculated as: 2 x (ARTCC Departure ops) + (ARTCC Overflight Ops)

Source: Office of Aviation Policy and Plans, Washington, DC 20591, Air Traffic Activity query, APO Data System, FAA APO Home Page, Internet WWW Site (Nov 19,1998). [60]

## References

---

- [1] Weidner, T., "Benefits Assessment Compilation of the En Route Descent Advisor (EDA) AATT Decision Support Tool," Seagull TR98188.52f, NASS AATT TO52. (December 2000)
- [2] Weidner, T., Mueller, T., "Benefits Assessment Compilation of En Route Data Exchange (EDX)," Seagull Technology, TM98188.27-01f, NASA AATT TO27. (December 2000)
- [3] Green, S.M., and Vivona, R., "En route Descent Advisor (EDA) Concept," Advanced Air Transportation Technologies (AATT) Project Milestone 5.10 Report, NASA Ames Research Center. (September 1999)
- [4] Vivona, R., Ballin, M., Green, S., Bach, R., and McNally, B.D., "A System Concept for Facilitating User Preferences in En Route Airspace," NASA TM4763. (November 1996)
- [5] National Aeronautics and Space Administration, "AATT Program Products Descriptions," Draft Manuscript, Advanced Air Transportation Technologies (AATT) Program Office, NASA Ames. (June 1998)
- [6] Weidner, T., Schleicher, D., Coppenbarger, R., "NASA/FAA En Route Data Exchange (EDX) Phase 2 Field Evaluation Project Plan," Seagull Technology, TR99185.04-01. (February 2000)
- [7] Davidson, T.G., Weidner, T., Birtcil, L., "En Route Descent Advisor Preliminary Benefits Assessment," Seagull TR98175.06 (December 1998)
- [8] Weidner, T., Davidson, T.G., "Preliminary En Route Data Exchange Potential Benefits Assessment," Seagull Technology, TR98175.9-01. (December 1998)
- [9] Swenson, H., et al, "Design & Operational Evaluation of the Traffic Management Advisor at the Fort Worth ARTCC," 1<sup>st</sup> USA/Europe ATM R&D Seminar, France. (June 1997)
- [10] Celio, J., Bowen, K., Winokur, D., Lindsay, K., Newberger, E., Sicenavage, D., "Free Flight Phase 1 Conflict Probe Operational Description," MITRE Technical Report MTR 0W00000100. (March 2000)
- [11] Davidson, T.G., Birtcil, L., "Sector Tools Potential Benefits Analysis," Seagull TR98154-01D. (draft April 1998)
- [12] Green, S., Goka, T., Williams, D., "Enabling User Preferences through Data Exchange," AIAA GNC Conference. (August 1997)
- [13] Cole, R., Richard, C., Kim, S., and Bailey, D., "An assessment of the errors in the 60 km Rapid Update Cycle wind forecasts relative to the needs of the Center TRACON Advisory System, and an assessment of the increase in accuracy due to augmentation of wind forecasts with near real-time MDCRS data via the Integrated Terminal Weather System," MIT/Lincoln Laboratory. (Jan 1998).
- [14] FAA, IFR En Route Low Altitude Chart, L-13 (February 26, 1998)
- [15] Weidner, T., Davidson, G., Coppenbarger, R. Green, S., "Modeling ATM Interruption Benefits," AIAA99-4296, AIAA GNC Conference. (June 1999)
- [16] CSSI Inc. , "Traffic Demand Scenarios" computer data files. (Sept 1998)
- [17] U.S. Department of Commerce, NOAA, National Ocean Service, "U.S. Government Flight Information Publication, U.S. Terminal Procedures, South Central," DFW BOWIE ONE Standard Terminal Arrival Route (STAR) and DFW COYOTE ONE Standard Instrument Departure Route (SID). (1997)
- [18] Davidson, T.G., Birtcil, L., "Comparison of Fuel Optimal, CTAS and FMS Time-of-Arrival Control Strategies for MD-80 Aircraft Trajectories," Seagull TR178-02. (September 98)
- [19] Davidson, T.G., Birtcil, L., "Comparison of Fuel Optimal, CTAS and FMS Time-of-Arrival Control Strategies for B-747 Aircraft Trajectories," Seagull TR178-03 (September 98)
- [20] Davidson, T.G., Birtcil, L., Green, S., "Comparison of CAS/EDA and FMS Time-of-Arrival Control Strategies," AIAA99-4230, Guidance, Navigation, and Control Conference. (August 1999)
- [21] Eurocontrol Experimental Centre, "User Manual for the Base of Aircraft Data (BADA) Revision 3.1," EED Note No. 23/97, Eurocontrol. (October 1998)
- [22] FAA, "Air Traffic Rules and Procedures Service, Air Traffic Control FAA Order 7110.65, USDOT. (1998)

- [23] Personal communication with Harry Swenson, NASA Ames Research Center, Moffett Field, CA. (April 2000)
- [24] Green, S., Vivona, R., Grace, M., "Field Evaluation of Descent Advisor Trajectory Prediction Accuracy for En route Clearance Advisories," AIAA98-4479, AIAA GNC Conference. (August 1998)
- [25] Mukai, C., "Design and Analysis of Aircraft Dynamics Models for the ATC Simulation at NASA Ames Research Center," Seagull TR92119-02. (March 1992)
- [26] FAA, "Economic Values for Evaluation of FAA Investment and Regulatory Programs," FAA-APO-98-8, Office of Aviation Policy and Plans. (June 1998)
- [27] FAA, "FAA, "FAA Aviation Forecasts Fiscal Years 1996-2007," Final Report FAA-APO-89-1, Office of Aviation Policy & Plans. (March 1989)
- [28] FAA, "FAA Aviation Forecasts Fiscal Years 1996-2007," Final Report FAA-APO-96-1, Office of Aviation Policy & Plans. (March 1996)
- [29] Chiang, Y, Klosowski, J, Lee, C. Mitchell, J., "Geometric Algorithms for Conflict Detection/Resolution in Air Traffic Management," 36th IEEE Conference on Decision and Control, San Diego, CA. (Dec 1997)
- [30] Weidner, T., Green, S., "Modeling ATM Automation Metering conformance Benefits," 3<sup>rd</sup> USA/Europe Air Traffic Management R&D Seminar. (June 2000)
- [31] Coppenbarger, R.A., "Enroute Climb Trajectory Prediction Enhancement Using Airline Flight-Planning Information," AIAA99-4147, Guidance Navigation & Control Conference. (August 1999)
- [32] Jackson, M., "Sensitivity of Trajectory Prediction in Air Traffic Management and Flight Management Systems," University of Minnesota, Ph.D Thesis under Zhao, Y. (December 1997)
- [33] Hunter, G., Weidner, T., Couluris, G., Sorensen, J., Bortins, R., "CTAS Error Sensitivity, Fuel Efficiency, and Throughput Benefits Analysis," Seagull Technology TR96150-02. (July 1996)
- [34] Williams, D., Green, S., "Flight Evaluation of Center-TRACON Automation System Trajectory Prediction Process," NASA/TP-1998-208439. (July 1998)
- [35] Green, S., Vivona, R., and Grace, M., "Field Evaluation of Descent Advisor Trajectory Prediction Accuracy for En route Clearance Advisories," AIAA-98-4479, AIAA GNC Conference. (August 1998)
- [36] Green, S., and Vivona, R., "Field Evaluation of Descent Advisor Trajectory Prediction Accuracy," AIAA 96-3764. (July 1996)
- [37] Kayton, M., and Fried, W.R., "Avionics Navigation Systems," Second Edition, John Wiley & Sons. (1997)
- [38] Benjamin, Stanley G., et al, "Aviation Forecasts From the RUC-2," 8<sup>th</sup> Conference on Aviation, Range, and Aerospace Meteorology, Dallas. (January 1999)
- [39] Crown Communications, Inc., "Center TRACON Automation Traffic Management Advisor Build 2 (TMA) Assessment - Final Report," Doc. No. CTASDS-BAPRPT-003, FAA. (Dec 1996)
- [40] Cole, R., Green, S., Jardin, M., Schwartz, B., Benjamin, S., "Wind Prediction Accuracy for ATM Decision Support Tools," 3<sup>rd</sup> USA/Europe ATM R&D Seminar. (July 2000)
- [41] Weidner, T., Davidson, T.G., Birteil, L., "Potential Benefits of User-Preferred Descent Speed Profile," Seagull TR98188.26-02f, NASS AATT TO26. (December 2000)
- [42] McNally, B.D., Bach, R., Chan, W., "Field Test Evaluation of the CTAS Conflict Prediction and Trial Planning Capability," AIAA98-4480, Guidance, Navigation, and Control Conference. (August 1998)
- [43] Bilimoria, K., "A Methodology for the Performance Evaluation of a Conflict Probe," AIAA98-4238, Guidance, Navigation, and Control Conference. (Aug 1998)
- [44] Personal Communication with McNally, B.D., and Bilimoria, K., NASA Ames Research Center. (1999)
- [45] Paielli, R., Erzberger, H., "Conflict Probability Estimation for Free Flight," Journal of Guidance, Control, and Dynamics, Vol. 20, No. 3. (May-June 1997)
- [46] Erzberer, H. Paielli, R. Isaacson, D., Eshow, M., "Conflict Detection and Resolution in the Presence of Prediction Error," 1<sup>st</sup> USA/Europe ATM R&D Seminar. (June 1997)

- [47] Krozel, J., Peters, M, Hunter, C.G., "Conflict Detection and Resolution for Future Air Transportation Management," Seagull Technology, TR97138-01. (April 1997)
- [48] Krozel, J., "Software Specifications for conflict detection and resolution maneuvers: Strategic Cases," Seagull Technology, TR98169-01. (February 1998)
- [49] Brudnicki, D., McFarland, A., "User Request Evaluation Tool (URET) Conflict Probe Performance and Benefits Assessment," MITRE CAASD, MP 9720000112. (June 1997)
- [50] McNally, B.D., Erzberger, H., Bach, W., Chan, W., "A Controller Tool for Transition Airspace," AIAA99-4298, Guidance Navigation, and Control Conference. (August 1999)
- [51] Warren, A., Ebrahimi, Y., "Vertical Path Trajectory Prediction for Next Generation ATM," 17th Digital Avionics Systems Conference, Bellevue, WA. (November 1998)
- [52] Datta, K., "Economic Effects of Increased Control Zone Sizes in Conflict Resolution," NASA/CR-1998-207889. (April 1998)
- [53] Federal Aviation Administration (FAA), "1997 Aviation Capacity Enhancement Plan," Office of System Capacity. (December 1997)
- [54] DenBraven, W., "Fully Automated Simulation of Air Traffic Control Concepts," Joint FAA/NASA CTAS/Datalink Workshop. (November 1994)
- [55] Personal communication with Danny Vincent, Traffic Management Supervisor, Ft. Worth ARTCC (ZFW). (September 2000)
- [56] ZFW ARTCC Radar Data (1996)
- [57] Paielli, Russell A., "Empirical Test of Conflict Probability Estimation," 2<sup>nd</sup> USA/Europe Air Traffic Management R&D Seminar (ATM98). (December 1998)
- [58] Eurocontrol, "Study of the Acquisition of Data from Aircraft Operators to Aid Trajectory Prediction Calculation," EEC Note No. 18/98. (September 1998)
- [59] FAA, "1997 Terminal Area Forecast (TAF) System," Office of Aviation Policy and Plans, FAA APO Home Page, Internet WWW Site. (October 1998)
- [60] FAA, Air Traffic Activity query, Office of Aviation Policy and Plans (APO) Data System, FAA APO Home Page, Internet WWW Site. (November 1998)
- [61] Slattery, R.A., and S.M. Green, "Conflict-Free Trajectory Planning for Air Traffic Control Automation, NASA Technical Memorandum 108790. (1994)